The effect of molecular composition on the properties of linear low density polyethylene

L Keulder

Thesis presented in partial fulfillment of the requirements for the degree of Master of Science at the University of Stellenbosch.

Study Leader: Dr A.J van Reenen. March 2008

Declaration

By submitting this thesis electronically, I declare that the entirety of the work contained therein is my own, original work, that I am the owner of the copyright thereof (unless to the extent explicitly otherwise stated) and that I have not previously in its entirety or in part submitted it for obtaining any qualification.

Date: March 2008

Abstract

In this study linear low density polyethylene (LLDPE), a copolymer consisting of ethylene and 1-butene, was fractionated by the use of temperature rising elution fractionation (TREF). These fractions were then analyzed by crystallisation analysis fractionation, ^{13}C NMR, high temperature size exclusion chromatography and DSC. The molecular distribution of the polymer was investigated. It was found that the polymer had a very broad distribution in its chemical composition. From these results it was also clear that the catalysts used for the polymerisation consist out of different active sites, producing chains with different molecular architecture.

Subsequently the polymer was fractionated again by TREF and certain fractions were removed and the remaining material recombined. The removed fractions and recombined material were analyzed by ^{13}C NMR, high temperature size exclusion chromatography, DSC and DMA. The results were compared with the bulk material and from this we could conclude the influence of the fractions removed on the material properties. This gave us more information on the influence of the chemical structure of the polymer on its mechanical properties. It was clear that by removing certain fractions with a certain chemical composition, the properties of the polymer are significantly influenced.

Opsomming

Tydens hierdie navorsing is lineêre lae digtheid poliëtileen, ‘n kopolimeer van etileen en 1-buteen, gefraksioneer deur temperatuurstyging eluering fraksionering (TREF). Hierdie fraksies is geanaliseer deur kristallisasie analise fraksionering (CRYSTAF), ^{13}C kern magnetiese resonans spektroskopie (^{13}C KMR), hoë temperatuur grootte uitsluitings chromatografie (HT-SEC) en differensiële skandeer kalorimetrie (DSC). Daar is ondersoek ingestel na die molekulêre samestellingsverpreiding van die polimeer en daar is gevind dat die polimeer ‘n wye verspreiding het t.o.v chemiese samestelling. Vanuit hierdie resultate is dit duidelik dat die katalis wat gebruik is vir die polimerisasie, uit vier verskillende tipes aktiewe setels bestaan wat kettings met verskillende molekulêre samestelling produseer. Die polimeer is weer gefraksioneer deur TREF en sekere fraksies is verwyder en die oorblywende materiaal is weer gekombineer. Die verwyderde fraksies sowel as die gekombineerde materiaal is geanaliseer deur ^{13}C KMR, HT-SEC, DSC en DMA. Die resultate is vergelyk met die oorspronklike materiaal en ons kon afleidings maak oor die invloed van die chemiese struktuur van die polimeer op die meganiese eienskappe van die polimeer. Dit was duidelik dat die verwydering van sekere materiaal met ‘n sekere chemiese samestelling, ‘n beduidende invloed het op die makroskopiese eienskappe van die polimeer.

Acknowledgements

I would like to thank the following people:

Dr. van Reenen – for all the guidance and support as my study leader

Gareth Harding – who was always willing to help and running the HT-SEC and CRYSTAF sample analysis

Elsa Malherbe – NMR sample analysis

Methuli Mbanjwa – DMA sample analysis

NRF and Sasol - for funding

Olefin research group

All my friends – especially Adine, Maggie and Morné who always listened and understood

My parents - for their continuing support throughout my studies

Table of Contents

List of Figures

List of Tables

List of abbreviations

BHT	2,6-di-tert-butyl-4-methylphenol
CRYSTAF	Crystallisation analysis by fractionation
DMA	Dynamic mechanical analysis
DSC	Differential scanning calorimetry
GC	Gas chromatography
HDPE	High density polyethylene
LDPE	Low density polyethylene
LLDPE	Linear low density polyethylene
MAO	Methylaluminoxane
Mn	Number average molecular weight
Mw	Weight average molecular weight
NMR	Nuclear magnetic resonance
ODCB	ortho-Dichlorobenzene
PD	Polydispersity
SCBD	Short chain branching distribution
SEC	Size exclusion chromatography
TCB	Trichlorobenzene
TREF	Temperature rising elution fractionation
UHMWPE	Ultra high molecular weight polyethylene

Chapter 1

Introduction

1.1 General overview

Polyethylene is one of the most widely used plastics in the world. This is due to the fact that the polymer has versatile chemical and physical properties and is regarded as ideal for use in many household and industrial applications [1].

Polyethylene can be classified according to type: high density polyethylene, low density polyethylene, linear low density polyethylene, plastomers and ultra high molecular weight polyethylene. The different classes are used in specific applications. The different applications are due to the unique molecular structure of each class. For instance ultra high molecular weight polyethylene has very good wear resistance and impact toughness [2].

The properties of any polymer are dependent on the molecular architecture of the material. All polyethylenes are simple, aliphatic hydrocarbons, yet they differ with respect to melting point, crystallinity, impact properties and tensile modulus, for example. These differences arise from variables such as molecular weight, molecular weight distribution, long– and short-chain branching and the molecular heterogeneity of the material. Past studies arising from this research group have focussed on the fractionation and characterization of commercial polyolefins, including LDPE, LLDPE, poly(propylene), propylene-1-pentene copolymers, propylene-ethylene random copolymers and propylene impact copolymers [3-8]. One key aspect is the ability to understand the role that the molecular species present in each polymer plays in determining the properties of the material as a whole. This study therefore focuses a fairly heterogeneous polymer like LLDPE. The goal was to see, if we selectively removed fractions from the polymer, the effect on macroscopic properties (thermal properties as well as mechanical properties) of the LLDPE in question.

The linear low density polyethylene selected for this study was a copolymer of ethylene and 1-butene.

1.2 Aim

In broad terms, the aim of the study was to fully characterise a commercially available LLDPE, and to ascertain whether selectively removing distinctly different fractions from the material would result in measurable changes in the polymer properties.

A copolymer such as LLDPE has a very complex molecular structure. This is because the α-olefin can be distributed in different ways through the polymer. The amount, type and distribution of the comonomer all influence the molecular make-up, and therefore the mechanical properties as well.

To fully characterise the polymer, we first needed to fractionate the polymer. We selected preparative temperature rising elution fractionation (TREF) for the fractionation. TREF is a technique that fractionates semi-crystalline polymers according to their crystallinity [9]. By characterizing these fractions fully, we can determine their chemical structure. Then by removing some of these fractions we can determine the influence of the chemical structure on the mechanical properties of the polymer. Individual objectives that were set out to meet the aim of the study are given below.

1.3 Objectives

- Fully characterizing the bulk material
- Fractionate the bulk material with the use of preparative TREF
- Characterizing each fraction fully by using, DSC, high temperature SEC and ^{13}C NMR
- Removing TREF fractions and recombining the rest of the material
- Characterizing the recombined material
- Determine the influence of the chemical structure on the mechanical properties of the polymer

1.4 Layout of the thesis

Chapter 1

In this chapter the objective and aim of this study is laid out.

Chapter 2

This chapter comprises a brief discussion on the historical and theoretical background of polyethylene, focussing mainly on LLDPE as a material.

The history of polyethylene is discussed and a brief overview is given on the catalysts used to produce these polymers, mainly focusing on the so-called Ziegler-Natta catalysts. The molecular properties of LLDPE are also discussed, with emphasis on crystallinity, branching, molecular weight and thermal properties.

The chapter concludes with a discussion on two fractionation techniques, TREF and CRYSTAF.

Chapter 3

The materials used are discussed. A layout is given of the experimental set-up of the fractionation and the analytical techniques used. This includes TREF, CRYSTAF, DSC, ^{13}C NMR, high temperature SEC, film preparation and DMA.

Chapter 4

An in-depth discussion of the characterization and fractionation of the material is presented, as well as a discussion of all the results obtained from the analytical processes performed.

Chapter 5

The conclusions drawn from the results we obtained from this study as well as recommendations for future work is presented.

1.5 References

1. Xie, T., K.B. McAuley, J.C.C. Hsu, and D.W. Bacon, *Gas Phase Ethylene Polymerization: Production Processes, Polymer Properties, and Reactor Modeling.* Industrial and Engineering Chemistry Research, 1994. **33**: p. 449-479.
2. Jauffrès, D., O. Lame, and F. Doré, *Microstructural origin of physical and mechanical properties of ultra high molecular weight polyethylene processed by high velocity compaction.* Polymer, 2007. **48**: p. 6374-6383.
3. Assumption, H.J., J.P. Vermeulen, W.L. Jarrett, L.J. Mathias, and A.J. Van Reenen, *High resolution solution and solid state NMR characterization of ethylene/1-butene and ethylene/1-hexene copolymers fractionated by preparative temperature rising elution fractionation.* Polymer, 2006. **47**: p. 67-74.
4. Harding, G.W. and A.J. Van Reenen, *Fractionation and Characterisation of Propylene-Ethylene Copolymers: Effect of the Comonomer on Crystallization of Poly(propylene) in the γ-phase.* Macromolecular Chemistry and Physics 2006. **207**: p. 1680-1690.
5. Kotsekoane, *Isolation and evaluation of extractable materials in commercial polyolefins.* MSc Thesis, University of Stellenbosch: Stellenbosch. 2007

6. Lutz, M., *Relationship between structure and properties of copolymers of propylene and 1-pentene.* PhD Thesis, University of Stellenbosch: Stellenbosch. 2006
7. Pretorius, M.S., *Characterization of molecular properties of propylene impact copolymers.* MSc thesis, University of Stellenbosch: Stellenbosch. 2007
8. Rabie, A.J., *Blends with Low-Density Polyethylene (LDPE) and Plastomers.* MSc Thesis, University of Stellenbosch: Stellenbosch. 2004
9. Wild, L., *Temperature Rising Elution Fractionation.* Advances in Polymer Science, 1990. **98**: p. 1-47.

Chapter 2

Historical and Theoretical Background

2.1 The history of polyethylene

Polyethylenes are generally regarded as being part of the polyolefin family, and can conveniently be divided into the following groups:

- Linear or **high density polyethylene**, with density values between 0.960-0.970 g/cm^3. These polymers are typically made by transition metal catalysts (Ziegler-Natta catalysts or Phillips catalysts), and at relatively low pressures.
- **Low density polyethylene**, which is made in a high pressure process by free radical polymerisation.
- **Linear low density polyethylene**, which are copolymers of ethylene and a α-olefin and have density values between 0.915-0.940 g/cm^3. These polymers are usually produced with Ziegler-Natta or Phillips catalysts, with the Unipol® gas-phase process as an example of a typical commercial production process.
- **Ultra high molecular weight polyethylene**, which is a group of linear polyethylene materials with a molecular weight about ten times than that of commercial high density polyethylene [1, 2].
- **Plastomers** are linear low density polyethylene type materials which have very low density values as well as low crystallinity [3]. These linear low density polyethylene materials are typically produced in solution by metallocene type catalyst systems [4].

J. Berzelius first used the word “polymeric” in 1832. Four Dutch chemists first used the word “olefin” and it is based on the term “olefiant”, which means oil-forming gas [5].

The development of polyethylene is generally regarded as having its origin in the 1930’s, with the development of the high pressure radical polymerisation. Before this time, however, there have been reports of polyethylene-like materials being prepared. There was Von Pechmann’s 1898 report [6] that diazomethane, when dissolved in ether yields a white substance on standing, and a subsequent report by Bamberger *et al*. [7] that this material melted at 128 °C and had a chemical structure of $(CH_2)_n$.

Other routes of producing polyethylene have also been suggested, with Arnold *et al*.

reporting that the Fischer-Tropsch reduction of carbon monoxide could be used to prepare

high molecular weight polyethylene with a melting temperature of 133 °C [8]. This patent was taken out in 1955, some 32 years after the discovery of the high temperature radical polymerisation of ethylene.

2.1.1 High pressure free radical polymerisation: LDPE

Low density polyethylene was the first commercial polyolefin to be produced [5]. In 1933, it was discovered accidentally in the laboratories of ICI in the United Kingdom by Fawcett and Gibson [1, 2, 9]. Just a small amount of solid polyethylene was produced at the research department of the Alkali Division of Imperial Chemical Industries Limited in March 1933. Repeating the experiment proved difficult, and only by improving the equipment to be able to handle high pressure were they able to produce eight grams of polymer. This was in December of 1935, and the decision was taken to commercially develop this material [9]. The development of polyethylene can thus be divided into several periods. From 1931-1935 the focus was on the effects of high pressure on the chemical reactions during the polymerisation process, while between 1935 and1939 a commercial manufacturing process was developed, culminating in commercial production in 1939 [10]. Between 1939 and 1945 the production of as much polyethylene as possible was the only concern, both in the UK and the USA. Du Pont made the first linear polyethylene by free-radical polymerisation at 50 - 80 °C and at a pressure of 707 Mpa. The product had a density of about 0.955 g/cm^3 and it had 0.80 alkyl substituents per 1000 carbon atoms [1].

2.1.2 Transition metal catalyzed polyethylenes: HDPE and LLDPE

J.P. Hogan and R.L. Bank at Phillips discovered in the 1950s that ethylene can be polymerised with catalysts which contained chromium oxide and was supported on silica. These catalysts became known as the Phillips catalysts. The first polymers prepared with these catalysts were homopolymers. In 1956 the commercial manufacture of HDPE started. The Phillips catalysts were also used for the first synthesis of copolymers of ethylene and α–olefins.

It was in this same time period (1953) that Karl Ziegler reported a new group of transition metal catalysts that could produce linear polyethylene. Subsequent to Natta's work on the polymerization of propylene involving these heterogeneous transition metal catalysts, these catalysts became known as the Ziegler–Natta catalysts [3]. The polyethylene produced with these catalysts had density of about 0.945-0.960 g/cm^3, and as a result, much higher crystallinity than the polymers produced by high pressure free radical processes. Typically

these linear polymers were prepared at 50-100 °C and atmospheric pressure and contained very few short-chain branches [1]. The Ziegler-Natta catalysts made it possible to produce polyethylene with a wide range of properties [3]. Du Pont, for example, produced linear low density polyethylene in the early 1970s, by adding alpha olefins like 1-hexene to ethylene during polymerisation [2].

Union Carbide Corp. produced a broad spectrum of LLDPE polymers with density values ranging between 0.915-0.950 g/cm^3 in 1977, through the Unipol® process. The Unipol® process utilized a fluidized-bed, gas phase technology [1].

In 1976, Kaminsky and Sinn reported a new range of catalysts for the production of polyethylene. These soluble transition metal catalysts contained a metallocene complex as pro-catalyst, and a organo-aluminium compound as cocatalyst [3]. Some more detail on these catalysts are given in Section 2.1.4.

2.1.3 UHMWPE

Ultra high molecular weight polyethylene were usually produced by a low pressure Ziegler-Natta catalyst system using organometallic compounds [11]. The process used can be either batch or continuous. They were usually produced by a slurry process. These polymers have extremely high molecular weights and density. Due to this fact, these polymers can be processed without any stabilizers or additives, because the long chains are not easily broken (resistant to scission) [12]. Recently metallocene catalysts have also been used to produce ultra high molecular weight polyethylene [13]. A high-pressure process can also be used to obtain polyethylene with a high molecular weight [14].

2.1.4 Metallocene catalysts: Plastomers

In the 1950s Breslow and Natta independently discovered metallocene catalysts. However these catalysts were not very active [15-18]. This catalyst system consisted of a bis(cyclopentadienyl) titanium compound, usually $(C_5H_5)_2TiCl_2$, and a dialkylaluminum chloride cocatalyst [15-19].

The significant breakthrough came in the 1980s when Kaminsky and Sinn discovered that when water was added to the catalyst system $(C_5H_5)_2TiCl_2/AlMe_3$, the activity was greatly increased [15, 16, 18] . When adding the water, hydrolysis of the $AlMe_3$ (used as cocatalyst) takes place and methylalumoxane (MAO) is formed [15-17, 20]. Subsequently, the use of $(C_5H_5)_2ZrCl_2$ (Cp_2ZrCl_2) as a catalyst, rather than the more unstable Cp_2TiCl_2 , was proposed, with MAO as a cocatalyst [15-18, 21]. MAO activates the catalyst by fast methylation and

partial demythylation, while also acting as a scavenger for impurities and potential catalyst poisons [15, 22]. The resulting MAO anion stabilizes the cationic catalytically active species.
The primary difference between metallocene catalysts and Ziegler-Natta catalysts is the fact that the metallocene catalysts are homogeneous in nature, and not heterogeneous like the Ziegler-Natta catalysts. This results in active sites that are far more homogeneous in nature in the case of the metallocene catalysts. As a result of this, metallocene catalysts produce polyethylene with a narrow molecular weight distribution [16, 18, 21]. The perceived activity of the metallocene catalysts is also much higher, as all the transition metals are available in catalytically active species, while the heterogeneous transition metal catalysts contain metal atoms that are inactive due to the crystalline nature of the material. [15].
The general mechanism for metallocene polymerisation is depicted in seen in Figure 2.1.

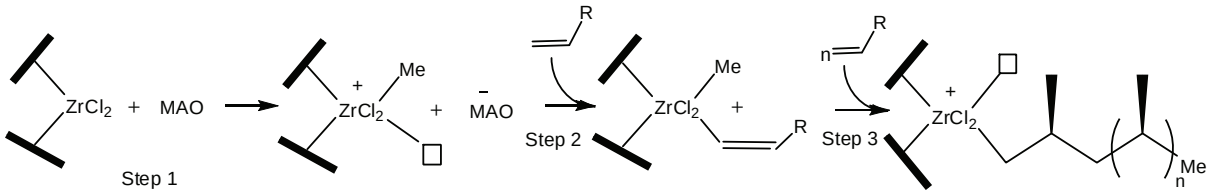

Figure 2.1 The mechanism for metallocene polymerisation [19]

The active species in metallocene catalyst is a ionic complex, comprising a metallocene cation and a MAO anion. As mentioned above, this is formed by the reaction between the MAO and the metallocene complex. The σ ligands (Cl^- or CH_3^-) are abstracted from the metallocene complex by the Al-centre of the MAO to form the ionic pair [15, 17, 19]. Krentsel *et al*. gives a very simple explanation of the polymerisation mechanism. The polymerisation begins when the α–olefin coordinates with the positively charged transition metal atom and then the insertion of the monomer into the Zr-Me bond takes place. This reaction takes place for all the monomer units to form a polymer chain.
Termination usually takes place through β-hydride elimination [17]. Because of the nature of the catalysts, very high comonomer content polymers can be produced, the so-called plastomer range of materials. Plastomers are generally defined as LLDPE materials with comonomer content of between 10 and 40 mole%. These materials have very low density (<0.915 g/dm3). Commercially these materials usually have 1-octene as comonomer.

2.1.5 Transition metal catalysts for propylene polymerisation: A brief history

A Ziegler-Natta catalyst is a catalyst that consists of two components. The first component is a transition metal compound, which can be a halide, or alkoxide, or alkyl or aryl derivative, of the group IV-VIII transition metals. The second component is a methyl alkyl or allyl halide of group I-III base metals. These two components then react to form a complex. The first component is usually called the catalyst or pro-catalyst, and the second component the cocatalyst [15, 17, 23]. The cocatalyst is responsible for generating the initial metal-carbon bond [24].

There are few "generations" of Ziegler-Natta catalysts. The first generation was characterised by catalysts that contained $TiCl_3 \cdot AlCl_3$ and $Al(C_2H_5)_2Cl$, but had very low productivity [22]. The stereospecificity of polypropylene produced by these catalysts was also very low; the fraction of isotactic polymer was only about 90%. The efficiency of the Ti needed to be improved, as this was responsible for the activity.

This led to the development of a catalyst with a much higher surface area by Solvay. The productivity increased by five times and the isotactic index was about 95%. This comprised the second generation catalysts [24].

The next development within this generation was the addition of a Lewis base to the catalyst system [22]. The Lewis bases acted as electron donors. The electron donors affect the kinetic and stereochemical behaviour of the catalyst. They increase the activity and stereoselectivity of the catalysts. The electron donors can form complexes by reacting with the components of the catalysts or the active centres [15]. In the third generation, catalysts were supported on $MgCl_2$. Catalysts comprised $TiCl_4$, a trialkyl-aluminum as a cocatalyst and as electron donors they used one or two Lewis bases [22]. When using two Lewis bases the first one was referred to as the "internal donor" and was added during preparation of the supported catalyst, and the second one as the "external donor" which was added during the addition of the cocatalyst to produce the active catalyst. The activity of these catalysts was very high, but there was still about 6-10% atactic polymer present in the polymer produced.

The fourth generation catalysts had better productivity and isotacticity. The better isotacticity was due to the use of a new combination of electron donors. As internal donors alkylphthalates were used and for external donors alkoxysilanes were used.

The fifth generation catalyst was discovered in the second part of the 1980's. 1, 3-Diethers were used as electron donors and if they were used as an internal donor, the activity and isotacticity was very high, without the need to use a Lewis base as an external donor [24]. It must be pointed out that organizing the catalysts in "generations" is a highly subjective exercise, and other descriptions than the one set out above might be found in literature.

2.2 The polymerisation mechanism of transition metal catalysts

Polymerisation with transition metal catalysts broadly consists of migratory insertion in alkyl-olefin complexes to cause chain growth and various mechanisms of chain transfer [25].

In the 1960s Cossee proposed a mechanism for Ziegler-Natta polymerisation [15]. In Figure 2.2 the general mechanism can be seen.

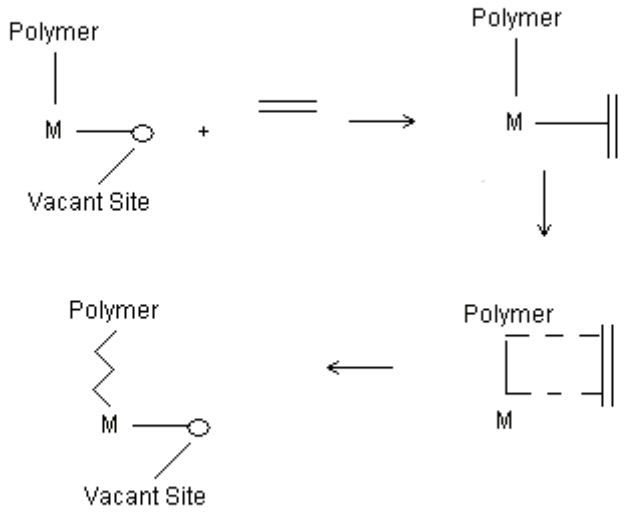

Figure 2.2 Cossee mechanism for Ziegler-Natta polymerisation

In the first step, the complexation of the monomer can be seen. This activates the double bond. Then the monomer is inserted into the metal-carbon bond. The vacant site is now available for the complexation of another monomer [26].

During the reaction of the catalyst with the cocatalysts, the exchange of the alkyl group of the organometallic component and the halogen atom of the transition metal compound takes place. The chemical bond formed with the transition metal is usually unstable. This causes the valence state of the metal to decrease. When the transition metal components contain $TiCl_3$ or VCl_3, the decrease of the valence state usually just occurs at the surface.

The ability of the metal-carbon bond to react with the double bond of the α-olefins is very important. The polymerisation activity of the catalysts is dependant on the α-olefin's insertion into the metal-carbon bond [17].

2.2.1 The effect of the catalyst chemistry on the structure and properties of LLDPE

When preparing LLDPE, the two different monomer molecules compete with each other to complex at the active site. The active centre then has a polymer chain attached to it, with the last inserted monomer being either ethylene or the α-olefin. The rate of the addition does not only depend on the type of α-olefin, but also on the chain-end [3]. There are four propagation reactions that control the arrangement of the two monomers (M_1 and M_2) in the chain.

$$\text{Polymer - M}_1\cdot + \text{M}_1 \xrightarrow{k_{11}} \text{Polymer - M}_1\text{ - M}_1\cdot \qquad \text{R}_{11} = k_{11}\left[\text{Polymer - } M_1\cdot\right]\left[M_1\right]$$

$$\text{Polymer - M}_1\cdot + \text{M}_2 \xrightarrow{k_{12}} \text{Polymer - M}_1\text{ - M}_2\cdot \qquad \text{R}_{12} = k_{12}\left[\text{Polymer - } M_1\cdot\right]\left[M_2\right]$$

$$\text{Polymer - M}_2\cdot + \text{M}_1 \xrightarrow{k_{21}} \text{Polymer - M}_2\text{ - M}_1\cdot \qquad \text{R}_{21} = k_{21}\left[\text{Polymer - } M_2\cdot\right]\left[M_1\right]$$

$$\text{Polymer - M}_2\cdot + \text{M}_2 \xrightarrow{k_{22}} \text{Polymer - M}_2\text{ - M}_2\cdot \qquad \text{R}_{22} = k_{22}\left[\text{Polymer - } M_2\cdot\right]\left[M_2\right]$$

The reactivity ratios, $r_1 = \frac{k_{11}}{k_{12}}$ and $r_2 = \frac{k_{22}}{k_{21}}$, can be measured. The rate of disappearance of the monomers is controlled by the reactivity ratios. They are also an indication as to how the monomer will be distributed throughout the chain [1, 27].

As seen in the previous section, active centres are formed between the transition metal components and the cocatalyst. During this reaction, the reduction of the transition metal takes place. Usually the supported catalysts $TiCl_4/MgCl_2$ consists of Ti_4^+. When the catalyst reacts with the AlR_3 some of the Ti_4^+ is reduced to Ti_2^+ and Ti_3^+. Due to this, Ziegler-Natta catalysts consist of many different active sites. These different active sites have different reactivity ratios and therefore produce copolymer molecules with different compositions and molecular weights. This causes copolymers produced with Ziegler-Natta catalyst to have a heterogeneous composition and a broad molecular weight distribution [3].

When considering the incorporation of α-olefins in ethylene, it must be taken into account that the biggest amount of comonomer will be inserted at the less sterically hindered active centres. The catalysts usually used for LLDPE have a very uniform distribution of active centres and the active centres is relatively unhindered [28].

The catalyst must also be able to copolymerise ethylene with the α-olefin. Ethylene has a very high reactivity; therefore, a high concentration of α-olefin is needed for copolymers with only about 4 mole% of α-olefin. The reactivity of the α-olefin in the copolymerisation depends on the catalyst type, and shape and size of the alkyl groups that are attached to the double bonds [3]. We know that LLDPE can be produced by Ti- or Cr-based catalysts. One of the differences between these two types of catalysts is that Ti-based catalysts produce polymers with a narrower molecular weight distribution than those produced with Cr-based catalysts.

Ziegler-Natta catalysts are usually supported (see Section 2.2.3). The most common use of support is $MgCl_2$. There are many reasons for this:

- It is inert to the chemicals that are used for polymerisation and it can be left in the final product, without influencing the properties
- It has a desirable morphology
- The crystalline form is the same as $TiCl_3$, because of the feature it can also incorporate $TiCl_4$
- It has a lower electron negativity than other metal halides. This will help to increase the productivity of the catalysts.
- It also enhances chain-transfer reactions, this can be seen in the fact that the number average molecular weight decreases with an increase in the Mg/Ti ratio. This leads to a narrower molecular weight distribution [18].

Polymerisation with transition metals uses the coordinated anionic mechanism. This occurs at low pressure and temperature. As mentioned above, propagation is through the monomer coordination and insertion into the metal-carbon bond [29]. The control of molecular weight distribution is very important when choosing a catalyst for ethylene/α-olefin copolymerisation [3]. Reaction temperature is very important w.r.t the control of molecular weight and the catalyst activity in Cr-based catalysts. It was found that the molecular weight increases up to a point as the reaction temperature is increased, where after it starts to decrease [18]. The molecular weight of the polymer can be controlled by altering the concentration of a chain-transfer agent and by the temperature of the reaction. Usually hydrogen is used as a chain-transfer agent [29]. There are a number of ways in which chain-transfer can occur. For Ziegler-Natta catalysts there are four types of chain-transfer: Chain-transfer to monomer, chain-transfer to hydrogen, chain transfer to aluminium and spontaneous transfer [28].

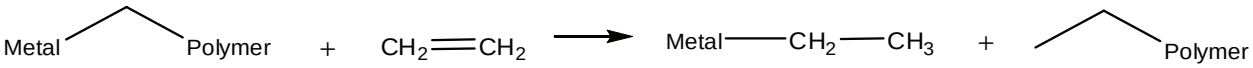

a) Transfer to monomer

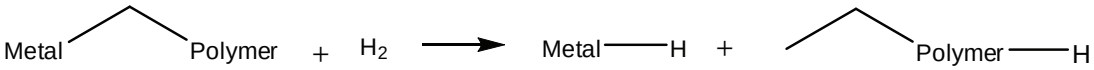

b) Transfer to Hydrogen

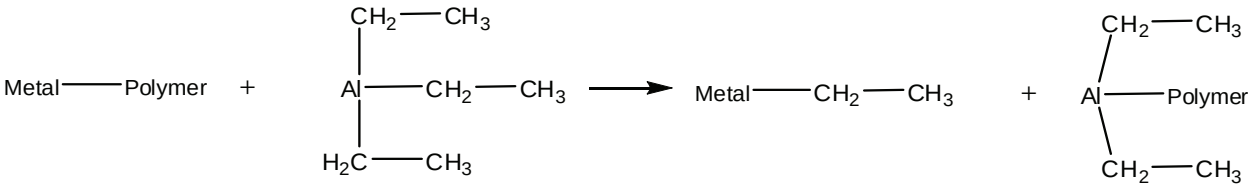

c) Transfer to Aluminium

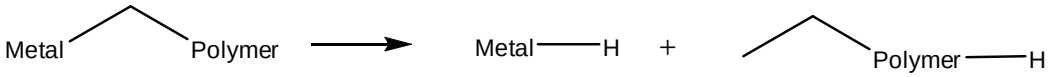

d) Spontaneous transfer

Figure 2.3 Four types of chain transfers in Ziegler-Natta catalysts [28]

The ratio of Al/Ti is also very important in controlling the molecular weight. When large amounts of unreacted $TiCl_4$ is present, it leads to a low molecular weight polymer [30].

It has also been found that the morphology of the polymer particle is influenced by the morphology of the supported catalyst, when it is supported on $MgCl_2$, the polymer particle will be of the same size and shape of the $MgCl_2$. This fact should also be taken into account when preparing a catalyst system [18].

2.2.2 Stereoregulation of α-olefin polymerisation

Natta discovered that the α–olefins polymerised with heterogeneous transition metal based catalysts are highly crystalline. They discovered the crystallinity is due to stereoregularity. During polymerisation, the monomer units are linked to each other in a certain order. This order is dependant on the catalyst and the conditions of the polymerisation [17].

Ziegler–Natta catalysts provide stereochemical control of the polymerisation. Polymers with a specific steric structure can be produced by choosing the right combination of catalyst and cocatalyst. The way in which the monomer complexes to the transition metal determines the stereochemical structure of the polymer [15]. The type of stereoregularity depends on the position of the R group attached to the polymer backbone [17].

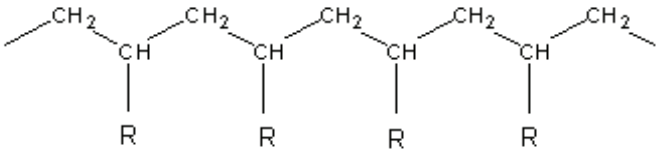

Figure 2.4 Illustration of the position of the R-group

When the monomer coordinates with the active centre of a prochiral olefin, it can give rise to either *si* or *re* coordination [15]. If there is no pattern in how the R groups are arranged the polymer is atactic or stereo-irregular [17]. This means that monomer coordinated randomly in the *si* and *re* coordination [15]. If all the R groups lie on the same side of the plane, the polymer is isotactic. When the R groups alternate between the above and below the plane, the polymer is syndiotactic [17].

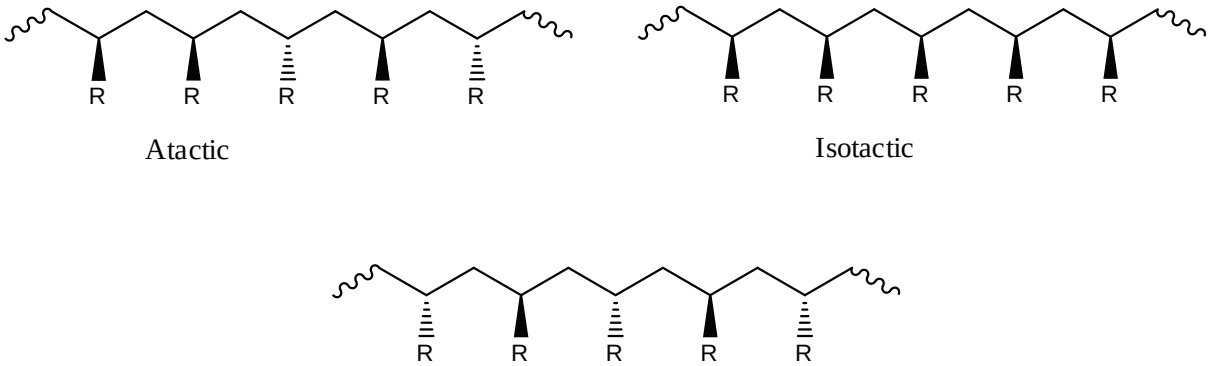

Figure 2.5 Different types of stereoregularity

There are two different ways in which the insertion of the monomer can take place.

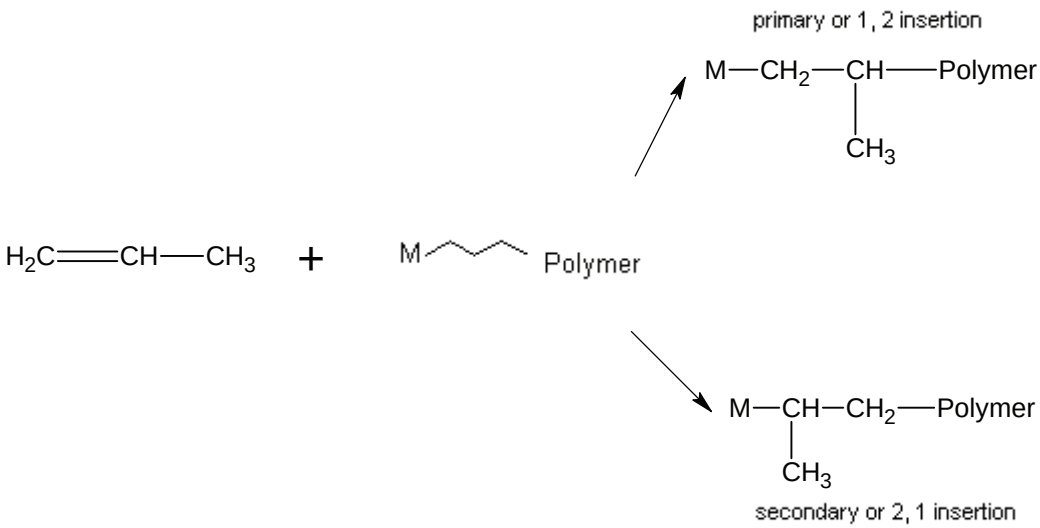

Figure 2.6 Two insertion ways of an α – olefin into the metal-carbon bond [24]

Stereoregulation can occur either through catalytic site control, also known as enantiomorphic site control, or through chain end control.

In stereoregulation due to the chain end control, the stereoselection is determined by the chirality of the last unit. This happens in homogeneous catalysts where the asymmetry of the active centre is not present [15, 24]. The steric interactions between the side groups of the monomers determines the way in which the next monomer is inserted [15].

Stereoregulation through catalytic site control usually occurs in heterogeneous catalyst systems. The initiating site is asymmetric and this causes the monomer to add always in the *re* or always in the *si* coordination. Therefore isotactic chains are formed [15, 24].

2.2.3 Physical state of the catalyst

The physical state of the catalyst is very important. The state of the catalyst can determine the morphology, stereoregularity, copolymer composition and microstructure of the polymer. It also influences the efficiency of the catalyst [23].

Ziegler–Natta catalysts are commonly classified according to the solubility of the transition metal components in the polymerisation medium. This was because inert hydrocarbon solvents were used to carry out polymerisation reactions with Ziegler–Natta catalysts [31].

Ziegler–Natta catalysts can be classified in three groups:

Homogeneous or soluble catalysts

The catalyst, including the cocatalyst and products of the reaction between the catalyst and cocatalyst, are soluble in the reaction solvent. Metallocene catalysts belongs to this group [17, 31].

Colloidal catalysts

The catalyst, which includes the transition metal compound, is soluble in the reaction solvent, but the reaction of the transition metal with the cocatalyst forms insoluble products [17].

Heterogeneous catalysts

The catalyst and the products of the reaction of the transition metal with the cocatalyst, is insoluble in the reaction solvent. This includes the supported Ziegler–Natta catalysts.

In the beginning, the catalysts were used without support, however there the introduction of supports increased the productivity of the catalyst and there was an improvement in the quality of the polymer. The supports used most frequently are $MgCl_2$ or silica [17].

These types of catalyst were very efficient for ethylene polymerisation. What happens with a supported catalyst is that the support acts as a high surface carrier. The transition metal salt can be fixed, chemically and/or physically, unto the surface of the support. The metal ions can become active centres, because they remain isolated [31].

2.3 Properties of polyethylene

2.3.1 Crystallinity

Polymers are either amorphous or semi–crystalline. Amorphous polymers do not have any crystalline regions; they just consist of randomly coiled chains. If the appropriate conditions of stress, pressure and temperature are achieved in semi–crystalline polymers, chains or part of the chains will conform in a specific order [32]. When the melting point of the polymer is reached, the crystalline areas will melt and will be in the same state as the amorphous parts of the polymer. When the polymer is then cooled to below its melting point, a semi – crystalline matrix will be formed [33]. The arrangement of the chains is complex because of the character of a polymer and the fact that there are crystalline and amorphous parts in the polymer. Studies through x–ray diffraction revealed the crystalline and amorphous components. The polymeric chain is in both crystalline and amorphous regions, because the crystalline micelle is smaller than the long–chain molecules [32]. The x-ray diffraction of low density polyethylene shows many sharp diffraction rings. This indicates that the molecules, or parts of the material, are arranged in a three-dimensional pattern. This suggests that the

chains are packed in an orderly fashion. The x-ray diffraction also shows diffused scattering patterns. This suggests that some parts of the material are amorphous [34]. It has been found for polyethylene that crystalline growth takes place in two steps. In the first step, folded chain crystals are formed and in the second step, the crystallite will thicken even more due to elevated temperature and pressure [32]. Studies have suggested that that the crystalline regions extend only a few hundred Ångström units in the chain direction, but through distortion and branching, they extend for much greater distances in the lateral direction. Polymer molecules consist of thousands of carbon atoms and therefore, taking into account the length in Ångströms in the chain direction, it suggests chains must be closely folded upon themselves during crystallisation. It is very unlikely that very branched or long molecules will be able to untangle themselves in a melted state and therefore it is suggested that one molecule participates in many crystalline regions and that crystalline regions are composed of pieces of a number of different molecules. The amorphous phase is comprised of those parts of the molecules that link the crystalline regions together. The linking of the amorphous and crystalline parts occurs in the following way: small pieces of neighbouring chains pack together straight and parallel and this form crystal nuclei. These nuclei then mainly grow through accumulation from pieces of other chains. The growth occurs as far as the molecular entanglement allows. The quoted size of a few hundred Ångström units in the chain direction usually represents the limit set by the first entanglement. Even in unbranched polymers, crystallisation is never complete. When more than one piece of a molecule is included in different crystalline regions, the intermediate pieces will not be crystallised [34].

In 1957, it was discovered that polyethylene could be crystallised in fine lamellae from a dilute solution. Crystallisation can either take place in bulk or solution. As mentioned before, when polymers are crystallised from solution the morphology is lamellarlike. The crystals have lozenge–shaped lateral lamellar conformation. The crystals are usually truncated which means the shorter faces are {100} and the longer faces are {110}. At low temperatures true lozenge lamella are formed and when concentration of the solution or the temperature are increased, mostly {100} face lamella are present. Due to the structure, molecular weight, concentration and temperature of the polymer, the shape of the lamella can be irregular.

When polymers are crystallised in the bulk the morphology of the crystallites are also lamellarlike. The crystallite and its surroundings consist of three regions: the crystalline region, here the structure is ordered, the interfacial region and the amorphous region. The amorphous region is not ordered and contains interconnections, which connect the crystallites, and this region is usually structurally isotropic. The interconnection can take place either by a chain connecting the two lamella directly or by entangling with chains from the other lamella [32].

The use of diffracted x-ray beams gave information on how polyethylene molecules are configured and the arrangement of them in the crystalline region. It was found that the CH_2 chains are packed together in the same manner as the crystal structure of normal paraffin hydrocarbons. The carbon atoms of each chain are linked together in the form of a zigzag plane. When the chains are packed side-to-side, their long axes are parallel, but the zigzag planes are not all parallel. Walter and Reding found that the lattice dimensions in the crystalline regions vary a little in different specimens. As the degree of branching increases, the unit cell expands a little. The notion of branching is to increase the amorphous material, but it seems that at the same time the crystal lattice expands. This means one of two things, either the small crystalline regions, which consists of unbranched chain segments, suffer very large strains that originate at the boundaries where branch points bring the regular structure to an end, or that in spite of major distortion, the crystal lattice can accommodate a limited number of branch points. Sometimes different crystal diffractions can be seen with x-ray diffraction. This is a second type of crystal structure where the CH_2 chains are packed in a different way than in the first type. Till [35], Keller [36] and Fischer [37] found with high density polyethylene that the thickness of the growth layers was only 100 Ångström, which suggest that each molecule is folded many times. It was concluded that the long-chain molecules was folded at more or less regular intervals, indicated by uniformity of the layer thickness.

Thick materials of polyethylene are usually opaque. The opacity is due to the scattering of light, which cannot be caused by the individual crystalline regions, which are too small. This light scattering is due to larger structural units [34].

When polymers are crystallised from the melt, spherulites can be observed. They are spherical symmetrical birefringent structures and when observed under an optical microscope, it displays a dark Maltese cross [32]. Spherulites form through the outwards growth from nucleation points and this growth comes to an end when neighbouring spherulites meet. The centres of the spherulites appear often sheaf-like. This suggests that a spherulite originates in a single-crystal and first grows into a rod-like form, due to distortion and branching, it spreads apart at the ends soon and a complete radial structure is formed. The growth in the directions at a right angle to the chain axes appears to be the fastest crystal growth. This can be explained as follows. The formation of crystal nuclei occurs where chains happen to lay more or less parallel. Growth can then occur either along the length of the chain through progressive straightening or tangential by the accumulation of pieces of other molecules. Growth along the length of the chain through progressive straightening is very difficult because the molecules in the crystal become entangled in any

direction, where growth in the tangential direction only needs the straightening re-orientation of neighbouring chains.

Spherulite size influences the mechanical properties of polyethylene to some degree. For example, when the material is rapidly cooled, the spherulite size is reduced, and the material is more flexible than a slow-cooled material. However, the spherulite size is not the only variable that affects the material, it is just one of many [34]. The loose fibrillar nonbanded type and the close packed, banded ring type, are the two main type of spherulites found. The texture of the spherulites depends on the chemical structure, crystallisation conditions and the molecular weight of the polymer. For example, when the polymer is relatively slow crystallised the ring spacing will be large, the Maltese cross will be distorted, and when looking at copolymers of ethylene, the flat lamella crystallites changes with the incorporation of a co–unit [32].

2.3.2 Branching

Linear low density polyethylene produced by Ziegler-Natta catalysts have a heterogeneous composition. Some of the molecules contain a large number of α-olefin units, while others have very few and can be seen as linear ethylene homopolymers [3]. Ziegler-Natta catalysts contains a range of active centres with different activity and this causes the heterogeneity in the chemical composition distribution [38, 39]. Branching in polyethylene can be in the form of long-chain branching or short-chain branching. Chain transfer reactions during free-radical polymerisation could result in both long and short chain branching, while copolymerisation with α-olefins causes regular length short branches, with the length of the branches determined by the size of the α-olefin [40]. Branches of polyethylene are terminated by either methyl or vinyl groups. Vinyl groups are only present in small amounts, therefore the number of methyl groups is representative of the number of branches [34]. Heterogeneity in linear low density polyethylene consists of two kinds: intramolecular, which state that all the molecules have the same short-chain branching, but that the distribution within one molecule is not uniform along the chain backbone, or it can be intermolecular, which means that among the molecules the short-chain branching distribution is not uniform, some molecules have more branching than others [41]. The properties of linear low density polyethylene are influenced by the amount of comonomer and the distribution of the comonomer in the polymer chain. When the comonomer is uniformly distributed throughout the polymer chain, the chemical composition is said to be narrow and when the chemical composition distribution is broad, the amount of comonomer is a function of the chain length [38]. Long-chain branching, which occurs in LDPE, influences largely the solution viscosity and melt

viscosity of the polymer, while short-chain branching mainly affects the melting point, density, hardness, chemical resistance, rigidity and so forth [42]. Many studies have been done to prove that short-chain branching influences the mechanical, physical and thermal properties of linear low density polyethylene [42-46]. It was found that the effect of molecular weight on crystallisation and melting is very small and that branching plays the biggest role [46]. By increasing the number of short-chain branches, the crystallinity and density of the polymer can be reduced. This is because the side chains do not crystallise and they are discarded into the interfacial or amorphous areas [45]. Longer short-chain branches inhibit the molecular chain folding of the polyethylene molecule into a growing crystal lamella. This increases the number of tie-molecules, which gives a stronger product [1]. It is also viewed that each branch point and chain end disrupts the ordering during crystallisation and therefore decreases the degree of crystallinity [40]. It was shown that with ethylene copolymers, that polymer will be more stable in solution, the shorter the ethylene sequence is between the branches. As the comonomer content increases the length of the ethylene sequences in between decreases, because of this the copolymer chains with more short-chain branching will crystallise at lower temperatures and will form thinner lamellae and fewer perfect crystallites [47].

2.3.3 Molecular weight

The properties of the polymer can be influenced in a great way by the molecular weight of the polymer. It is complicated to calculate the molecular weights of polymers due to the fact that all the chains in a polymer molecule is not all the same length [48]. To provide detailed information on the molecular weight distribution, weighted–average molecular weight (M_w) and number–average molecular weight (M_n) are used. The polydispersity is given by the ratio M_w/ M_n and this represents the width of the molecular weight distribution [3, 34]. The number-average molecular weight is the weight of the molecules divided by the number of molecules in the polymer:

$$\overline{Mn} = \frac{\sum M_i n_i}{\sum n_i}$$

M_i Is the molecular weight of molecules with a certain size i and the number of that size is n_i.

The weighted-average molecular weight is calculated as follow:

$$\overline{Mw} = \frac{\sum M_i w_i}{\sum w_i}$$

The total weight of molecules with a size i is given by w_i.

For a heterogeneous polymer the two types of molecular weight will not be the same, because the small molecules will have a large effect on reducing the number-average weight and the large molecules will have a great effect on the weighted-average molecular weight [34].

As mentioned before, molecular weight can influence the properties of the polymer. Sometimes above a critical molecular weight, the crystallinity decreases as the molecular weight increases. This is due to the fact that the longer chains cannot be incorporated into the crystalline structure [45].

2.3.4 Melting

Polyethylene melts over a wide temperature range and not at a sharply defined temperature [34, 49]. Crystallinity, polydispersity, molecular weight, morphology and structural irregularities all influence the melting temperature range [49]. The crystalline areas melt as the temperature rises and the amount of amorphous material increases. The two-phase structure of polyethylene causes this melt pattern. Movement in the amorphous areas is freer and the rise of temperature makes some of the strained molecules on the crystalline boundaries move into the amorphous areas. The small crystals will also melt before the larger crystals [34].

The melting of polymers is a first-order transition. The transformation temperature in a first-order phase transition and is independent of the concentration of the phase if melting takes place under constant pressure [49]. The melting point of a polymer is given by the following equation:

$$T_m = \frac{\Delta H}{\Delta S}$$

Where ΔH is the enthalpy of fusion, or the heat of crystallisation, and ΔS is the entropy of fusion, or the change of entropy [34, 49]. The range of the melting point is due to the variation in the entropy, if it is assumed that ΔH is the same for each unit. The distribution of the molecular weight does not influence the melting point that much, except if there are many small molecules with a molecular weight less than 1 500 g/mol. In low density polyethylene, the branches will have the same effect as low molecular weight material on the melting behaviour of the polymer. Flory's theory on the melting point of copolymers explains it [34].

According to this theory, the melting point decreases with an increase in the α-olefin content in compositionally uniform ethylene copolymer. This is given by Flory's equation:

$$\frac{1}{T_m} - \frac{1}{T_m^\circ} = -\frac{R}{\Delta H_u} \cdot \ln p$$

where T_m° is the melting point of the linear polyethylene in Kelvin, T_m is the melting point of the copolymer in Kelvin, ΔH_u is the heat of fusion per crystallised ethylene unit and p is the probability of ethylene-ethylene linking in a copolymer chain [3, 49]. The value of p is calculated by:

$$p = \frac{r_1 F}{1 + r_1 F}$$

where $r_1 F$ is a function of the reactivity ratio product, $r_1 r_2$, and the copolymer composition ration, f [3]. Experiments have shown that the short-chain branching in linear low density polyethylene is responsible for the unique melting of these polymers [39, 50].

Three areas of chain relaxation were established for polyethylene, through dynamic mechanical analysis.

The α-relaxation is associated with reorientation of the amorphous regions in the lamella. The position and the intensity of this peak depends on the thickness of the crystalline lamellae and the higher the content of copolymer, the smaller the relaxation peak.

The β-relaxation is associated with movement of large chain fragments in the amorphous regions. This peak increases as the α-olefin content increases, because then the amorphous region will increase.

The γ-relaxation is attributed to the crankshaft motion of the short amorphous chain fragments [3].

2.4 Characterization of polyolefins through fractionation

Linear low density polyethylene is a copolymer consisting of ethylene and a α–olefin. The properties of the polymer is affected by the molecular weight, molecular weight distribution, the amount of comonomer and the composition of the copolymer [3].

2.4.1 Temperature rising elution fractionation (TREF)

The introduction of comonomers like butene and hexene, in a polyethylene chain, influences the crystallinity. The comonomers are however not uniformly distributed. In the production of linear low density polyethylene, multiple-site-type Ziegler–Natta catalysts are used. This influences the chemical composition distribution of the polymer. The chemical composition

distribution of these polymers is usually bimodal in nature [51]. In ethylene copolymers, the content of the short chain branches determines the crystallinity of the polymer. The determination of the short chain branching distribution (SCBD) is very important, because both the SCBD and the molecular weight distribution influence the polymer properties. The SCBD also provides information on the nature of the catalyst as well as the polymerisation mechanism [52]. Short chain branching diminishes the crystallinity and this leads to lower density and dissolution temperature [53].

Temperature rising elution fractionation (TREF) is an analytical technique which separates semi – crystalline polymers according to their difference in molecular structure or composition [53, 54].

Desreux and Spiegels [55] first describe the fractionation of polyethylene according to composition in 1950 and Shiriyama *et al.* [56] first named the technique TREF. The development of analytical TREF by Wild *et al*. in the 1970s established this technique in the polyolefin industry [51, 57].

TREF can only fractionate semi – crystalline polymers and not amorphous polymers. TREF works on the bases that different molecular structures will have distinct crystallinities and these different crystallinities will have different dissolution temperatures. TREF makes use of the different dissolution temperatures, which will give information about the crystallinity and this in turn will say something about the molecular structure [58]. The higher the degree of crystallinity, the higher the dissolution temperature will be [48].

TREF can be divided in two steps, precipitation and elution. In preparation for the first step, the polymer is dissolved in a suitable solvent at a high temperature. The dissolved polymer is then mixed with an inert support material. The solution is then slow cooled and then fractionates according to crystallinity. As the temperature drops, the layers will deposit in order of decreasing crystallinity (increasing in branching) on to the support. The fraction that is the most crystalline will deposit first on o the support and the least crystalline fraction will deposit last. In the second step, the polymer/support mixture is packed into a column and eluted with a solvent at steadily increasing temperature. The fractions elute in reverse order to that of crystallisation on to the support. As the temperature increases, the solvent dissolves the fractions with increasing crystallinity (decreasing in branching). The fraction with the least crystallinity elutes first and the fraction which is the most crystalline will elute last [3, 48, 51-54, 57-59]. The most common solvents used are xylene, trichlorobenzene, *o* – dichlorobenzene or α – chloronaphthalene [51, 58].

There are two ways to operate TREF, analytical and preparative TREF [57, 58, 60].

Analytical TREF is usually automated and connected to other analytical instruments. The fractions are collected frequently while the temperature is increasing and then monitored by

an on-line detector. The structure of the fractions is determined by using a calibration curve. The columns and the sample size of analytical TREF is smaller than those employed in preparative TREF. The technique is faster than preparative TREF, but less information about the polymer microstructure can be obtained than is the case with preparative TREF [52, 54, 57, 58, 61].

In preparative TREF the sample is fractionated into a number of fractions, according to predetermined temperatures. These fractions are collected at relevant temperature intervals and are analyzed off-line [52-54, 58, 61].

Desreux and Spiegels [55] was the first to carry out a preparative fractionation of polyethylene. They established that the separation was depended on crystallinity and not so much molecular weight. Wijga, Van Schooten and Boerma [62] made some refinements to the procedure. They designed a system for the gradient elution fractionation of polypropylene. Their column was made of glass. They dissolved 1g of polypropylene in 50 ml of kerosene solvent at 135 °C and loaded it into the column packed with ground firebrick. The solution was then allowed to cool down to room temperature. The elution process was divided into many steps and it took place between 30 °C and 150 °C. Shirayama, Okada and Kita described a system for the fractionation of low density polyethylene. They dissolved 4 g of polymer in hot xylene and slow–cooled it on to 1 400 g sea sand as support material. The cooled mixture was then placed in a 7 x 38 cm column. Elution took place between 50 °C and 80 °C. A temperature controlled oil–bath was used to give constant temperature [57].

In the earlier studies no attention was paid to the cooling rate of the polymer solution, but in all the later studies the polymer solution was slow cooled. The general view was that a controlled cooling step was necessary to get reproducible separation of the polymer. Wild and Ryle concluded in their studies that to get optimum separation the cooling rate must at minimum be 2 K/hour. Under these conditions a linear relationship could be seen between the degree of short chain branching and separation temperatures for many polyethylenes [57].

Both analytical and preparative TREF have been and still are being used by numerous researchers to fractionate polymers according to their short-chain distribution to obtain more information on how the short-chain branching distribution affects the polymer properties [38-41, 43, 44, 46, 50, 63-66].

2.4.2 Crystallisation analysis fractionation (CRYSTAF)

This analytical technique investigates the chemical composition distribution of semi-crystalline polymers. CRYSTAF and TREF are based on the same fractionation principles

and the result of these two techniques are usually comparable [51, 54, 61, 67-69]. CRYSTAF was first reported by Monrabel in 1991 [70].

The difference between the two techniques is that CRYSTAF is less time consuming. TREF consists out of a crystallisation and elution step, whereas CRYSTAF only consists of a crystallisation step [54, 61, 67]. Other advantages of CRYSTAF over TREF is the fact that CRYSTAF uses less solvent for analysis and in CRYSTAF no support is needed. The fact that there is no elution step avoids the effect of peak broadening, which is sometimes caused by the non-ideal environment of the column and the support [54, 68].

The crystallisation step takes place in solution during constant cooling and the concentration of the polymer in solution is examined as a function of the crystallisation temperature [67, 68]. This gives a cumulative concentration profile and when the derivative of the cumulative profile is taken, the amount of polymer crystallised at each temperature can be obtained [61, 67-69].

CRYSTAF works on the same basis as TREF; the first data points in CRYSTAF are taken at temperatures above crystallisation. Then as the temperature decreases the fractions with the highest crystallinity, less branching, will precipitate out. When this happens, a sharp drop in the solution concentration can be seen on the cumulative plot. As the temperature drops, the fractions precipitate out with decreasing crystallinity and thus increasing branch content. The last data point, at the lowest temperature, corresponds to the amorphous fraction which is still in solution [51, 61, 69].

The commercial CRYSTAF mostly in use is the one developed by Polymer Char, Spain. It contains five stirred steel vessels in which the crystallisation takes place. These vessels are placed inside an oven in which the temperature can be controlled [51, 54, 61, 67-69]. Trichlorobenzene (TCB) is usually the preferred solvent to dissolved the samples in the vessels [51, 61, 67, 69], but other solvents like *o*-dichlorobenzene (ODCB), perchloroethylene and α-chloronaphthalene can also be used [51, 68, 69]. ODCB is preferred because of the fact that it has a freezing point of -17.5 °C, which is lower than that of TCB. This is useful when fractionation must occur at low temperatures [68].

The fact that 5 steel vessels are used, gives CRYSTAF an advantage over TREF in the fact that up to 5 samples can be analyzed simultaneously [51, 67, 68].

The sample size used is usually between 0.03-0.01%, this means that about 10-30 mg of sample is placed inside a reactor with 30 ml of solvent [51].

Some molecular structures and operating conditions, have an effect on CRYSTAF.

- The effect of number average molecular weight

It was found that below a certain number average molecular weight the crystallisation temperature decreases. However, the crystallisation temperature is independent of molecular

weight when the molecular weight is high. It ha also been shown that with polyethylene with decreasing molecular weight the CRYSTAF profile broadens. This is because with higher molecular weight, the crystallisation temperature becomes independent of the chain length and all the chains more or less crystallise at the same temperature. With lower molecular weight, the length of the short chains influences the crystallisation temperature and the profile broadens. This means that when samples with low molecular weight are analyzed, the CRYSTAF peak temperatures are affected. If the sample contains some very low molecular weight material, the estimated chemical composition distribution might be broader than the real chemical composition distribution [61, 69].

- The effect of comonomer content

The CRYSTAF profiles becomes broader with an increase in the comonomer content [61, 69].

- The effect of cooling rate

A slower cooling rate will shift the CRYSTAF profiles to a higher temperature [61].

- The effect of co-crystallisation

When a blend of polymers has different crystallisabilities, there is minimal to no co-crystallisation. If the two polymers do have the same crystallisabilities, the effect can be significant [61]. The two factors that regulates the co-crystallisation is the match of the chain crystallisabilities and the cooling rate [69].

If we look at CRYSTAF vs. TREF, there are some differences. As mentioned before, CRYSTAF is less time-consuming. Analytical TREF also has a continuous elution signal, whereas CRYSTAF has discontinuous sampling. There are also temperature differences between the two profiles analyzing the same sample. This is due to the undercooling/supercooling effect of CRYSTAF. This happens because CRYSTAF is measured during the crystallisation step, whereas TREF is measured during the melting step [51, 68].

2.5 References

1. Doak, K.W., *Ethylene Polymers*, in *Encyclopedia of Polymer Science and Engineering*, J.I. Kroschwitz, Editor. 1985, John Wiley & Sons: New York. p. 383-436.
2. Seymour, R.B., *General Purpose Thermoplastics*, in *Polymeric Composites*, R.B. Seymour, Editor. 1990. p. 120-136.

3. Krentsel, B.A., Y.V. Kissin, V.J. Kleiner, and L.L. Stotskaya, *Copolymers of Ethylene and Higher a-Olefins*, in *Polymers and Copolymers of Higher a-Olefins*. 1997, Hanser Publishers: Munich. p. 243-335.
4. Shanks, R.A. and G. Amarasinghe, *Crystallisation of blends of LLDPE with branched VLDPE.* Polymer, 2000. **41**: p. 4579-4587.
5. Seymour, R.B., *History of polyolefins*, in *Handbook of polyolefins*, C. Vasile and R.B. Seymour, Editors. 1993, Marcel Dekker: New York. p. 1-7.
6. Von Pechmann, H., *Ueber Diazomethan und Nitrosoacylamine.* Chemische Berichte, 1898. **31**: p. 2640-2646.
7. Bamberger, E. and F. Tschirner, *Ueber die Einwirkung von Diazomethan auf B-Arylhydroxylamine.* Chemische Berichte, 1900. **33**(1): p. 955-959.
8. Arnold, H.R. and E.C. Herrick, in *US Patent 2726218*. 1955: United States of America.
9. Swallow, J.C., *The History of Polythene*, in *Polythene: The technology and uses of ethylene polymers*, Renfrew and Morgan, Editors. 1960, Illffe & Sons Ltd.: London. p. 1-10.
10. Raff, R.A.V. and E. Lyle, *Historical Developements*, in *Crystalline Olefin Polymers Part 1*, R.A.V. Raff and K.W. Doak, Editors. 1965, John Wiley & Sons: New York.
11. Joo, Y.L., O.H. Han, H.-K. Lee, and J.K. Song, *Characterization of ultra high molecular weight polyethyelene nascent reactor powders by X-ray diffraction and solid state NMR.* Polymer, 2000. **41**.
12. Coughlan, J.J. and D.P. Hug, *Ethylene Polymers*, in *Encyclopedia of Polymer Science and Engineering*, J.I. Kroschwitz, Editor. 1985, John Wiley & Sons: New York. p. 490-494.
13. Resconi, L., U. Giannini, and T. Dall'Occo, *MAO-free Metallocene Catalysts for Ethylene (Co)Polymerization*, in *Metallocene-Based Polyolefins: Preparation, Properties and Technology*, J. Scheirs and W. Kaminsky, Editors. 2000, John Wiley & Sons Ltd.: Chichester. p. 69-102.
14. Akimoto, A. and A. Yano, *New Developements in the Production of Metallocene LLDPE by High-Pressure Polymerization*, in *Metallocene-Based Polyolefins: Preparation, Properties and Technology*, J. Scheirs and W. Kaminsky, Editors. 2000, John Wiley & Sons Ltd.: Chichester. p. 287-308.
15. Huang, J. and G.L. Rempel, *Ziegler-Natta Catalysts for Olefin Polymerizations: Mechanistic Insights from Metallocene Systems.* Progress in Polymer Science, 1995. **20**: p. 459-526.

16. Imanishi, Y. and N. Naga, *Recent developements in olefin polymerizations with transition metal catalysts.* Progress in Polymer Science, 2001. **26**: p. 1147-1198.
17. Krentsel, B.A., Y.V. Kissin, V.J. Kleiner, and L.L. Stotskaya, *Brief Review of the Principles of Olefin Polymerization*, in *Polymers and Copolymers of Higher a-Olefins*. 1997, Hanser Publishers: Munich. p. 1-21.
18. Xie, T., K.B. McAuley, J.C.C. Hsu, and D.W. Bacon, *Gas Phase Ethylene Polymerization: Production Processes, Polymer Properties, and Reactor Modeling.* Industrial and Engineering Chemistry Research, 1994. **33**: p. 449-479.
19. Kaminsky, W. and A. Laban, *Metallocene catalysis.* Applied Catalysis A: General, 2001. **222**: p. 47-61.
20. Simpson, D.A. and G.A. Vaughan, *Ethylene Polymers, LLDPE*, in *Polymer Science and Technology*, J.I. Kroschwitz, Editor. 2003, John Wiley & Sons: Hoboken. p. 441-482.
21. Benham, E. and M. McDaniel, *Ethylene Polymers, HDPE*, in *Polymer Science and Technology*, J.I. Kroschwitz, Editor. 2003, John Wiley & Sons: Hoboken. p. 382-412.
22. Soga, K. and T. Shiono, *Ziegler-Natta Catalysts for Olefin Polymerizations.* Progress in Polymer Science, 1997. **22**: p. 1503-1546.
23. Boor, J., *Ziegler-Natta Catalysts and Polymerizations*. 1979: Academic Press Inc.
24. Moore, E.P., *Polypropylene Handbook*. 1996, Munich: Hanser Publishers.
25. Mecking, S., *Olefin Polymerization by Late transition metal Complexes - A Root of Ziegler Catalysts Gains New Ground.* Aangewandte Chemie International Edition, 2001. **40**: p. 534-540.
26. Böhm, L.L., *The Ethylene Polymerization with Ziegler Catalysts: Fifty Years after the Discovery* Aangewandte Chemie International Edition, 2003. **42**: p. 5010-5030.
27. Maraschin, N., *Ethylene Polymers, LDPE*, in *Polymer Science and Technology*, J.I. Kroschwitz, Editor. 2003, John Wiley & Sons: Hoboken. p. 412-424.
28. Chadwick, J.C., *Ziegler-Natta Catalysts*, in *Polymer Science and Technology*, J.I. Kroschwitz, Editor. 2003, John Wiley & Sons: Hoboken. p. 517-536.
29. James, D.E., *Linear Low Density Polyethylene* in *Encyclopedia of Polymer Science and Engineering*, J.I. Kroschwitz, Editor. 1985, John Wiley & Sons: New York. p. 441-482.
30. Goppel, J.M. and R.N. Haward, *Manufacturing Processes: Ziegler Polymerization*, in *Polythene: The technology and uses of ethylene polymers*, Renfrew and Morgan, Editors. 1960, Iliffe and Sons Ltd.: London. p. 17-27.
31. Boor, J., *Initial Physical State of the Catalyst*, in *Ziegler - Natta Catalysts and Polymerizations*. 1979, Academic Press Inc. p. 154-167.

32. Fatou, J.G., *Morphology and Crystallization in Polyolefins*, in *Handbook of Polyolefins*, C. Vasile and R.B. Seymour, Editors. 1993, Marcel Dekker: New York. p. 155-227.
33. Giles, H.F.J., J.R.J. Wagner, and E. Mount, *Extrusion - The definitive Processing Guide & Handbook*. 2005: William Andrew Publishing/Plastic Design Library.
34. Bunn, C.W., *The Structure of Polythene*, in *Polythene: The technology and uses of ethylene polymers*, Renfrew and Morgan, Editors. 1960, Iliffe and Sons Ltd.: London. p. 87-130.
35. Till, P.H., *The growth of single crystals of linear polyethylene.* Journal of Polymer Science, 1957. **24**: p. 301-306.
36. Keller, A., *Single crystals in polymers: evidence of a folded-chain configuration.* Philosophical Magazine, 1957. **2**: p. 1171-1175.
37. Fischer, E.W., *Step and spiral crystal growth of high polymers.* Zeitschrift fuer Naturforschung, 1957. **12a**: p. 753-754.
38. Starck, P., *Studies of the Comonomer Distributions in Low Density Polyethylenes Using Temperature Rising Elution Fractionation and Stepwise Crystallization by DSC.* Polymer International, 1996. **40**: p. 111-122.
39. Usami, T., Y. Gotoh, and S. Takayama, *Generation Mechanism of Short-Chain Branching Distribution in Linear Low-Density Polyethylenes.* Macromolecules, 1986. **19**: p. 2722-2726.
40. Wild, L., T.R. Ryle, D.C. Knobeloch, and I.R. Peat, *Determination of Branching Distributions in Polyethylene and Ethylene Copolymers.* 1981: p. 441-455.
41. Kong, J., X. Fan, Y. Xie, and W. Qiao, *Study on Molecular Chain Heterogeneity of Linear Low-Density Polyethylene by Cross-Fractionation of Temperature Rising Elution Fractionation and Successive Self-Nucleation/Annealing Thermal Fractionation.* Journal of Applied Polymer Science, 2004. **94**: p. 1710-1718.
42. Shirayama, K., S.-I. Kita, and H. Watabe, *Effects of Branching on some Properties of Ethylene/ a-Olefin Copolymers.* Die Makromolekulare Chemie, 1972. **151**: p. 97-120.
43. Fazeli, N., H. Arabi, and S. Bolandi, *Effect of branching characteristics of ethylene/1-butene copolymers on melt flow index.* Polymer Testing, 2006. **25**: p. 28-33.
44. Gupta, P., G.L. Wilkes, A.M. Sukhadia, R.K. Krishnaswamy, M.J. Lamborn, S.M. Wharry, C.C. Tso, P.J. DesLauriers, T. Mansfield, and F.L. Beyer, *Does the length of the short chain branch affect the mechanical properties of linear low density polyethylenes? An investigation based on films of copolymers of ethylene/1-butene, ethylene/1-hexene and ethylene/1-octene synthesized by a single site metallocene catalyst.* Polymer, 2005. **46**: p. 8819-8837.

45. Shan, C.L.P., J.B.P. Soares, and A. Penlidis, *Mechanical properties of ethylene/1-hexene copolymers with tailored short chain branching distributions.* Polymer, 2002. **43**: p. 767-773.

46. Zhang, M., D.T. Lynch, and S.E. Wanke, *Effect of molecular structure distribution on melting and crystallization behavior of 1-butene/ethylene copolymers.* Polymer, 2001. **42**: p. 3067-3075.

47. Sarzotti, D.M., J.B.P. Soares, L.C. Simon, and L.J.D. Britto, *Analysis of the chemical composition distribution of ethylene/a-olefin copolymers by solution differential scanning calorimetry: an alternative technique to Crystaf.* Polymer, 2004. **24**: p. 4787-4799.

48. Mays, J.W. and A.D. Puckett, *Molecular Weight and Molecular Weight Distribution of Polyolefins*, in *Handbook of Polyolefins*, R.B. Seymour, Editor. 1993, Marcel Dekker: New York. p. 133-153.

49. Fatou, J.G., *Melting of Polyolefins*, in *Handbook of Polyolefins* C. Vasile and R.B. Seymour, Editors. 1993, Marcel Dekker: New York. p. 229-294.

50. Mirabella, F.M., J. Ford, and E.A. Ford, *Characterization of Linear Low-Density Polyethylene: Cross-Fractionation According to Copolymer Composition and Molecular Weight.* Journal of Polymer Science: Part B: Polymer Physics, 1987. **25**: p. 777-790.

51. Monrabel, B., *Temperature Rising Elution Fractionation and Crystallization Analysis Fractionation*, in *Encyclopedia of Analytical Chemistry*. 2000, John Wiley & Sons Ltd: Chichester. p. 0874-8084.

52. Xu, J. and L. Feng, *Application of temperature rising elution fractionation in polyolefins.* European Polymer Journal, 2000. **36**: p. 867-878.

53. Glöckner, G., *Temperature Rising Elution Fractionation: A review.* Journal of Applied Polymer Science: Applied Polymer Symposium, 1990. **45**: p. 1-24.

54. Fonseca, C.A. and I.R. Harrison, *Temperature Rising Elution Fractionation*, in *Modern Techniques for Polymer Characterisation*, R.A. Pethrick and J.V. Dawkins, Editors. 1999, John Wiley & Sons Ltd: Chichester. p. 1-13.

55. Desreux, V. and M.C. Spiegels, *Fractionation of polythene by extraction.* Bulletin des Societes Chimiques Belges, 1950. **59**: p. 476-789.

56. Shirayama, K., T. Okada, and S. Kita, *Distribution of short-chain branching in low density polyethylene.* Journal of Polymer Science, 1965. **3**: p. 907-916.

57. Wild, L., *Temperature Rising Elution Fractionation.* Advances in Polymer Science, 1990. **98**: p. 1-47.

58. Soares, J.B.P. and A.E. Hamielec, *Temperature rising elution fractionation of linear polyolefins.* Polymer, 1995. **36**: p. 1639-1654.
59. McHugh, M.A. and V.J. Krukonis, *Supercritical Fluid Extraction*. 1994, Elsevier. p. 201-205.
60. Feng, Y. and J.N. Hay, *The measurement of compositional heterogeneity in a polypropylene-ethylene block copolymer.* Polymer, 1998. **39**(26): p. 6723-6731.
61. Anantawaraskul, S., J.B.P. Soares, and P.M. Wood-Adams, *Fractionation of Semicrystalline Polymers by Crystallization Analysis Fractionation and Temperature Rising Elution Fractionation.* Advances in Polymer Science, 2005. **182**: p. 1-54.
62. Wijga, P.W., J. Van Schooten, and J. Boerma, *Fractionation of polypropylene.* Makromolekulare Chemie, 1960. **36**: p. 115-132.
63. Faldi, A. and J.B.P. Soares, *Characterization of the combined molecular weight and composition distribution of industrial ethylene/a-olefin copolymers.* Polymer, 2001. **42**: p. 3057-3066.
64. Gabriel, C. and D. Lilge, *Comparison of different methods for the investigation of the short-chain branching distribution of LLDPE.* Polymer, 2001. **42**: p. 297-303.
65. Mirabella, F.M., *Correlation of the Elution Behavior in Temperature Rising Elution Fractionation and Melting in the Solid-State and in the Presence of a Diluent of Polyethylene Copolymers.* Journal of Polymer Science: Part B: Polymer Physics, 2001. **39**: p. 2819-2832.
66. Wang, C., M.-C. Chu, T.-L. Lin, S.-M. Lai, H.-H. Shih, and J.-C. Yang, *Microstructures of a highly short-chain branched polyethylene.* Polymer, 2001. **42**: p. 1733-1741.
67. Anantawaraskul, S., J.B.P. Soares, and P.M. Wood-Adams, *Effect of Operation Paremeters on Temperature Rising Elution Fractionation and Crystallization Analysis Fractiontion.* Journal of Polymer Science: Part B: Polymer Physics, 2003. **41**: p. 1762-1778.
68. Britto, L.J.D., J.B.P. Soares, A. Penlidis, and B. Monrabal, *Polyolefin Analysis by Single-Step Crystallization Fractionation.* Journal of Polymer Science: Part B: Polymer Physics, 1999. **37**: p. 539-552.
69. Soares, J.B.P. and S. Anantawaraskul, *Crystallization Analysis Fractionation.* Journal of Polymer Science: Part B: Polymer Physics, 2005. **43**(1557-1570).
70. Monrabel, B., *Crystallization Analysis Fractionization*, in *United States Patent 5 2220390*. 1991: United States of America.

Chapter 3

Experimental Techniques

3.1 Materials

3.1.1 Polymer

Linear low-density polyethylene was obtained from Sasol Polymers. The grade was LM3040P, which is a copolymer of ethylene and 1-butene with a MFI of 30.

3.1.2 Stabilizer

A mixture of Irganox 1010 and Irgafos 168 (see
Figure 3.1 and 3.2) was used as thermal stabilizers during the TREF procedure to prevent degradation during the slow cooling stage. During the elution step of the TREF procedure, the elution solvent (xylene) was stabilized with 2,6-di-tert-butyl-4-methylphenol (BHT).

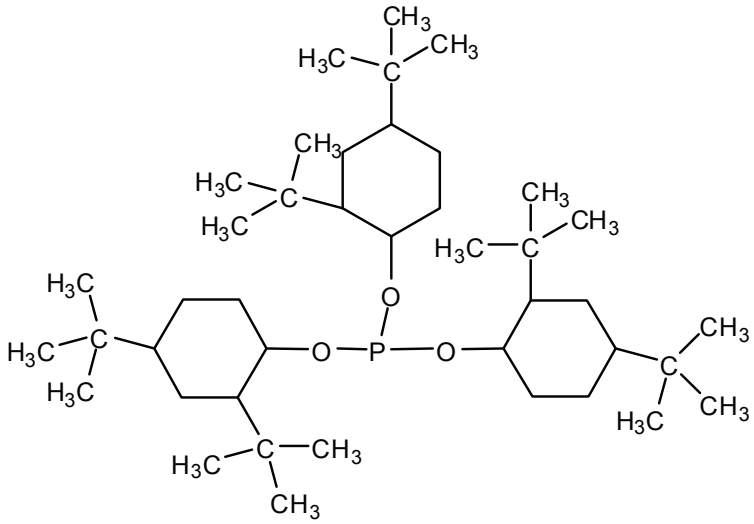

Tris (2, 4 - di - tert - butylphenyl)phosphite

Figure 3.1 Irgafos 168

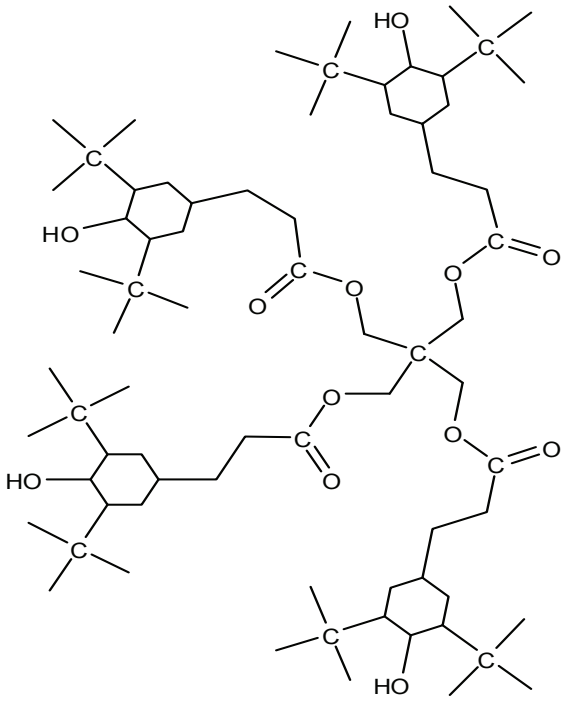

Figure 3.2 Irganox 1010

3.1.3 Solvent

In all the TREF experiments, xylene (Aldrich, 99% purity) was used as received.

3.2 Analytical techniques

3.2.1 Temperature rising elution fractionation (TREF)

This technique involves the fractionation of a semi-crystalline polymer according to crystallinity or short-chain branching.

For experimental purposes, TREF was divided into three steps:

1. Cooling

Typically 3 g polymer and 0.06 g stabilizer were dissolved at 130 °C in 300 mL of xylene in a glass reactor. The mixture was stirred throughout the solution process. Preheated sea sand (130 °C) was then added to the reactor. Enough sand was added to ensure that no polymer solution was visible above the level of the sand. The reactor was then placed in a preheated oil-bath (130 °C), and fitted with a condenser.

Typically, up to 4 reactors could be cooled in a single step.
The oil-bath was kept at 130 °C for 2 hours and then the solution was cooled from 130 °C to 20 °C at a rate of 1 °C/min.
The slow cooling rate is very important to ensure good separation according to crystallinity [1].

2. Elution

When the polymer solution has cooled down to 20 °C, the solution and the support (sea sand) is placed in steel column. The column had a length of 15 cm and an internal diameter of 7 cm. A schematic representation is shown in Figure 3.3.
The column has a temperature probe, which is inserted through the bottom. This allows for the temperature inside the column to be monitored. The solvent flows along the outside of the column in a coiled copper tube (6 mm diameter) before entering the column at the top (Figure 3.4). This allows the solvent temperature to reach the required temperature before being passed into the column [2]. To prevent channelling of the solvent, the solvent flow on entering and exiting the column is spread by the use of glass beads and glass wool. The loading of the column proceeds in the steps of glass beads, glass wool, sand/polymer solution mixture, and more glass wool.
The column was then placed into a modified GC oven (Varian Model 3700). The heating program of the GC oven was then used to program the heating of the column inside the oven. At predetermined temperature intervals, the column was flushed with solvent (300 mL at a flow rate of 40 mL/min) and these fractions were collected for polymer recovery. The flow rate was maintained by using a solvent pump (FML “Q” Pump, Model QG150). The xylene used for the elution step was stabilized with 0.0125% BHT.

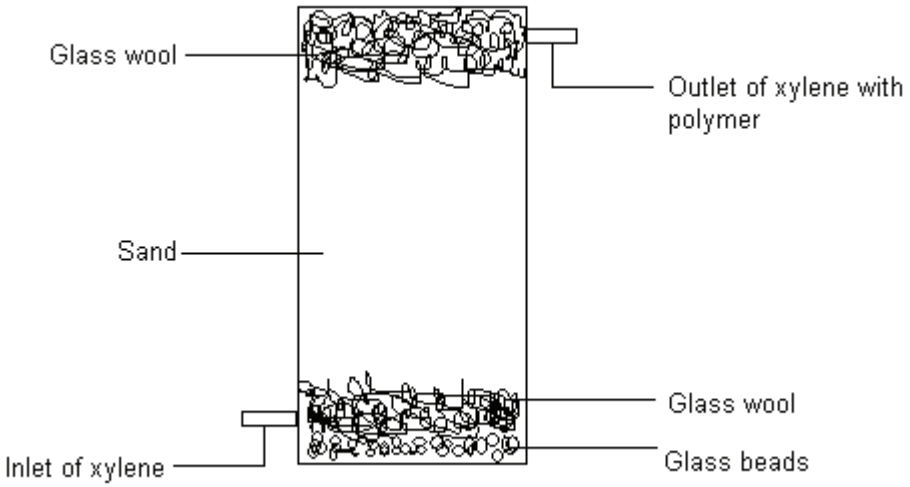

Figure 3.3 Schematic of TREF elution column

Figure 3.4 TREF elution column

3. Recovery of material

The fractions were then transferred to a round bottom flask and the solvent removed under reduced pressure on a rotary evaporator (water vacuum, 60 °C). The polymer was then removed from the flask after washing with acetone and placed in pre-weighed glass vials (20 mL). The polymer fractions were dried in a vacuum oven at 60 °C for 24 h.

3.2.2 Crystallisation analysis fractionation (CRYSTAF)

CRYSTAF is based on the same principles as TREF, but consists only of a crystallisation step [3-5]. The crystallisation analysis fractionation was done on a CRYSTAF commercial

apparatus model 200, manufactured by Polymer Char S.A. (Valencia, Spain). Typically, 1.5 mg of polymer was dissolved in 30 mL of solvent (TCB). Up to 5 samples could be analyzed simultaneously.

3.2.3 Differential scanning calorimetry (DSC)

DSC was used to determine the melting point and the percentage crystallinity. DSC analyses were done on a TA Instruments Q100 DSC. The instrument was calibrated using indium metal according to a standard procedure. About 2-5 mg (carefully weighed) of each sample was used to do the analysis. The analysis procedure comprised the following (all DSC measurements were conducted in a nitrogen atmosphere).

The sample was weighed off and sealed in a standard DSC pan. The sample was then heated to 150 °C at a rate of 10 °C/min and then equilibrated at 150 °C for 5 minutes. The sample was then cooled down to -40 °C at a rate of 10 °C/min and then left to equilibrate at that temperature for 5 minutes. The sample was then heated again to 150 °C at a rate of 10 °C. The second heating was used for analysis of the melting behaviour of the polymer.

3.2.4 Size exclusion chromatography

Molecular weight and polydispersity were determined with high temperature SEC. 1.5-2 mg of polymer was dissolved in 2 mL of 1, 2, 4-trichlorobenzene containing 0.0125% 2, 6-di-tert-butyl-4-methylphenol (BHT) and dissolved at 160 °C. Molecular weights were determined on a PL-GPC 220 High Temperature Chromatograph from Polymer Laboratories at 145 °C. The 4 columns were packed with polystyrene/divinylbenzene copolymer (PL gel MIIXED-B [9003-53-6]) from Polymer Laboratories. Each column had a length of 300 mm and a diameter of 7.5 mm. The particle size was 10 μm. A differential refraction index detector was used. The calibration of the instrument was done with monodisperse polystyrene standards (Easical from Polymer Laboratories).

3.2.5 Nuclear magnetic resonance (NMR)

The ^{13}C NMR of the unfractionated polymers, as well as the fractions obtained by TREF were recorded. These spectra were used to determine the comonomer content present in each sample. Typically, about 65 mg of each sample was placed in a NMR tube and dissolved in 5 mL of 1, 2, 4-trichlorobenzene/C_6D_6. The 1, 2, 4-trichlorobenzene/C_6D_6 was used in 5:1 ratio.

The ^{13}C and ^{1}H spectra were obtained on a Varian VXR 300 MHz instrument. A pulse angle of 45 degrees and an acquisition time of 0.82 seconds were used.
The comonomer percentage was calculated according to the equation:

$$\text{Comonomer} = \frac{(\alpha\ \text{Br carbon}/2) + \text{Br carbon}}{\text{Total backbone carbons}}$$

The peaks associated with all the backbone carbons were integrated and the integrals of the peaks assigned to the branching carbon and the carbons α to branching were then used to determine the comonomer content (mole%) using the equation above. The percentage of the carbons α to branching were divided by two, because there are two carbons α branching, and the percentage of the branching carbons are added together.

3.2.6 Film preparation

Films were pressed for the DMA analysis. Films of both 50 µm and 100 µm thick were pressed in a Grasby Specac 15.011 ton press. A small amount of material was pressed between pieces of aluminium foil at 180 °C in multiple steps. The film was pressed for 5 minutes at 5 Mpa, then for another 5 minutes at 5 Mpa, then for another 10 minutes at 10 Mpa and then again for 10 minutes at 10 Mpa.

3.2.7 Dynamic mechanical analysis (DMA)

The DMA analysis was done on a Perkin Elmer DMA 7e in the tensile mode at ambient temperature. The samples had a thickness of 50 µm and 100 µm and a sample width of 4.5 mm and sample length of 2.2 cm. The method used was static force scan, 200 mN to 6000 mN at 200 mN/min.

3.3 References

1. Wild, L., *Temperature Rising Elution Fractionation.* Advances in Polymer Science, 1990. **98**: p. 1-47.
2. Rabie, A.J., *Blends with Low-Density Polyethylene (LDPE) and Plastomers.* MSc Thesis, University of Stellenbosch: Stellenbosch. 2004

3. Anantawaraskul, S., J.B.P. Soares, and P.M. Wood-Adams, *Fractionation of Semicrystalline Polymers by Crystallization Analysis Fractionation and Temperature Rising Elution Fractionation.* Advances in Polymer Science, 2005. **182**: p. 1-54.
4. Anantawaraskul, S., J.B.P. Soares, and P.M. Wood-Adams, *Effect of Operation Parameters on Temperature Rising Elution Fractionation and Crystallization Analysis Fractionation.* Journal of Polymer Science: Part B: Polymer Physics, 2003. **41**: p. 1762-1778.
5. Fonseca, C.A. and I.R. Harrison, *Temperature Rising Elution Fractionation*, in *Modern Techniques for Polymer Characterisation*, R.A. Pethrick and J.V. Dawkins, Editors. 1999, John Wiley & Sons Ltd: Chichester. p. 1-13.

Chapter 4

Results and Discussion

4.1 Characterization of bulk material

4.1.1 TREF analysis

The bulk linear-low density polyethylene (LLDPE, Sasol Grade LM3040P, henceforth called Sample A) was fractionated by preparative TREF. The individual fractions were fully characterised. Results of a typical TREF experiment are shown in this section. It must be remembered that for the fraction removal/recombination experiments a TREF experiment was run for each case; so for the removal and recombination of each fraction a similar TREF run was conducted and small differences might be found in the molecular constitution of the LLDPE so fractionated. Therefore the results given below must be regarded as typical for this particular LLDPE.

The amount of material that is obtained form each TREF fraction cannot be directly compared to the other fractions obtained, because the sample temperature intervals are not always the same. To address this issue, the weight obtained from each fraction is divided by the temperature interval between two successive fractions in order to get a weighted percentage. In Table 4.1, the TREF fractionation data for the original LLDPE can be seen.

Table 4.1 TREF fractionation data

Sample	T (°C)	W_i%	W_i%/ΔT
A1	25	10.5	0.4
A2	50	6.6	0.7
A3	60	8.6	0.9
A4	70	12.7	1.3
A5	80	19.7	2.0
A6	90	22.6	2.3
A7	100	17.0	1.7
A8	120	2.3	0.1

The results in Table 4.1 show that most of the material elutes between 80-100 °C. In Figure 4.1, the distribution of the fractions is shown schematically.

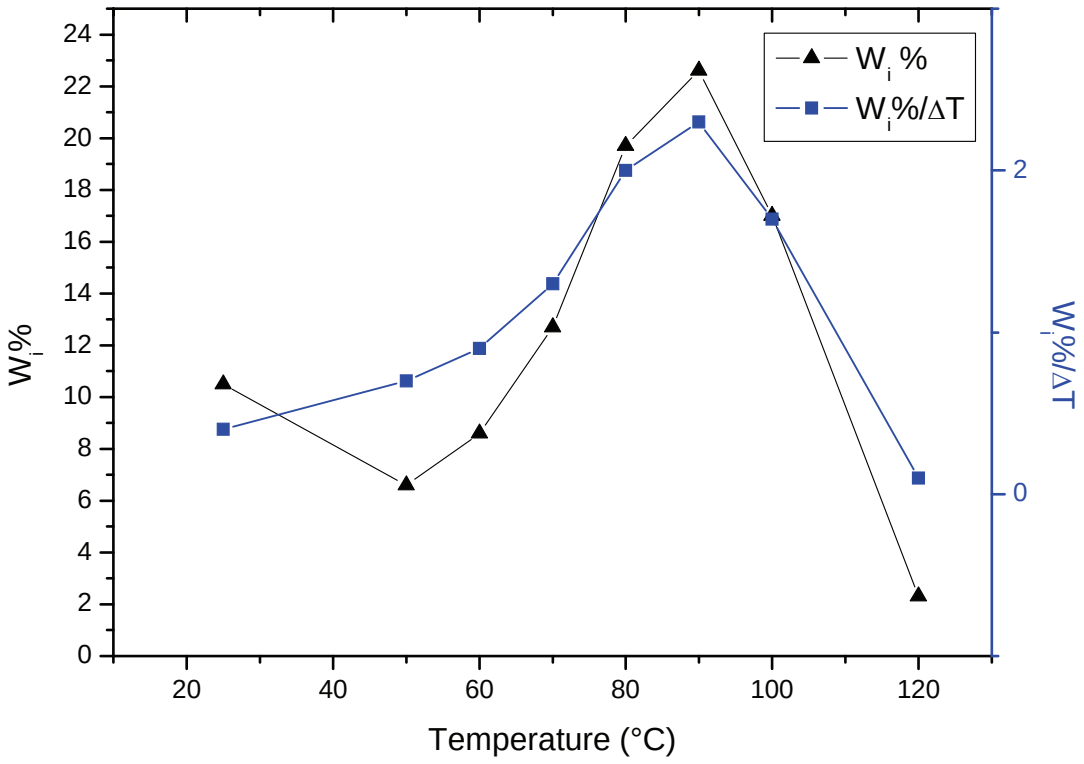

Figure 4.1 TREF elution weight distribution

The distribution of the eluted material is relatively broad, which indicates that there is a broad distribution in the chemical composition of the chains of the polymer. It is well known that TREF operates by fractionating according to crystallinity. It is also known that the most crystalline material, with less branching, will elute at the higher temperatures and the least crystalline material, with the most branching, will elute at lower temperatures [1]. The branching in LLDPE is due to comonomer insertion. These side-chain branches influence the crystallinity. Transition metal catalysts have more than one active site and LLDPE made with these catalysts will not have a uniform distribution of side-chains, as different active sites will produce polymers with different amounts of comonomer included. TREF curves of LLDPE have been reported to show bimodality [1-3]. The bimodality is explained by the different active sites of the catalyst which produce the polymer [1, 3-6]. The bimodality also indicates the broad compositional heterogeneity of these polymers [4]. In the case of bimodality, it was explained that a certain active site will produce polymer with a high amount of comonomer

and this is usually the peak seen at the lower temperatures. Another active site will have a low affinity for comonomer and this is the peak seen at the higher elution temperatures [4, 7, 8]. In the case of this polymer, no bimodality is seen in the elution curve of TREF. This might be because not enough data points are present to distinguish between the different active sites. Because we are working over a wide range of temperatures, the TREF is not sensitive enough to pick up the difference. The CRYSTAF trace (see Figure 4.2), clearly shows this bimodality.

The chains of LLDPE will have different amounts of the comonomer (short chain branching) and therefore will have different crystallinities. This will be reflected in the TREF results, as crystallinity will affect the amount of material that will elute at a certain temperature. There are two features visible in the TREF profile. In the first instance, there is a large soluble fraction and in the second instance a very broad distribution of molecular species is shown, even though most of the material elutes between 90 and 100 °C. The evidence for this is in the fact that the amount of material eluted for each fraction is quite substantial with the exception of the 120 °C fraction.

4.1.2 CRYSTAF analysis

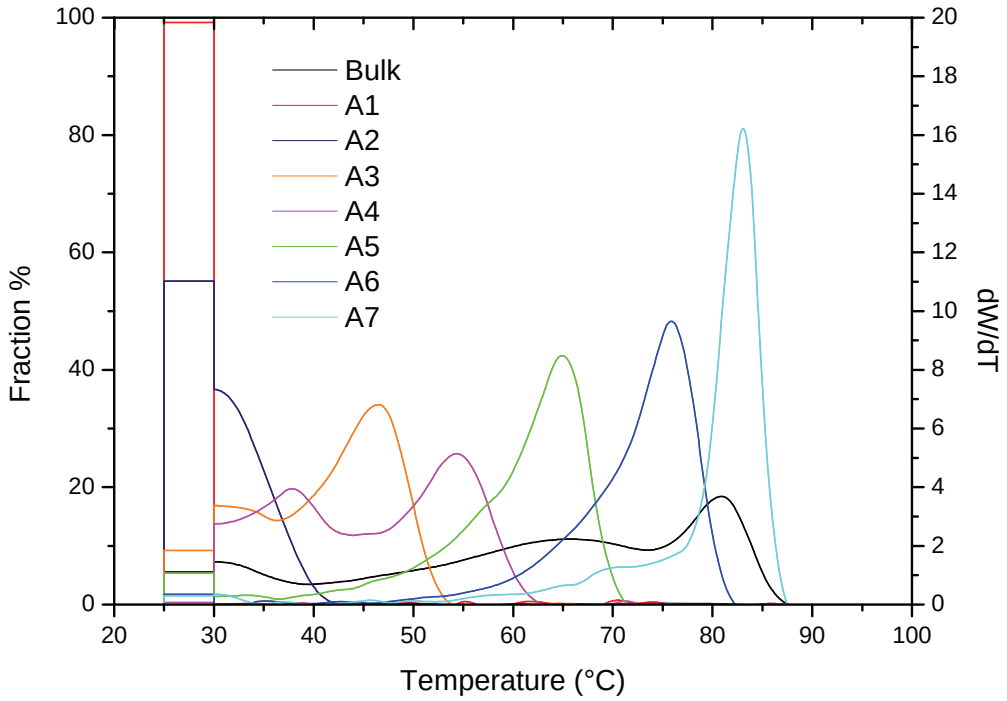

Figure 4.2 CRYSTAF analysis of TREF fractions and bulk LLDPE

From the CRYSTAF results of the bulk material a bimodal chemical distribution can clearly be seen. There is a relatively sharp peak between 80 – 90 °C and a broader peak stretching from about 35 – 75 °C. As mentioned before this bimodality is due to the multiple active sites of Ziegler–Natta catalysts [9, 10]. When looking at A1, the fraction taken from 0-25 °C, we can see it contains a large soluble fraction, comprising about 99% of the material. No crystalline material appears to be present, although a very small amount might be present as some small peaks are just visible in the CRYSTAF spectrum (see Table 4.2). From the results represented in Figure 4.2 we can see that the higher the elution temperature of the fraction is, the more crystalline the material. This agrees with the result we obtained from TREF.

Table 4.2 CRYSTAF crystallisation data

Sample	Peak 1 Temperature (°C) and area (%)	Peak 2 Temperature (°C) and area (%)	Peak 3 Temperature (°C) and area (%)	Peak 4 Temperature (°C and area)
A1	48.9 (0.2)	61.7 (0.2)	70.5 (0.3)	74 (0.1)
A2	30.0 (44.4)	49.7 (0.1)	66.5 (0.1)	
A3	30.0 (20.2)	46.5 (70.7)	64.6 (0.1)	
A4	37.8 (43.8)	54.3 (55.7)	71.3 (0.1)	
A5	33.3 (1.8)	64.9 (93.3)		
A6	42.6 (0.4)	75.9 (98.2)		
A7	30.0 (0.9)	45.7 (0.5)	71.1 (10.7)	83.1 (85.9)
Bulk	30.0 (10.2)	65.7 (53.1)	80.9 (31.1)	

In Table 4.2 the peak temperatures assigned by CRYSTAF can be seen. From here we can also see the heterogeneity of the catalysts. For the first sample, a very high soluble fraction is observed. The peaks assigned are very small and cannot be seen on the profile. For the next samples, (A2-A4) three peaks could be detected, then for A5-A6 only two peaks could be assigned. For the last sample, multiple peaks could again be detected.
Again, we can see from CRYSTAF that there is a broad distribution in the molecular species and that there are more than one active site present.

4.1.3 Analysis of molecular structure

The molecular weight values of the TREF fractions are given in Table 4.3, as are the polydispersity (PD) values. This is also presented graphically in Table 4.3

Table 4.3 Molecular weight and polydispersity of TREF fractions

Sample	Mn	Mw	PD
A1	37400	82800	2.2
A2	32700	133000	4.1
A3	45000	154000	3.4
A4	54200	159000	2.9
A5	60300	173000	2.9
A6	82400	220000	2.7
A7	113000	263000	2.3
A8	87500	201000	2.3
Bulk	73603	278523	3.8

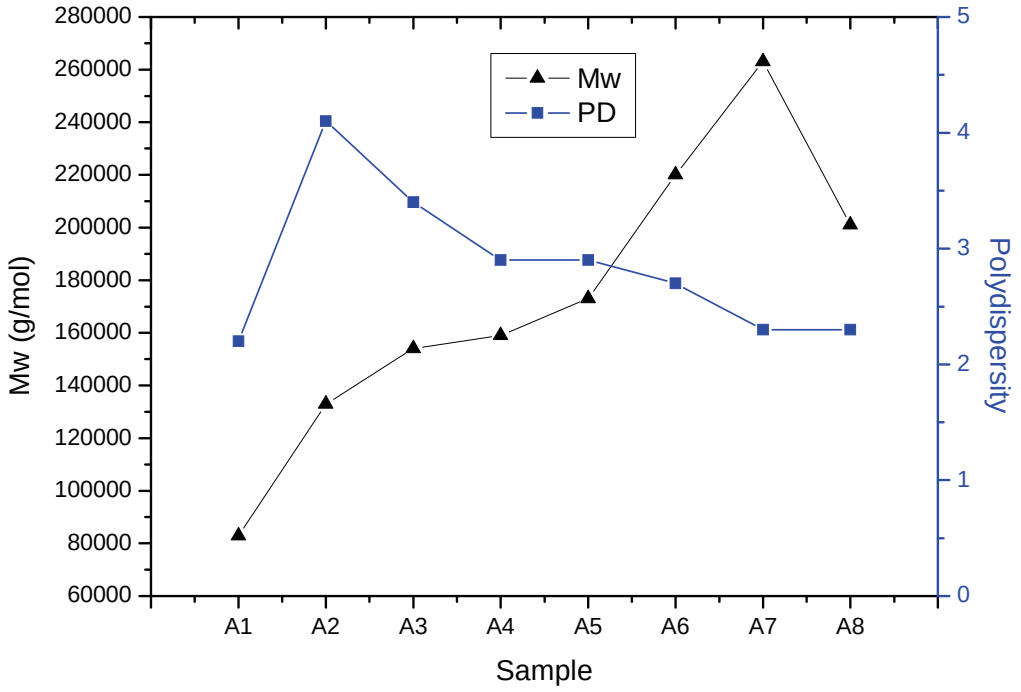

Figure 4.3 Molecular weight and polydispersity

The general trend is that molecular weight increases as the elution temperature increases. Wild et al. showed that the molecular weight decreases with an increase in the short-chain branching as do other papers [7, 11-13]. We already know that at higher elution temperatures there is less short-chain branching. The last fractions' molecular weight is lower than the previous one. This can be because some lower molecular weight material is

trapped between the chains when it crystallises. We have observed this phenomena in other polymers as well [14]. The TREF results indicate that the fractions that are the least crystalline also have the lowest molecular weight and the highest polydispersity. According to theory, TREF does not separate according to molecular weight [13, 15], although in our case the higher molecular weight fractions appear to elute at higher temperatures. To differentiate between possible molecular weight effects and crystallinity effects, we also determined the comonomer content by ^{13}C NMR, as well as the crystallinity and melting by DSC (see Section 4.1.2). The ^{13}C NMR peaks of the fractions were assigned according to ACD Chem labs predictor. The comonomer content was determined by integration of the peaks associated with the backbone carbons and relating this to the peaks associated with backbone carbons at the branch points. The following equation was used to calculate the mole% comonomer:

$$\text{Comonomer} = \frac{\left(\alpha \text{ Br carbon}/2\right) + \text{Br carbon}}{\text{Total backbone carbons}} \quad (4.1)$$

In Figure 4.4, the ^{13}C NMR of sample A2 can be seen. Peaks are assigned as shown in Figure 4.5.

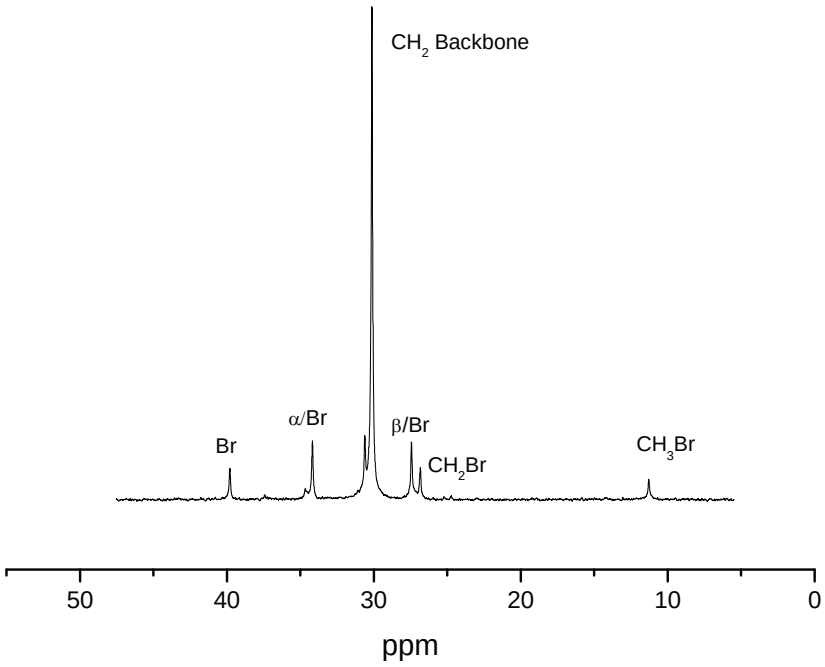

Figure 4.4 ^{13}C NMR of sample A2

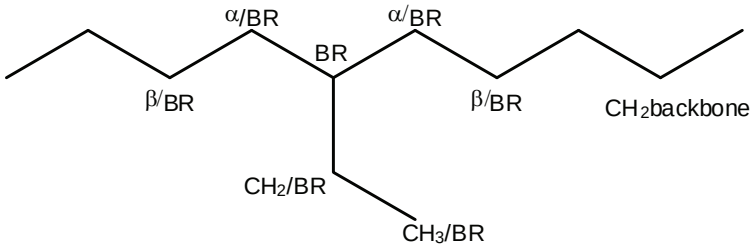

Figure 4.5 Structure of 1-Butene/LLDPE

Table 4.4 Comonomer content of each fraction

Sample	Fraction Temperature (°C)	Comonomer %	Ethylene %	Ratio Ethylene/Butene	Gram of fractions	Grams of butene	% of total Butene
A1	25	8.7	91.3	0.1978	0.2841	0.05618	21.7
A2	50	8.2	91.8	0.1845	0.1796	0.03314	12.8
A3	60	6.9	93.1	0.1536	0.2323	0.03569	13.8
A4	70	6.6	93.4	0.1463	0.3457	0.05056	19.5
A5	80	3.7	96.3	0.0788	0.5347	0.04214	16.3
A6	90	2.1	97.9	0.0454	0.6145	0.02790	10.8
A7	100	1.2	98.8	0.0243	0.4612	0.01121	4.3
A8	120	1.9	98.2	0.0390	0.0618	0.00241	0.9
bulk		3.2	96.9	0.0674			

In Table 4.4 it can be seen that the comonomer content decreases with an increase in the elution temperature. This is what will be expected from theory [4-7, 15, 16]. TREF fractionates according to crystallinity. The chains in the fraction collected at 25 °C will be the least crystalline. Comonomer decreases crystallinity, because the chains cannot pack close together. It will therefore be expected that the highest comonomer content will be in the fractions collected at the lowest temperatures. When looking at the comonomer distribution it is interesting to note that the room temperature fraction contains a very high percentage of all the butene in the copolymer (about 22%). Around 16-19% butene is in the fractions eluted at 70 and 80°C. The 1-butene content of the other major fractions is about 10-12%, while the highest elution temperature that produces a sizable fraction has only 4% of all the butene in the copolymer included. Based on this we postulate that there appears to be at least four different types of active sites that produce LLDPE. This is also illustrated quite clearly if we look at the butene content of the individual fractions, 8-9 mole% for the 25 and 50 °C fractions, 6-7% for the 60 and 70 °C fractions, 3% for the 80 °C and 1-2% for the 100-120 °C fraction. Similarly this four active sites produce molecular weights of 80 000 -130 000, 150 000-160 000, 170 000, and 200 000-260 000. We can illustrate this quite well by plotting the butene content (as a percentage of the total butene content) of the fractions, and assigning

the fractions to “active sites” or “molecular species”, the latter being defined as the type of polymer produced by the active sites.

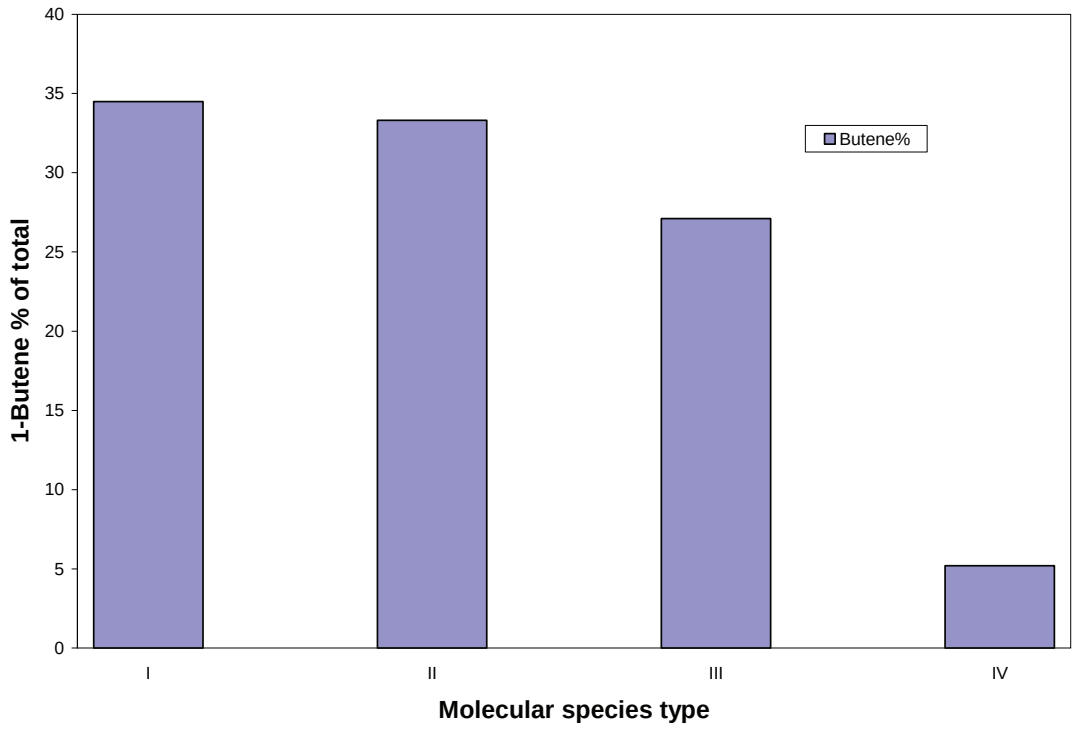

Figure 4.6 Distribution of 1-butene content

The trend shown in Figure 4.6 clearly illustrates the distribution of 1-butene. We need to consider this when we discuss the effect of the removal of fractions from the polymer and the subsequent effects on the properties of the polymer. The trend clearly indicates that most of the 1-butene in the polymer is in fractions eluted at the lower temperatures. Similarly, we can plot the average molecular weight for the different “molecular species”. Molecular weights were averaged taking the amount of material into consideration (Figure 4.7).

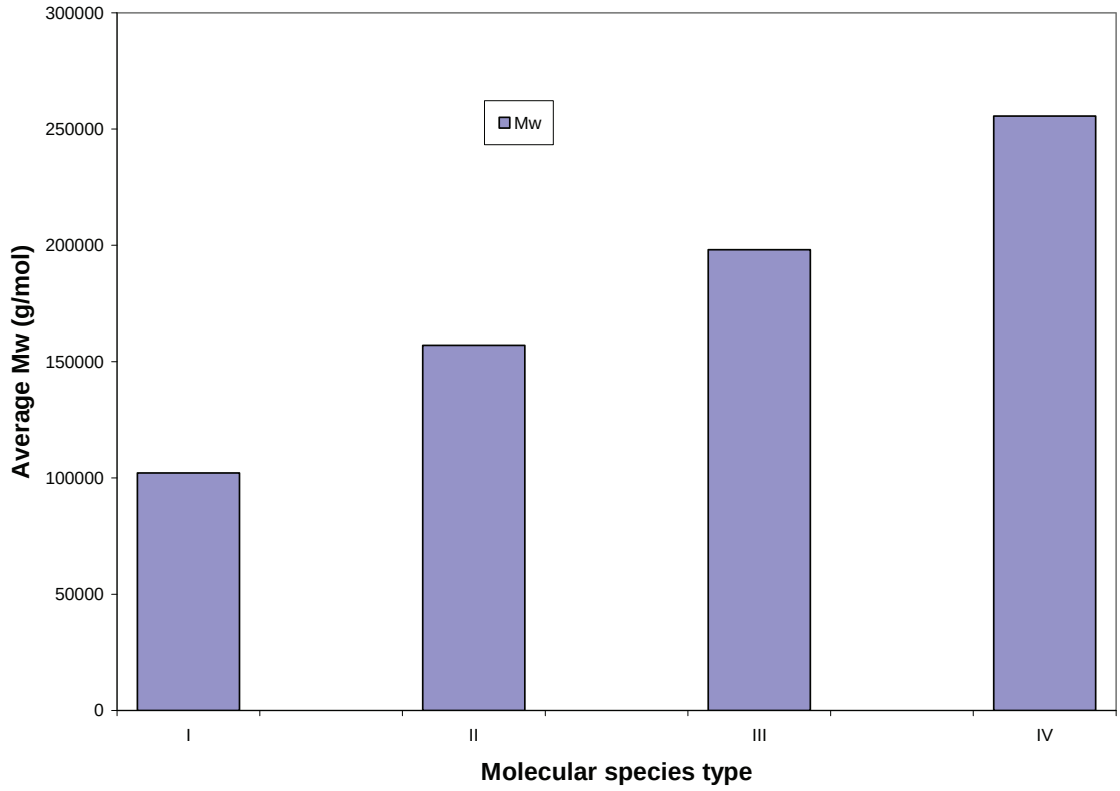

Figure 4.7 Distribution of average molecular weight

From these result we can clearly see that TREF fractionates according to crystallinity and that the branching influence the crystallinity of the polymer. The more branching there is present in a fraction, the less that fractions' crystallinity is. We also saw that there are four active sites present and that each active site produces polymer with a difference in molecular weight and amount of comonomer.

4.1.4 Crystallinity and melting

The melting endotherms were used to calculate the crystallinity. The degree of crystallinity was calculated relating the enthalpy from the melting endotherm and relating it to the melting enthalpy of a 100% crystalline LLDPE, which was 290 J/g [17, 18].

In Figure 4.8 the waterfall plot (the graphs are offset in the y-direction) of the fractions can be seen.

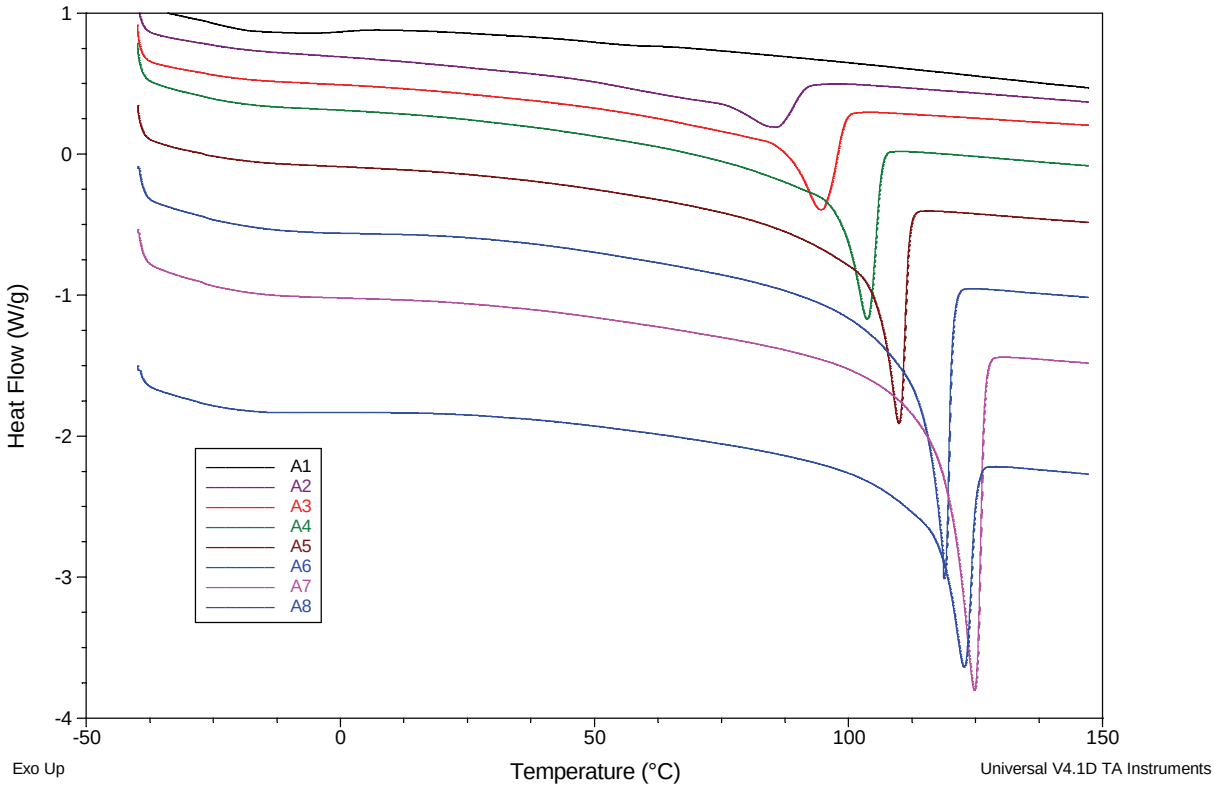

Figure 4.8 Waterfall plot of melting endotherms for LLDPE

From the graph, it can be seen that the melting point of each fraction shifts to higher temperature as the elution temperature at which the fraction was collected increases. The area under the peaks also seems to get broader with an increase in elution temperature.

LLDPE usually shows a broader melting peak, than for instance HDPE. A multipeak endotherm is usually seen for copolymers of ethylene containing more than 15 mol% 1-alkene [11]. Kong *et. al*. also found that with an increase in the short-chain branching a decrease in crystallinity and melting point temperature is observed. Short-chain branching influences the crystallinity and melting of the polymer [19]. If we subdivide the melting regions in the same way as we did for the molecular weight and comonomer content, we define the melting for the active sites as: I up to 85 °C, II up to 105 °C, III up to 110 °C and IV up to 125 °C.

Table 4.5 DSC Results for TREF fractions

Sample	T_e (°C)	T_m (°C)	ΔH_m (J/g)	Crystallinity (%)
A1	25			none
A2	50	85.6	33.8	11.7
A3	60	94.4	52.7	18.2
A4	70	103.6	87.6	30.2
A5	80	109.9	109.8	37.9
A6	90	118.8	150.6	51.9
A7	100	124.8	174.7	60.2
A8	120	122.7	118.5	40.9
Bulk		122.7	104.1	35.9

It can be seen from the data that the crystallinity increases as the elution temperature increases. That is exactly what is expected when using temperature rising elution fractionation [1, 5-7, 15, 20-23]. The melting temperature (Tm) also increases with increasing elution temperature. This coincides with the increased crystallinity in this case, which indicates that the perfection of the crystals are greater, which can be attributed to the decrease in the comonomer content.

We conclude from this that the more branching a fraction contains, the less crystalline that fraction is and the lower the melting point will be. Again, four active sites could be established.

4.2 Removal of TREF fractions

In this set of experiments, a single fraction was removed form the LLDPE after the completion of the TREF run. For 8 different factions to be removed, at least 8 samples of the LLDPE had to be fractionated according to TREF. From each sample a single fraction was removed, and the remainder of the material recombined and analyzed. In each case the fraction that was removed was also characterised by NMR and DSC.

4.2.1 TREF analysis

Fractionated material was selectively recombined after removing an individual fraction obtained by TREF in each case. For example, the fraction eluted at 120 °C might be removed and the rest of the polymer recombined.

Table 4.6 TREF fraction removal data

Sample	Temperature of fraction removed (°C)	W_i% removed
B1	<25	6.6
B2	27-50	7.4
B3	51-60	10.9
B4	61-70	12.9
B5	71-80	15.9
B6	81-90	19.8
B7	91-100	14.4
B8	101-120	15.6

In Table 4.6, the weight percentage of each fraction removed is shown.

Again, it can be seen that with some fractions you remove more material than with others. When results are discussed, we need to consider this fact.

4.2.2 Molecular weight and comonomer content, recombined material

In Table 4.7 the molecular weight and polydispersity of the recombined samples can be seen.

Table 4.7 Molecular weight and polydispersity of recombined material

Temperature of fraction removed (°C)	Mn (g/mol)	Mw (g/mol)	PD
<25	86400	255000	3.2
26-50	70300	257000	3.7
51-60	63700	244000	3.8
61-70	57000	234000	4.1
71-80	56400	229000	4.1
81-90	59400	221000	3.7
91-100	63500	226000	3.6
101-120	64300	108000	2.2
Bulk	73603	278523	3.8

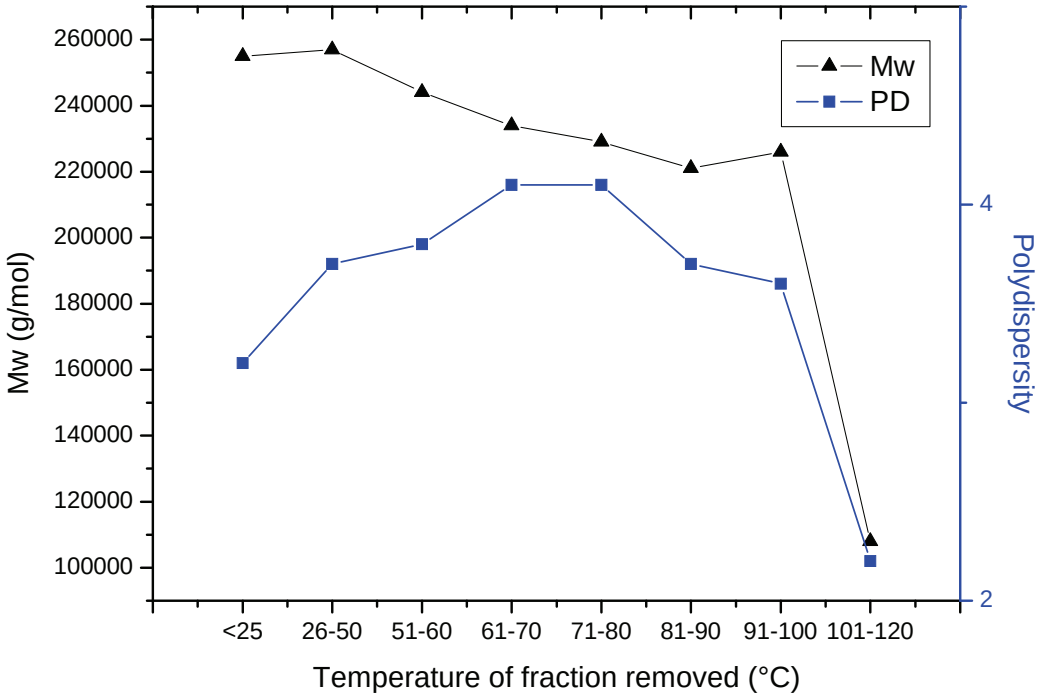

Figure 4.9 Molecular weight and polydispersity distribution

After the removal of the room temperature soluble fraction, the remaining material has a lower apparent molecular weight than the original bulk material, which is unexpected, as the fraction that is removed has quite a low molecular weight (Table 4.3). It is possible that removal of the more highly branched lower molecular weight material from the sample affects the size exclusion mechanism of the remaining material and thereby affects the overall GPC profile of the material. Within the rest of the series, however, the molecular weight of the fraction that is removed tends to increase as the elution temperature increases (Table 4.3), while the overall tendency is for the remaining material to have a slightly decreased molecular weight. The molecular weight remains in the region of 226 000 to 255 000 g/mole, and the polydispersity remains fairly constant (3.8 for the unfractionated material to a low value of about 3.2). This indicates that molecular weight distribution is fairly even throughout the sample even though crystallinity may vary. From these results it appears unlikely that molecular weight, or polydispersity will be a major variable in determining the properties of the final product (after recombination).

The ^{13}C NMR spectrum of the material remaining after the A6 fraction (81-90 °C) was removed can be seen in Figure 4.10. Other spectra are shown in the appendix. In Table 4.8 the comonomer content of both the fractions removed as well as the remaining material is shown.

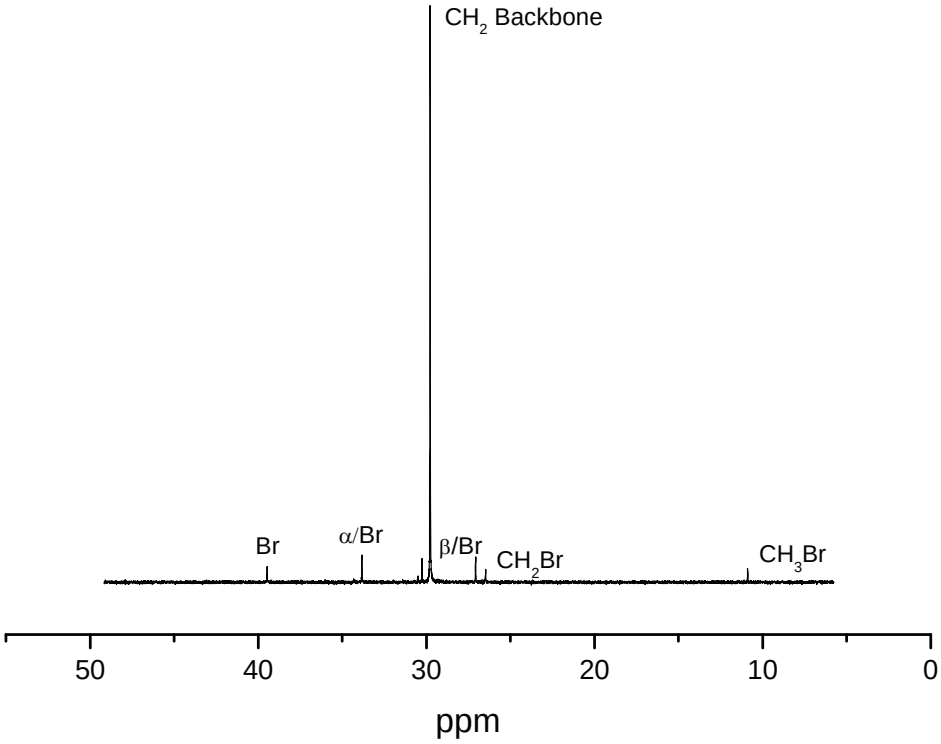

Figure 4.10 ^{13}C NMR spectrum of material without A6 fraction

Table 4.8 Comonomer content of recombined and fraction removed

Fraction removed	Comonomer % of fraction removed	Comonomer % of recombined material	Crystallinity of fraction removed	Crystallinity of recombined material
Bulk		3.15		35.9
>25	11.0	2.1	none	34.2
25-50	6.7	2.3	8.5	46.1
51-60	3.9	3.6	17.6	32.9
61-70	3.9	3.6	28.1	36.2
71-80	2.7	4.5	39.7	37.8
81-90	1.6	4.8	54.8	34.8
91-100	0.9	4.9	66.5	37.5
100-120	0.7	2.9	39.5	32.9

It is evident from Table 4.8 and Figure 4.11 that as material with higher comonomer content is removed, the remaining material has correspondingly lower commoner content. This is affected by the amount of material removed as well. For example, when the room temperature soluble fraction is removed, or the fraction eluted at 50 °C, we see a sharp decline in comonomer content of the remaining material, as a large amount of the total butene is found in these fractions (about 40%). On the other hand, when a significant amount of material with low comonomer content is removed, for example the fraction eluting at 90 °C (about 20% of the total polymer, but with a low comonomer content), the overall concentration of 1-butene in the remaining polymer increases. What would be interesting here is to compare the crystallinity versus comonomer content before and after removal of the fractions.

The general trend is that the comonomer content increases, the higher the temperature of the fraction removed. When looking at the characterization, we can see that the comonomer content of the 50 °C fraction is high, so when this fraction is removed it suggests that the comonomer content of the remaining material will be low. Moreover, as the temperature of the fractions removed increased the comonomer content will increase. When the room temperature fraction is removed, it is expected that the comonomer content will be very low. The trend can be seen in Figure 4.11.

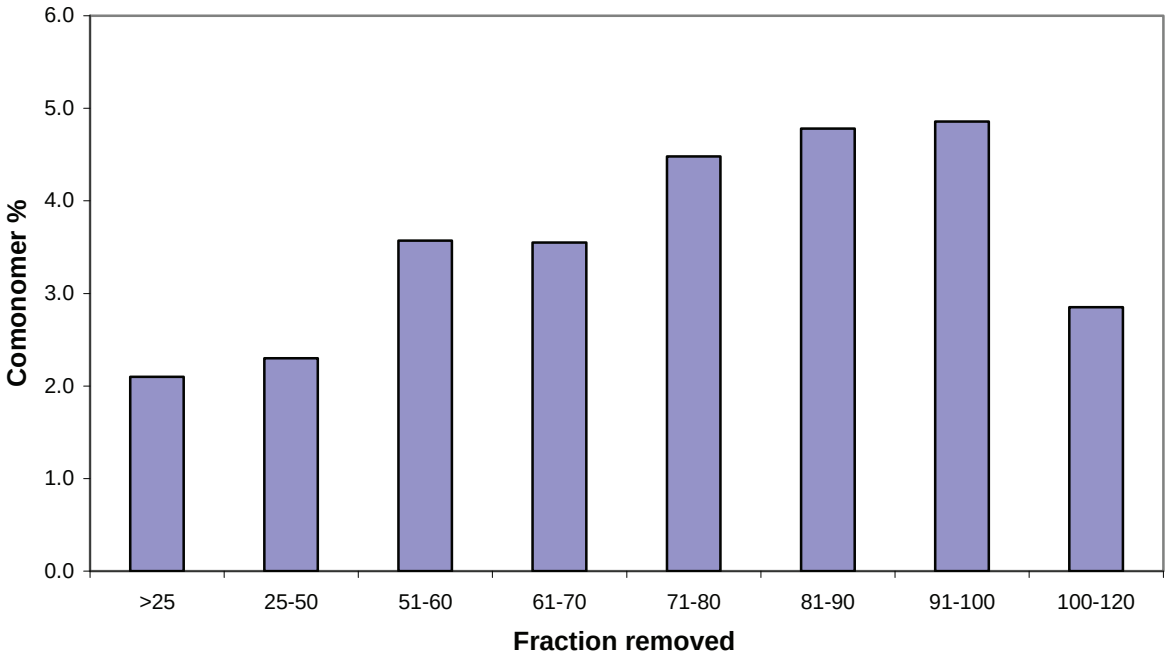

Figure 4.11 Comonomer percentage distribution of remaining material

These results showed that the molecular weight and the polydispersity do not have a great influence on the properties of the final product. It also showed that the comonomer percentage do not only depend on the amount of comonomer removed, but also on the amount of material removed.

4.2.3 Crystallinity and melting

Each sample's crystallinity and melting point were determined by DSC. The data for the fractions removed are presented in Table 4.9, while the data for the recombined materials are shown in Table 4.10, and graphically in Figure 4.12.

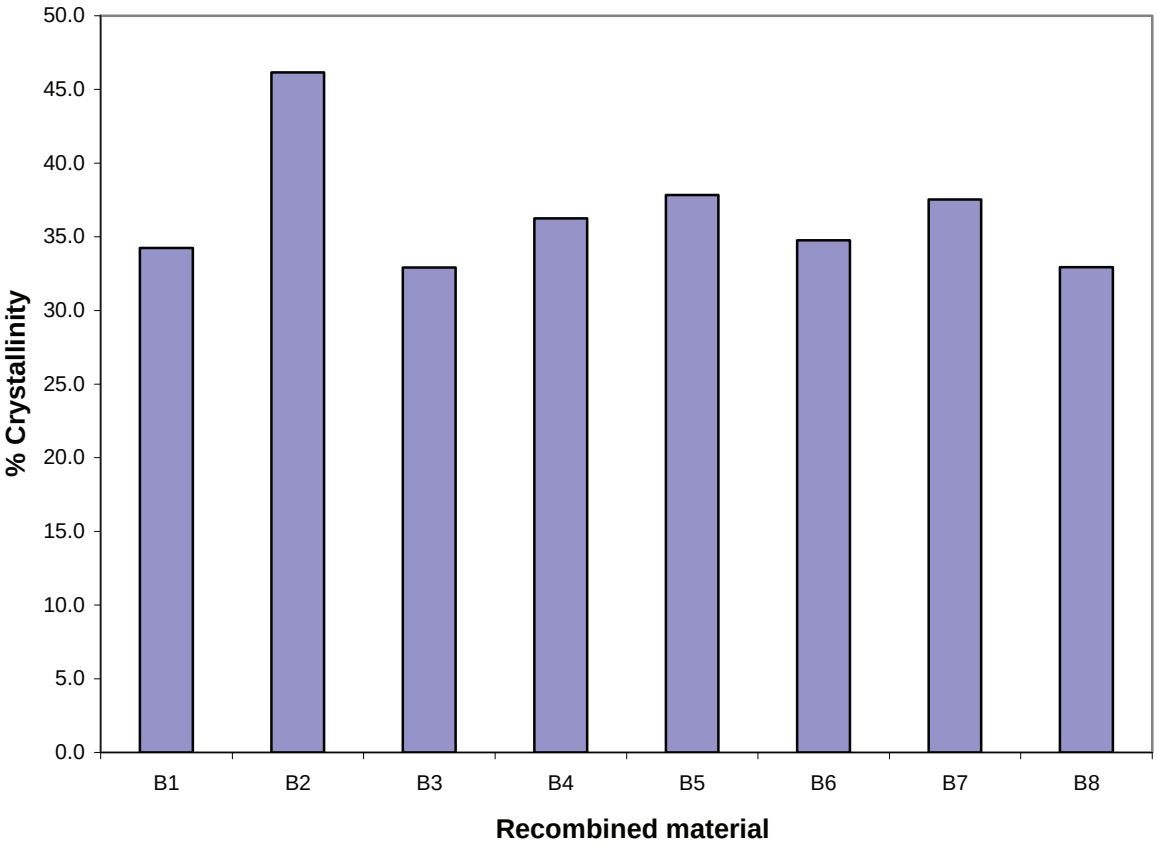

Figure 4.12 % Crystallinity of recombined material without certain fractions

Table 4.9 DSC data of the fractions removed

Temperature of fraction removed (°C)	T_m (°C) of fraction removed	ΔH_m (J/g) of the fraction removed	Crystallinity of the fraction removed
<25			none
25-50	84.6	24.5	8.5
51-60	93.6	51.2	17.6
61-70	103.4	81.6	28.1
71-80	110.3	115.1	39.7
81-90	118.5	158.8	54.8
91-100	124.7	192.9	66.5
101-120	119.3	114.6	39.5

Table 4.10 DSC data of recombined material without certain fractions

Sample	T (°C) of fraction removed	T_m (°C) of recombined material	ΔH_m (J/g) of recombined material	Crystallinity (%) of recombined material
B1	<25	121.5	99.3	34.2
B2	25-50	119.5	133.8	46.1
B3	51-60	116.8	95.5	32.9
B4	61-70	121.2	105.1	36.2
B5	71-80	119.9	109.7	37.8
B6	81-90	117.9	100.8	34.8
B7	91-100	116.0	108.8	37.5
B8	101-120	112.3	95.5	32.9
bulk		122.7	104.1	35.9

The general trend is that the crystallinity of the remaining material goes down as the temperature of the fractions removed increases. This is the opposite trend than what is seen in the characterization. This trend can be explained by the fact that by removing the <25 °C fraction, more amorphous material are removed and therefore the crystallinity of the remaining material will be high. When removing the 101-120 °C fraction, more crystalline material is removed and therefore the crystallinity of the remaining material is less. It was also seen that the room temperature fraction contains more short-chain branches, therefore when this fraction is removed it will be expected that the crystallinity will be higher because there are less side-chains that could impede crystallisation. This once again brings us to the relationship between comonomer and crystallinity. This is plotted for the samples in Figure 4.13

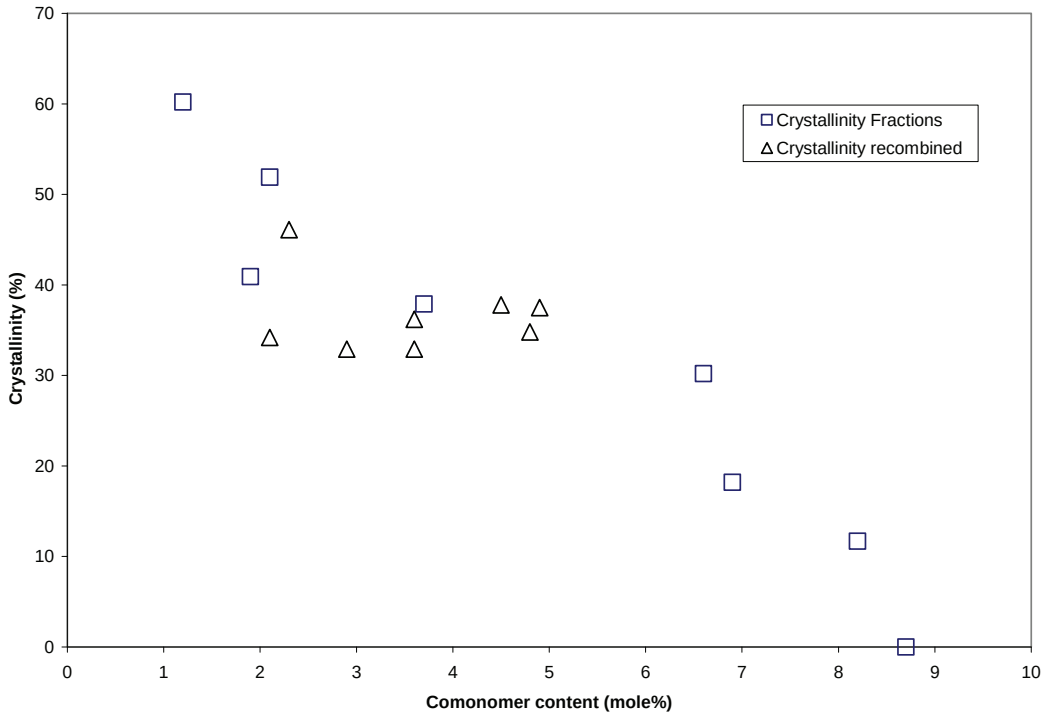

Figure 4.13 Comparison between the comonomer % and crystallinity for TREF fractions and recombined material

What we see in Figure 4.13, is a comparison of the effect of comonomer content in the individual fractions as obtained by TREF and crystallinity (open squares), and similar for the recombined materials (open triangles). It is clear that for the individual fractions obtained from TREF, we see a clear relationship between the comonomer content and the crystallinity. This is expected, as the more comonomer, the less crystalline the material. When we remove certain fractions and recombine the rest of the material, we see that with the exception where a lot of non-crystalline material is removed, there is very little correlation between comonomer content and crystallinity. This indicates that the effect of the comonomer is actually quite limited with regard to the crystallinity, and that for the most part, the comonomer containing chains are excluded from the crystalline regions of the polymer.

4.2.4 Mechanical properties

The information gathered from the DMA experiments were initially difficult to interpret. A typical stress/strain curve is shown in Figure 4.14. As it was in many cases extremely

difficult to calculate single point modulus values, we initially attempted to get an idea of the differences in yield point of the samples. This was done by calculating an "extrapolated yield onset" by drawing lines on the linear portions of the curves proper to the yield point and after the yield point (when cold drawing occurred). This is illustrated in Figure 4.14.

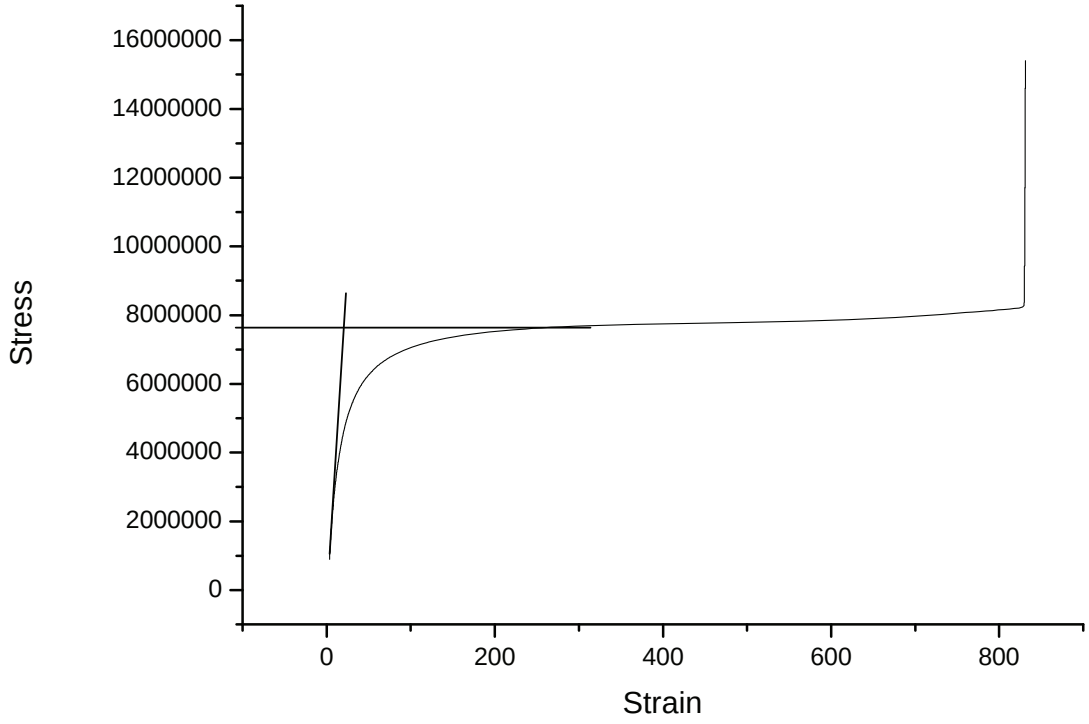

Figure 4.14 Stress/Strain graph of sample B5. Stress given in Pa, strain in %

The plateau stress and extrapolated yield onset were calculated by taking the point of intersection between the two tangent lines. These values are very objective, and can vary depending on the accuracy of drawing the lines, but at least give an indication of the material properties.

Table 4.11 Plateau Stress and Extrapolated yield strain for recombined material

Sample	Plateau Stress	Extrapolated yield strain
Bulk	11939000	38.41
B1	11098000	15.35
B2	8556900	16.61
B3	8996500	27.70
B4	11587000	18.01
B5	7634700	20.97
B6	8216100	17.72
B7	7853300	14.98
B8	9476600	22.41

From Table 4.11 it can be seen that if the amorphous material is taken out, like in sample B1, the material appears to yield at a lower strain value than for the bulk material. This is to be expected, as we should be decreasing the flexibility and ductlility of the material. The plateau stress also decreases as we take out more crystalline material. This should be expected, as the more amorphous the material is, the less stress is needed to yield the material. However, the unexpected results are the fairly low values for the yield strain when more crystalline materials are removed (samples B4 to B8).

The biggest problem that we faced was the fact that the DMA data for different samples seldom started at exactly the same point. In some cases the first recorded strain value was as low as 0.24%, while in other cases the first recorded value was at 5% strain. It was therefore virtually impossible to take, for example, the 5% modulus value for all samples. In order to overcome this problem we obtained modulus values by calculating the slope for all the curves (using the raw data) for the following cases:

- From the start of the analysis to a strain value of 10%
- From the start of the analysis to a strain value of 2% from the start.
- For the region of 7 to 10 % strain for all the samples.

In the latter case the correlation of linear regression was consistently above 0.99 (R^2 value). Results are shown schematically in Figure 4.15.

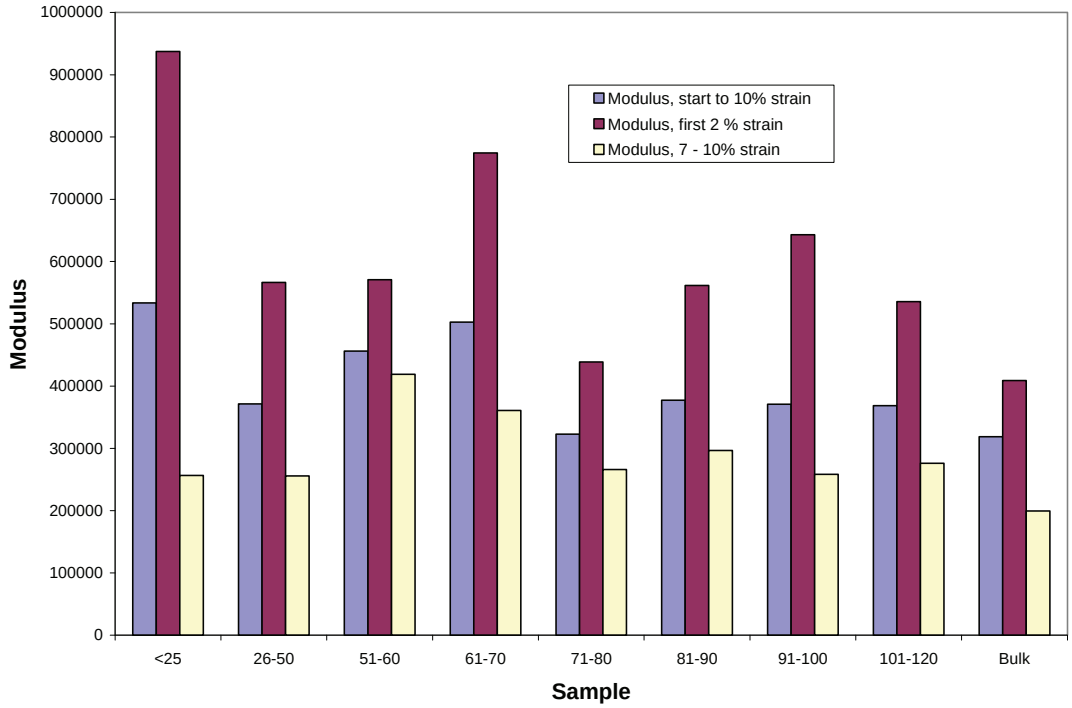

Figure 4.15 Modulus data of recombined material

As can be seen from Figure 4.15, the trends are all the same, although the variations differ in intensity for the values obtained by different methods.

When removing the amorphous material, that is the fraction collected at <25 °C, there is a definite increase in the modulus. This is to be expected. The soluble fraction is removed, leaving behind a material which is more crystalline overall, and this will cause an increase in modulus. At the same time, the molecular weight of the material removed is quite low, and this amorphous, low molecular weight material might very well act as a plasticiser. Overall we see three general areas in Figure 4.15. In the first instance, we see that removing the less crystalline material (<25 °C and 26 – 50 °C, molecular species I) we see a higher modulus than for the bulk material. For the cases where we removed 51 – 60 °C and the 61 – 70 °C fractions (molecular species II) we see a significant increase in the modulus compared to the bulk material, while removing the more crystalline material (fractions from 71 – 80 °C, 81 – 90 °C, 91 – 100 °C and 101 – 120 °C, molecular species III and IV) we see modulus values much in the same range as the bulk material. As the latter material contains most of the higher molecular weight material, as well as the more crystalline material (Table 4.9) we would expect the modulus to decrease as the fractions are removed. Yet this is clearly not the case. If we look at Table 4.10, we see that the crystallinity of the recombined fractions is virtually identical, despite the fact that these materials have had crystalline

material removed. Significantly, though, the peak melting temperature is decreased for all these materials, compared to the bulk material. This indicates fewer very large crystals. This does not seem to influence the modulus at all. What is really significant is the large increase in modulus that is evident when fractions B3 and B 4 (Table 4.10) are removed. These are materials with low to intermediate crystallinity (28 to 40%), have low melting temperatures (93 and 103 °C) and contain about 4 mole% comonomer (about a third of the comonomer in the material). This shows that this material has predominantly small crystals, with crystalline growth being inhibited by the short-chain branching. These materials would typically be at the interface between the amorphous and crystalline regions, and could very well contribute significantly to the amount of tie molecules. It is therefore postulated that these materials significantly affect the material properties, by imparting flexibility and possibly impact properties. It is even possible that these materials act as compatibilisers for the amorphous and crystalline regions, thereby increasing the influence of the amorphous materials on the bulk properties of the materials. Removing these materials result in fewer tie molecules, more perfect crystals (after removal of the B4 fraction the melting temperature of the recombined material is similar to that of the bulk material) and a more effective exclusion of the amorphous fractions from the crystalline material. This all resulted in significantly higher modulus values.

It would have been an interesting experiment to be able to investigate impact properties of these materials as well, as this could further illuminate the possible reasons for the phenomena as seen here, but with the limited amounts of material available from the p-TREF experiments, this was not possible.

4.3 References

1. Monrabel, B., *Temperature Rising Elution Fractionation and Crystallization Analysis Fractionation*, in *Encyclopedia of Analytical Chemistry*. 2000, John Wiley & Sons Ltd: Chichester. p. 0874-8084.
2. Faldi, A. and J.B.P. Soares, *Characterization of the combined molecular weight and composition distribution of industrial ethylene/a-olefin copolymers.* Polymer, 2001. **42**: p. 3057-3066.
3. Usami, T., Y. Gotoh, and S. Takayama, *Generation Mechanism of Short-Chain Branching Distribution in Linear Low-Density Polyethylenes.* Macromolecules, 1986. **19**: p. 2722-2726.

4. Anantawaraskul, S., J.B.P. Soares, and P.M. Wood-Adams, *Fractionation of Semicrystalline Polymers by Crystallization Analysis Fractionation and Temperature Rising Elution Fractionation.* Advances in Polymer Science, 2005. **182**: p. 1-54.

5. Fonseca, C.A. and I.R. Harrison, *Temperature Rising Elution Fractionation*, in *Modern Techniques for Polymer Characterization*, R.A. Pethrick and J.V. Dawkins, Editors. 1999, John Wiley & Sons Ltd: Chichester. p. 1-13.

6. Xu, J. and L. Feng, *Application of temperature rising elution fractionation in polyolefins.* European Polymer Journal, 2000. **36**: p. 867-878.

7. Wild, L., *Temperature Rising Elution Fractionation.* Advances in Polymer Science, 1990. **98**: p. 1-47.

8. Soares, J.B.P. and A.E. Hamielec, *Temperature Rising Elution Fractionation*, in *Modern Techniques for Polymer Characterization*, R.A. Pethrick and J.V. Dawkins, Editors. 1999, John Wiley & Sons Ltd: Chichester. p. 15-55.

9. Britto, L.J.D., J.B.P. Soares, A. Penlidis, and B. Monrabal, *Polyolefin Analysis by Single-Step Crystallization Fractionation.* Journal of Polymer Science: Part B: Polymer Physics, 1999. **37**: p. 539-552.

10. Monrabel, B., *Crystallization Analysis Fractionation*, in *United States Patent 5 2220390*. 1991: United States of America.

11. Mirabella, F.M., J. Ford, and E.A. Ford, *Characterization of Linear Low-Density Polyethylene: Cross-Fractionation According to Copolymer Composition and Molecular Weight.* Journal of Polymer Science: Part B: Polymer Physics, 1987. **25**: p. 777-790.

12. Shan, C.L.P., J.B.P. Soares, and A. Penlidis, *Mechanical properties of ethylene/1-hexene copolymers with tailored short chain branching distributions.* Polymer, 2002. **43**: p. 767-773.

13. Wild, L., T.R. Ryle, D.C. Knobeloch, and I.R. Peat, *Determination of Branching Distributions in Polyethylene and Ethylene Copolymers.* 1981: p. 441-455.

14. Harding, G.W., *The fractionation and characterization of propylene-ethylene random copolymers.* MSc Thesis, University of Stellenbosch: Stellenbosch. 2005

15. Soares, J.B.P. and A.E. Hamielec, *Temperature rising elution fractionation of linear polyolefins.* Polymer, 1995. **36**: p. 1639-1654.

16. Wang, C., M.-C. Chu, T.-L. Lin, S.-M. Lai, H.-H. Shih, and J.-C. Yang, *Microstructures of a highly short-chain branched polyethylene.* Polymer, 2001. **42**: p. 1733-1741.

17. Sarzotti, M.D., J.B.P. Soares, L.C. Simon, and L.J.D. Britto, *Analysis of the chemical composition distribution of ethylene/a-olefin copolymers by solution differential scanning calorimetry: an alternative technique to Crystaf.* Polymer, 2004. **45**: p. 4787-4799.

18. Wright, K.J. and A.J. Lesser, *Crystallinity and Mechanical Behavior Evolution in Ethylene-Propylene Random Copolymers.* Macromolecules, 2001. **34**: p. 3626-3633.

19. Kong, J., X. Fan, Y. Xie, and W. Qiao, *Study on Molecular Chain Heterogeneity of Linear Low-Density Polyethylene by Cross-Fractionation of Temperature Rising Elution Fractionation and Successive Self-Nucleation/Annealing Thermal Fractionation.* Journal of Applied Polymer Science, 2004. **94**: p. 1710-1718.

20. Glöckner, G., *Temperature Rising Elution Fractionation: A review.* Journal of Applied Polymer Science: Applied Polymer Symposium, 1990. **45**: p. 1-24.

21. Krentsel, B.A., Y.V. Kissin, V.J. Kleiner, and L.L. Stotskaya, *Copolymers of Ethylene and Higher a-Olefins*, in *Polymers and Copolymers of Higher a-Olefins*. 1997, Hanser Publishers: Munich. p. 243-335.

22. Mays, J.W. and A.D. Puckett, *Molecular Weight and Molecular Weight Distribution of Polyolefins*, in *Handbook of Polyolefins*, R.B. Seymour, Editor. 1993, Marcel Dekker: New York. p. 133-153.

23. McHugh, M.A. and V.J. Krukonis, *Supercritical Fluid Extraction*. 1994, Elsevier. p. 201-205.

Chapter 5

Conclusions

5.1 Conclusions

The aim of the study was to investigate the influence of the chemical composition of the polymer on its mechanical properties by using TREF as a fractionation technique. We successfully achieved the following objectives:

- The bulk material was fully characterized.
- The LLDPE was successfully fractionated by the use of preparative TREF. The TREF distribution was very broad and indicated that the distribution of the molecular species was very broad for the polymer.
- All the fractions were analyzed using High Temperature SEC, ^{13}C NMR and DSC. From these results we concluded that TREF fractionates according to crystallinity and that the amount of branching influences the crystallinity. Although we know that TREF does not fractionate according to molecular weight, it could be seen that the molecular weight increases with an increase in the fractionation temperature. It was also seen that the catalysts consists of four different active sites, producing polymer with a difference in crystallinity, molecular weight and comonomer content. The distribution of the comonomer in the copolymer shows quite clearly that most of the comonomer resides in the more soluble, less crystalline fractions of the polymer.
- TREF fractions were also successfully removed and the remaining material recombined.
- The removed fractions as well as the recombined material were analyzed using, high temperature SEC, ^{13}C NMR, DSC and DMA. The analysis showed that as we remove more crystalline material, the remaining materials' crystallinity drops. This trend was not seen when looking at the molecular weight and comonomer content.

This showed us that final properties are influenced by the crystallinity of the polymer.
It was also concluded that the molecular weight and polydispersity differences exhibited by the polymers analyzed, did not influence the properties of this polymer that much and that there are no correlation for this polymer between the crystallinity and the comonomer content. It seems that the chains that contain comonomer are largely excluded from the crystalline regions.

As can be seen from the results obtained, we have shown that there is definite relationship between the chemical composition of the polymer and its mechanical properties. To this end, the removal of lower melting material, with reasonably high comonomer content, had the greatest effect on the modulus of the material when removed.

5.2 Future work

The DMA analysis was a challenge, because so little material is available to press films, and it is difficult to perform DMA analysis on such small strips of material. Therefore, it is recommended to analyse these polymers using a tensile tester, which can be used on such small samples.

It might also be interesting to compare these results with another LLDPE polymer with a different α–olefin to see if these results can act as a model for all LLDPE polymers.

Appendix A: ^{13}C NMR Data

Bulk material

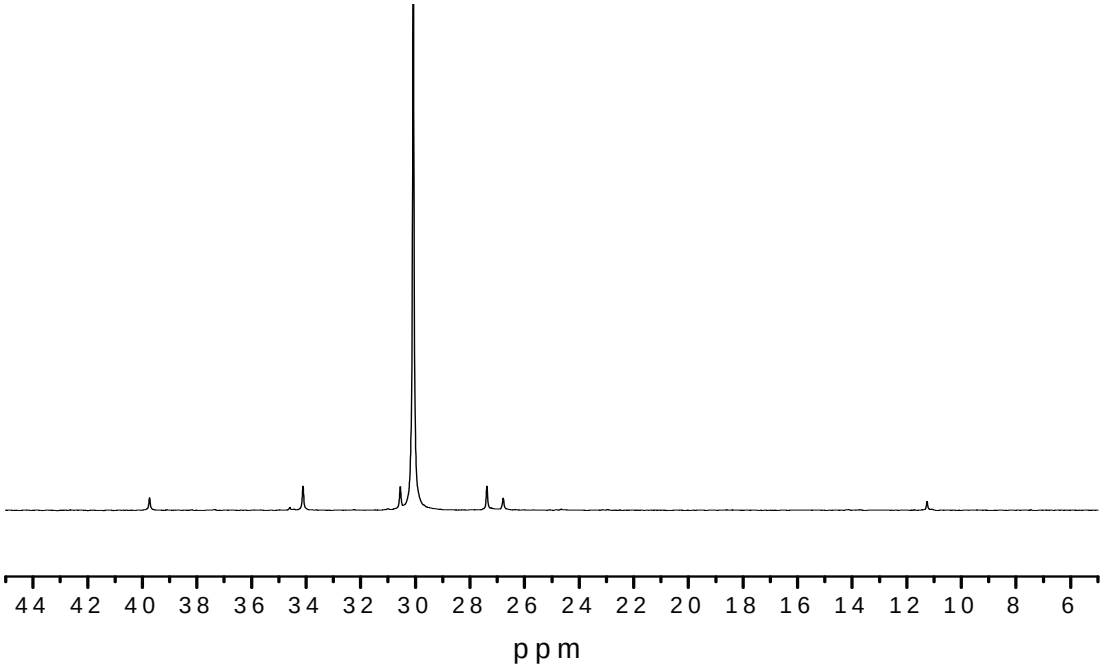

Figure A.1 Bulk material

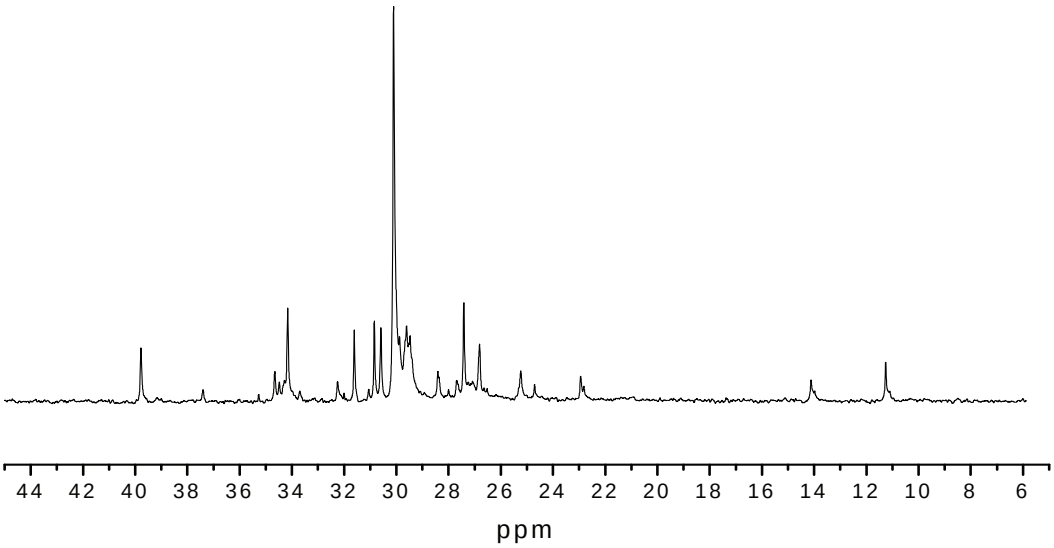

Figure A.2 ^{13}C NMR of sample A1

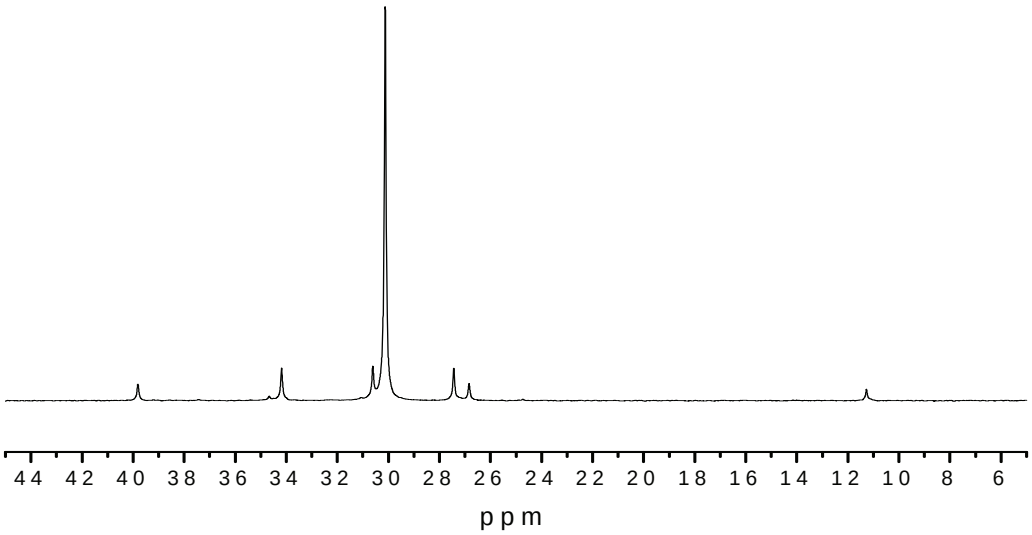

Figure A.3 ^{13}C NMR of sample A3

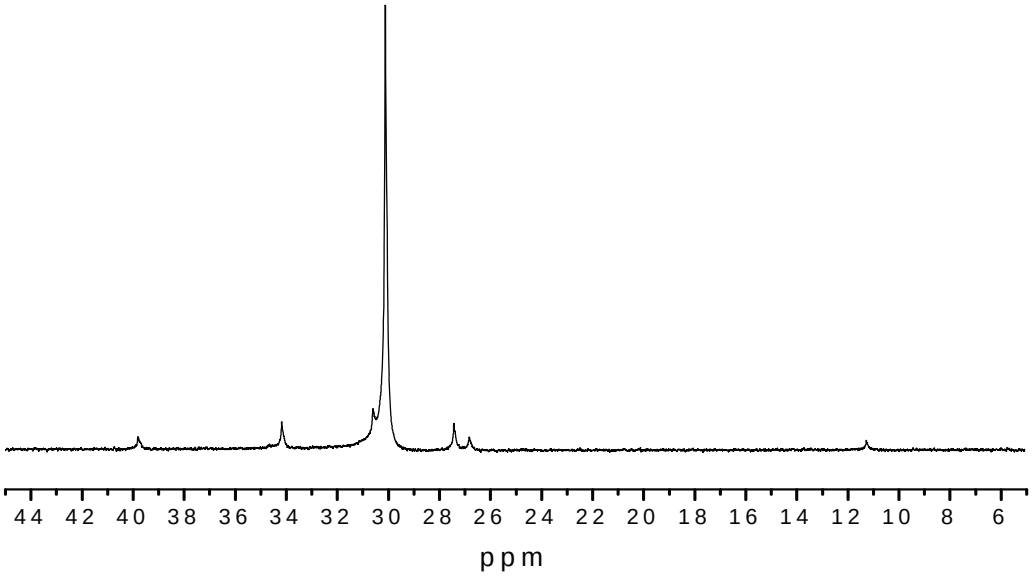

Figure A.4 ^{13}C NMR of sample A4

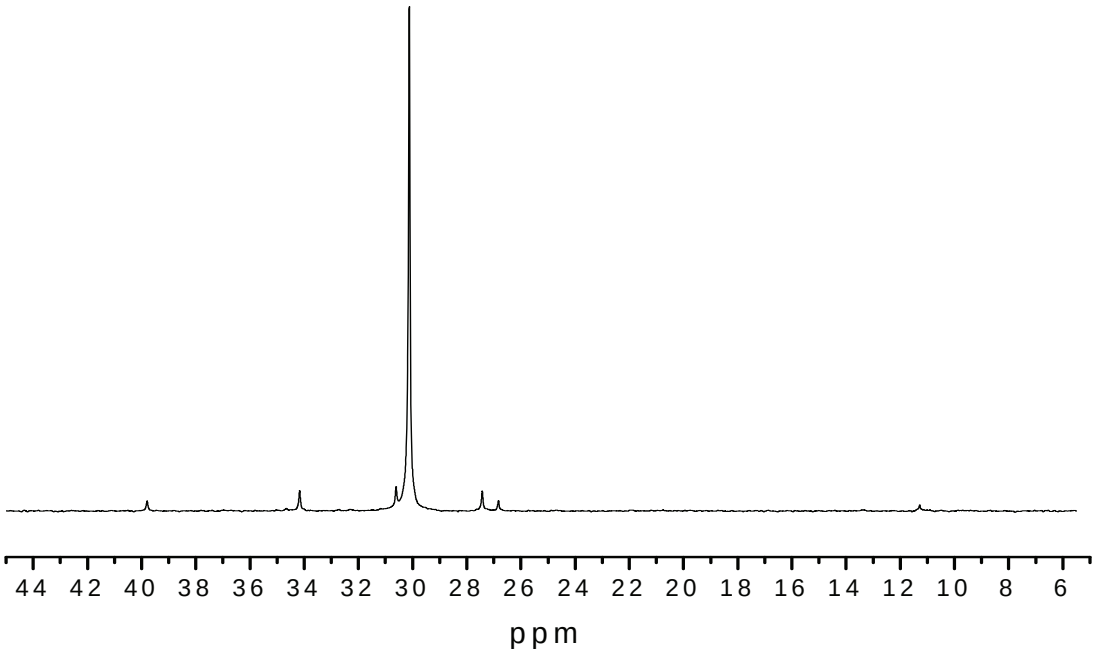

Figure A.5 ^{13}C NMR of sample A5

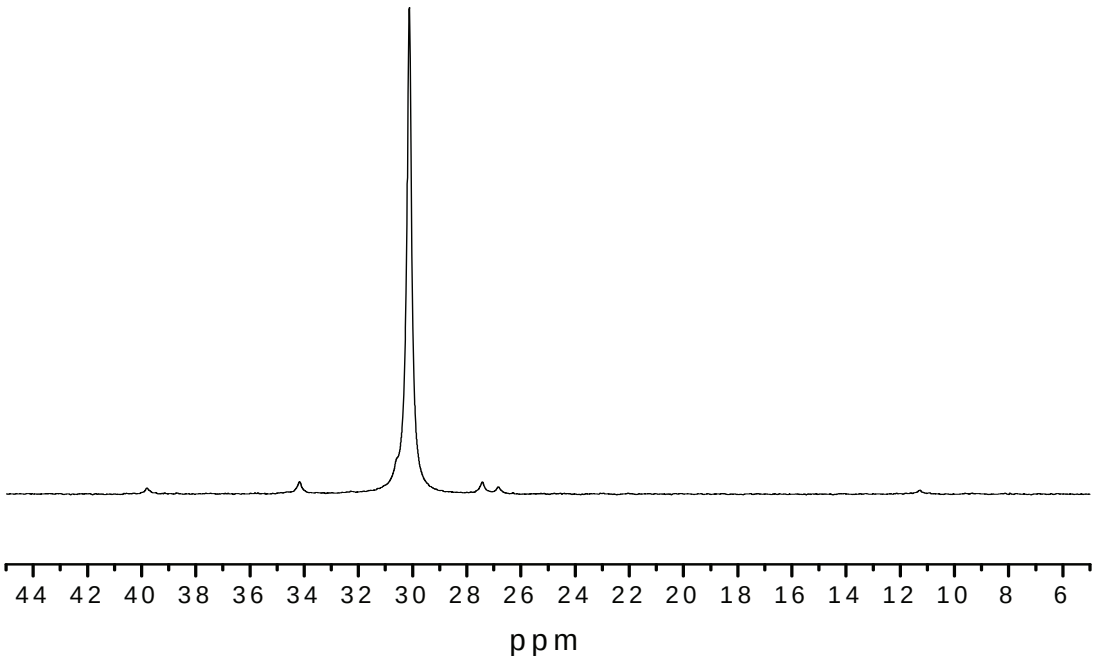

Figure A.6 ^{13}C NMR of sample A6

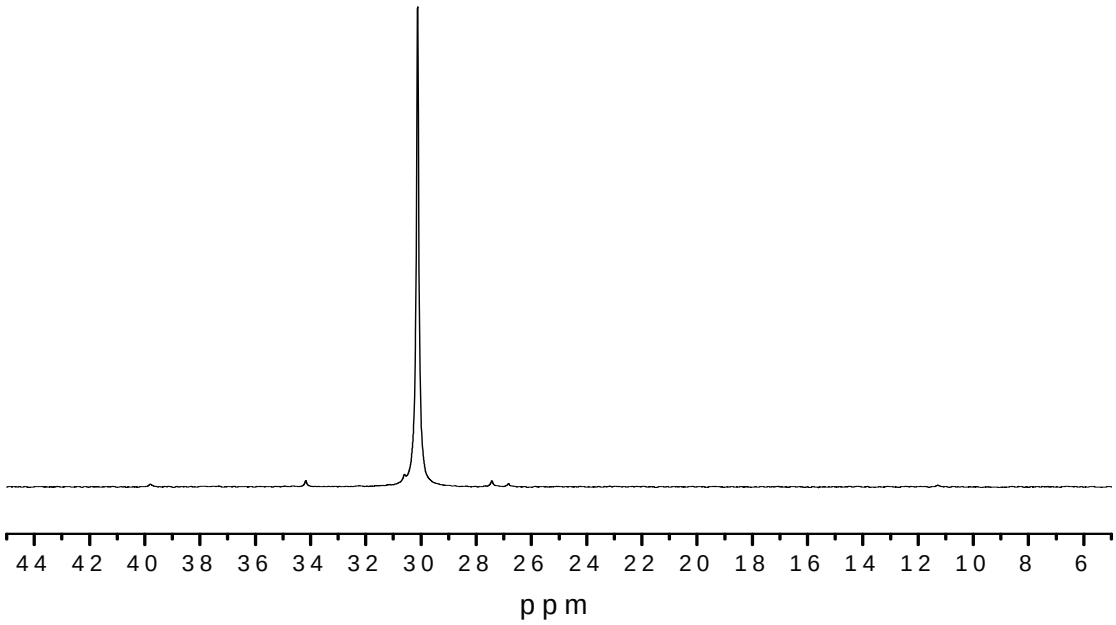

Figure A.7 ^{13}C NMR of sample A7

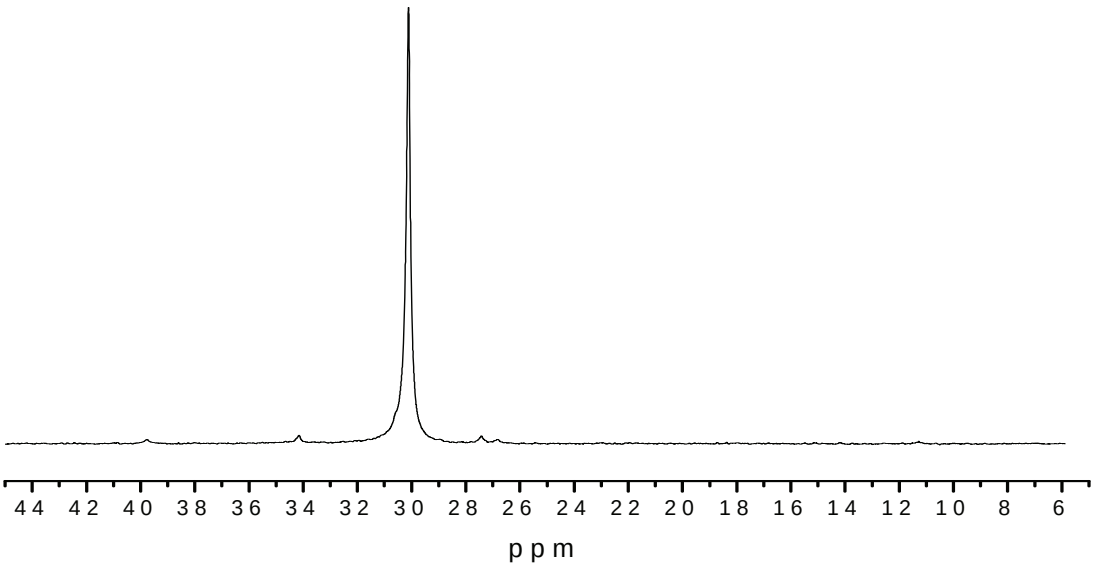

Figure A.8 ^{13}C NMR of sample A8

Recombined material

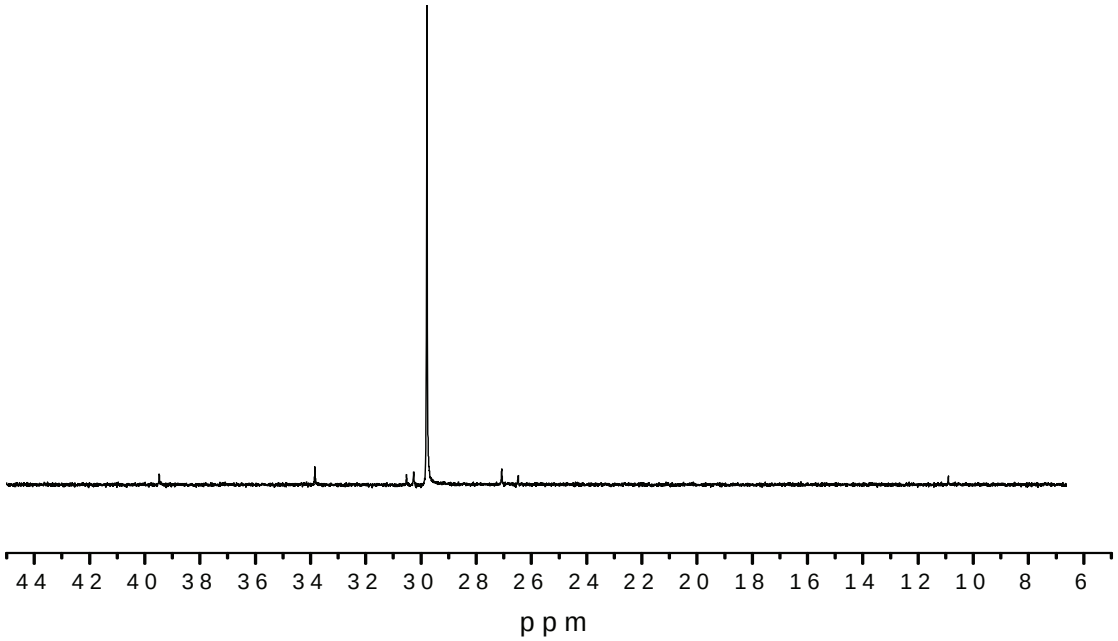

Figure A.9 ^{13}C NMR of sample B1

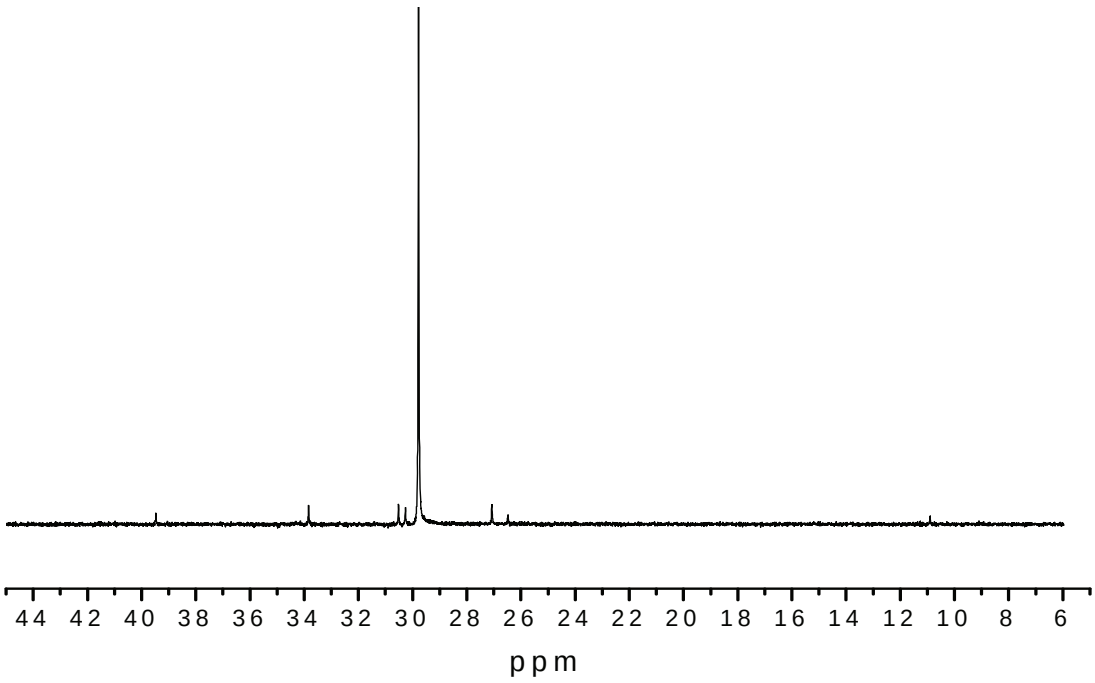

Figure A.10 ^{13}C NMR of sample B2

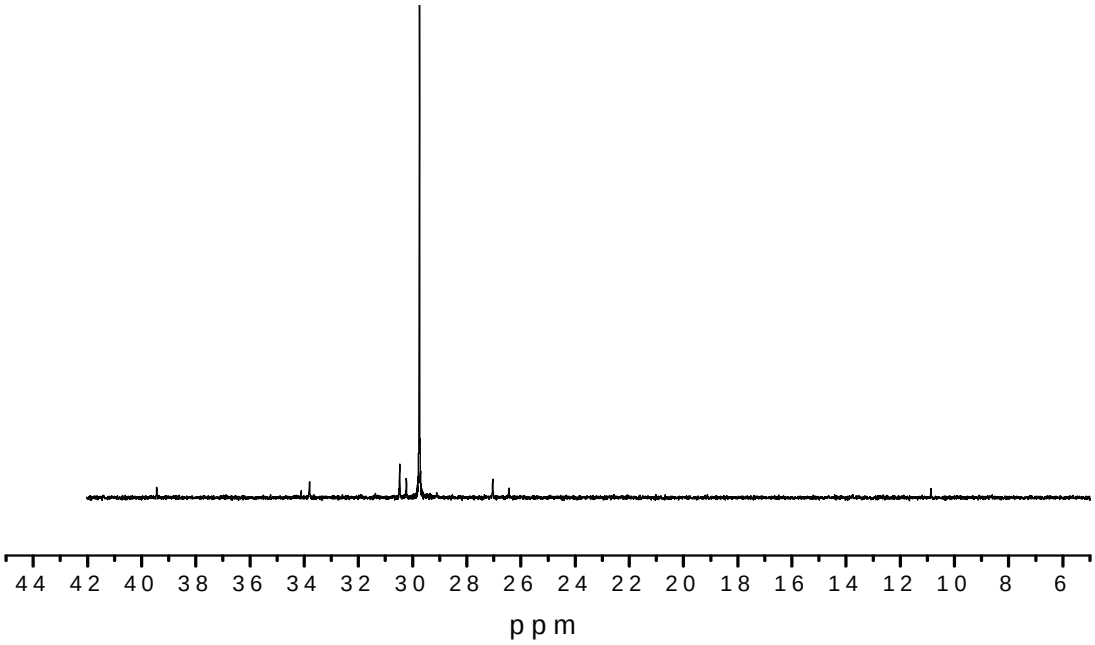

Figure A.11 ^{13}C NMR of sample B3

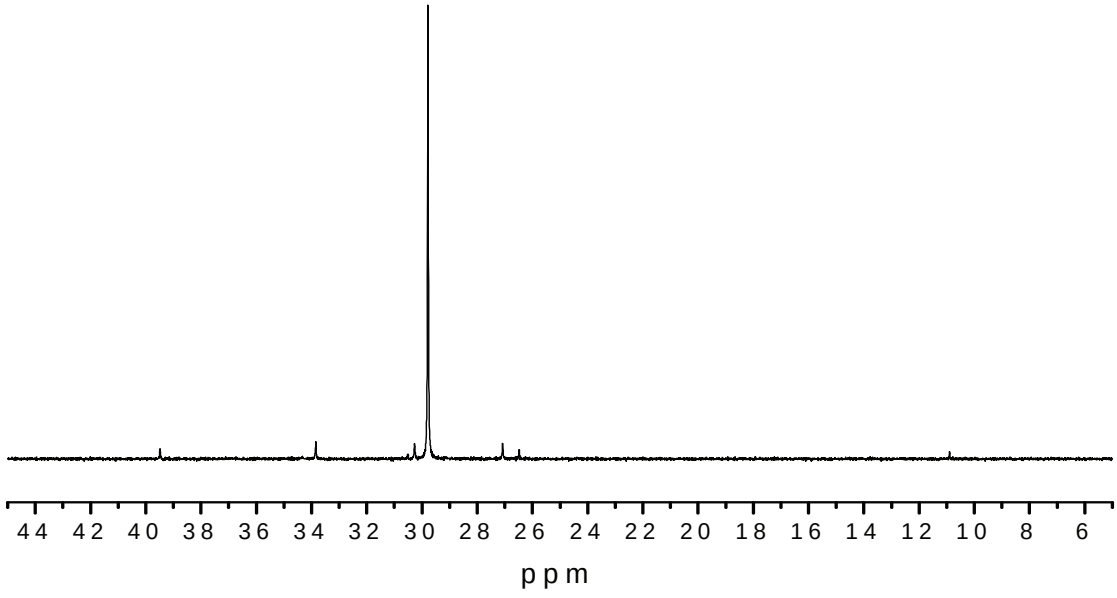

Figure A.12 ^{13}C NMR of sample B4

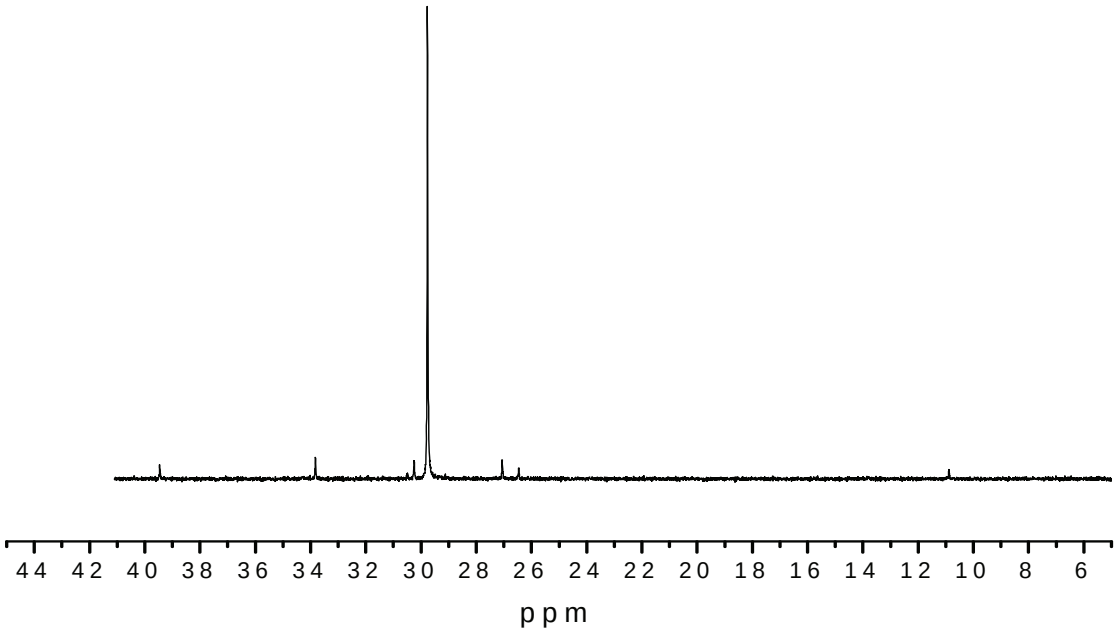

Figure A.13 ^{13}C NMR of sample B5

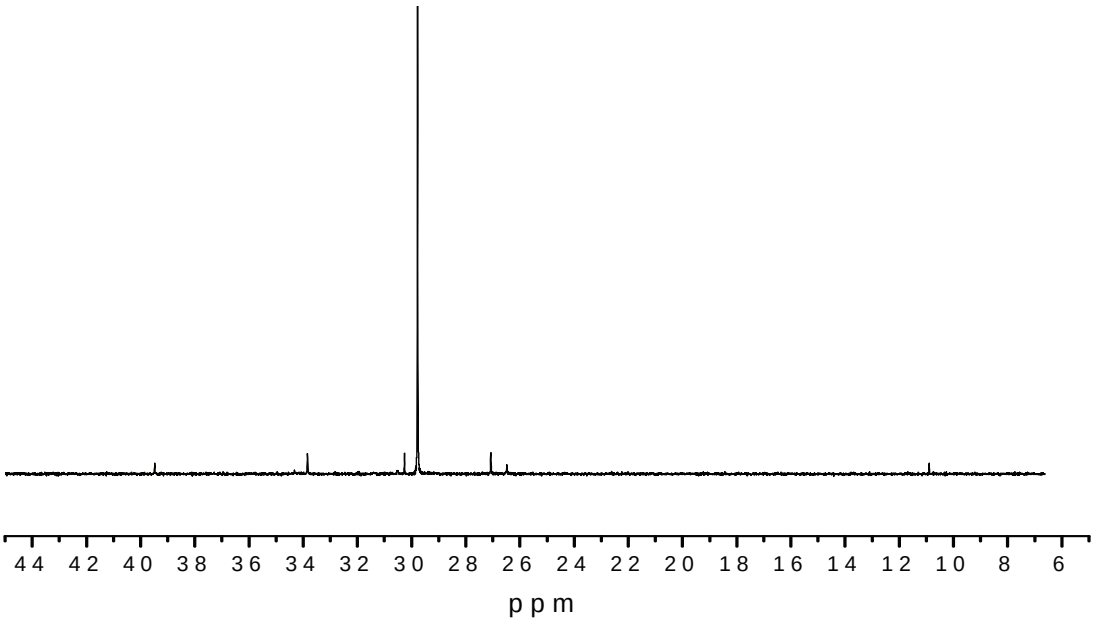

Figure A.14 ^{13}C NMR of sample B7

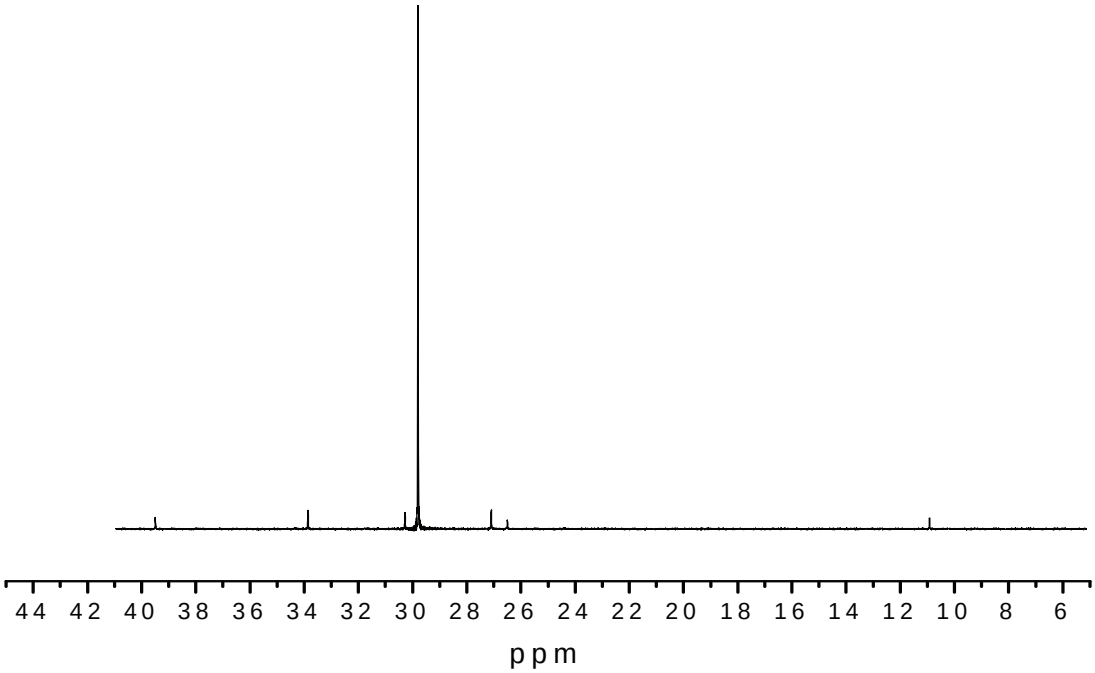

Figure A.15 ^{13}C NMR of sample B8

Removed Fractions

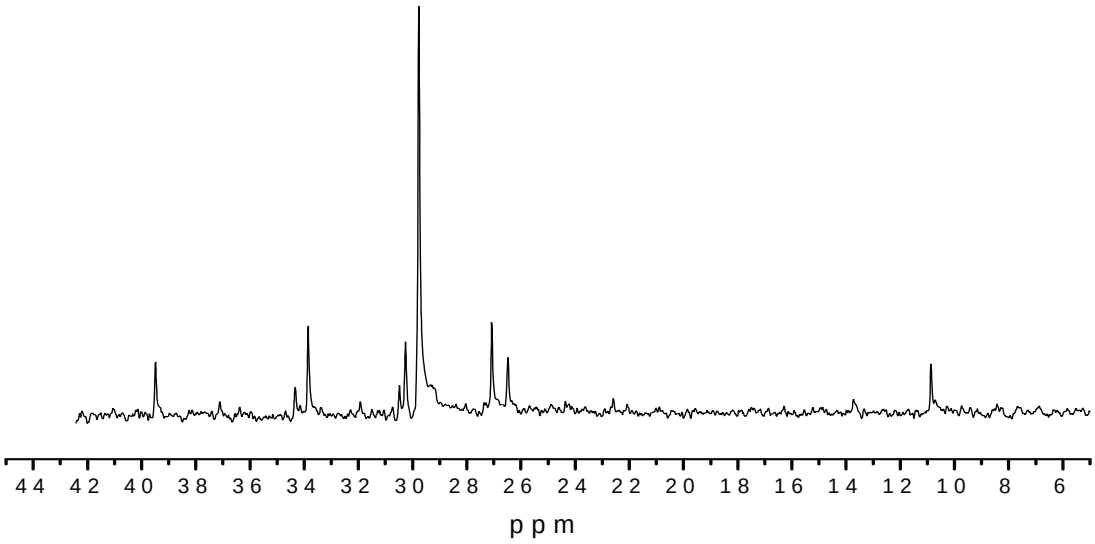

Figure A.16 <25 °C

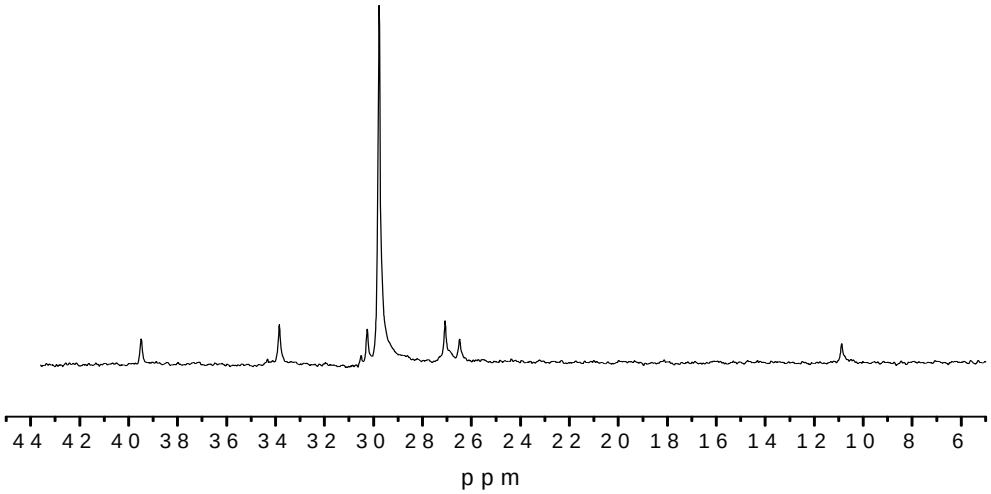

Figure A.17 26-50 °C

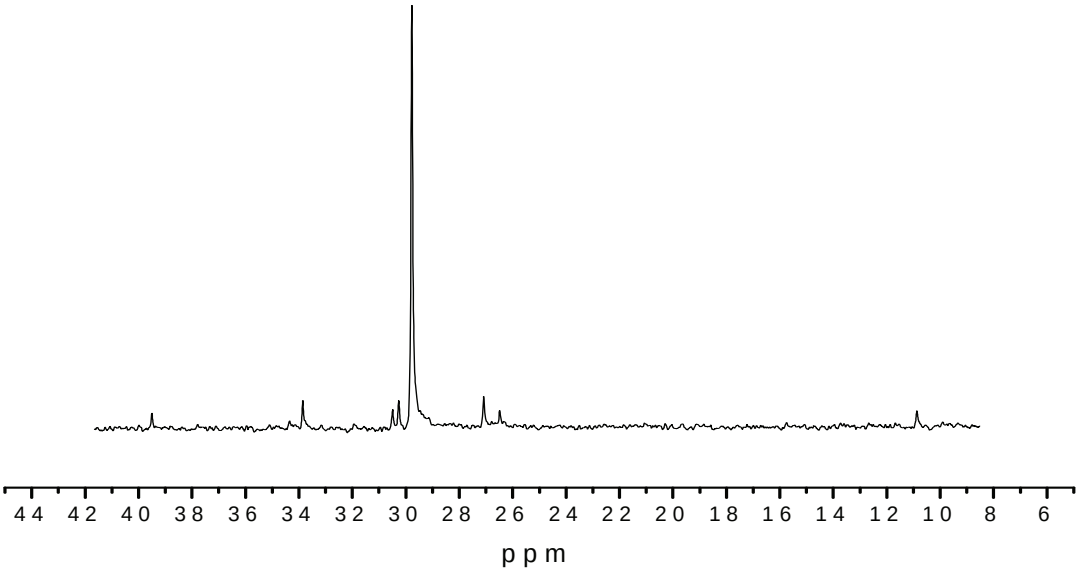

Figure A.18 51-60 °C

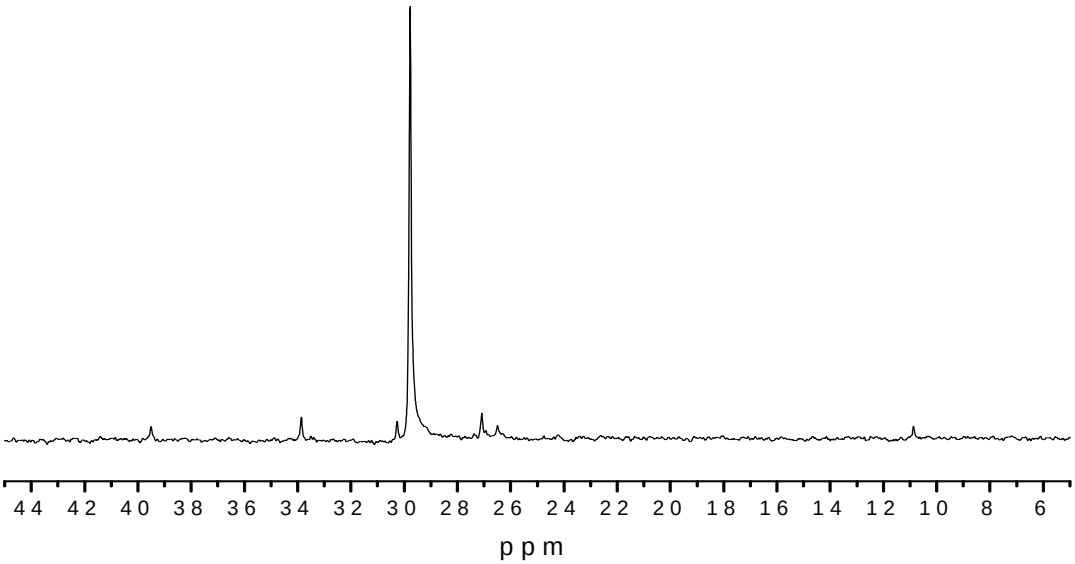

Figure A.19 61-70 °C

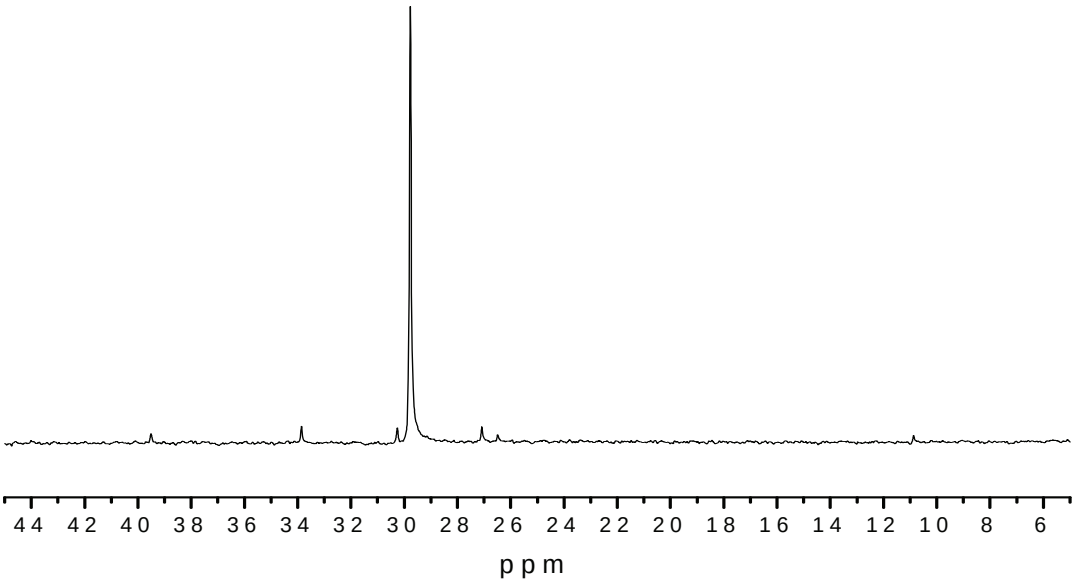

Figure A.20 71-80 °C

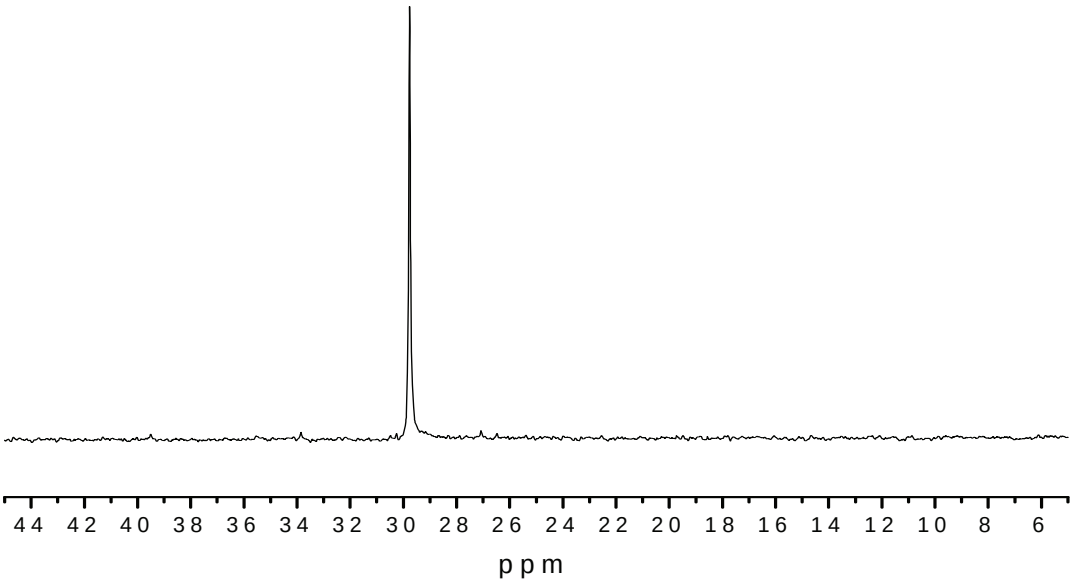

Figure A.21 81-90 °C

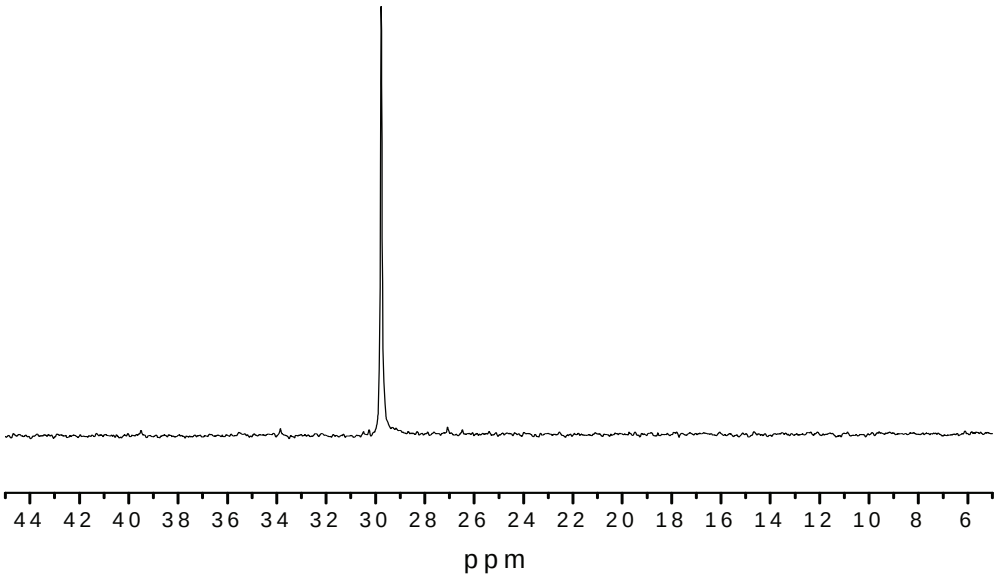

Figure A.22 91-100 °C

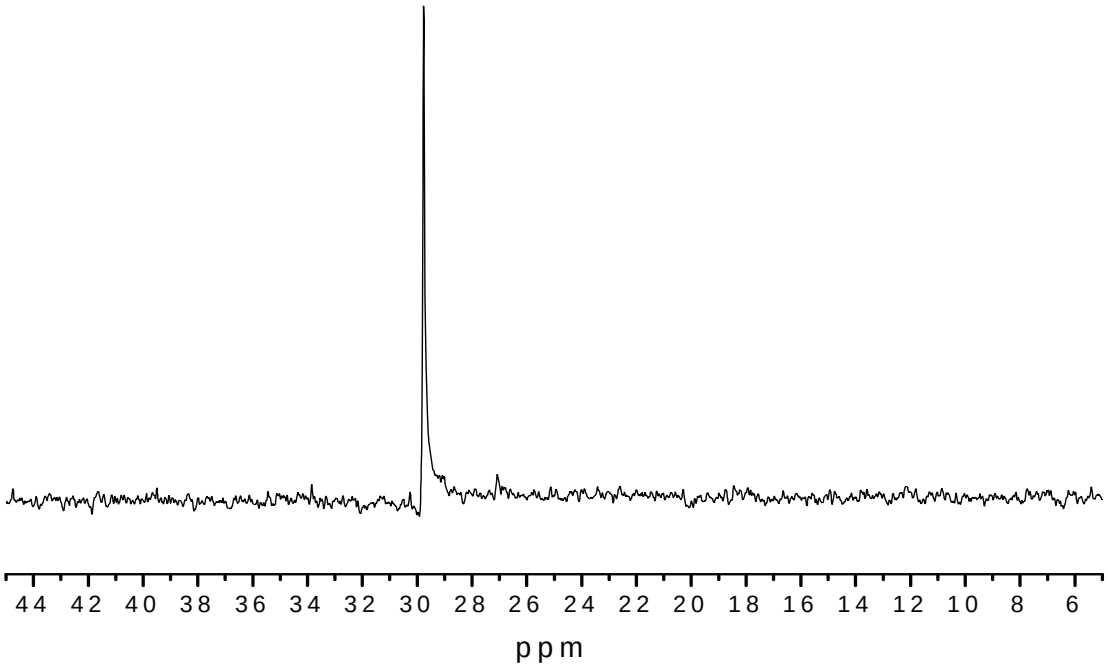

Figure A.23 101-120 °C

Appendix B: DMA Data

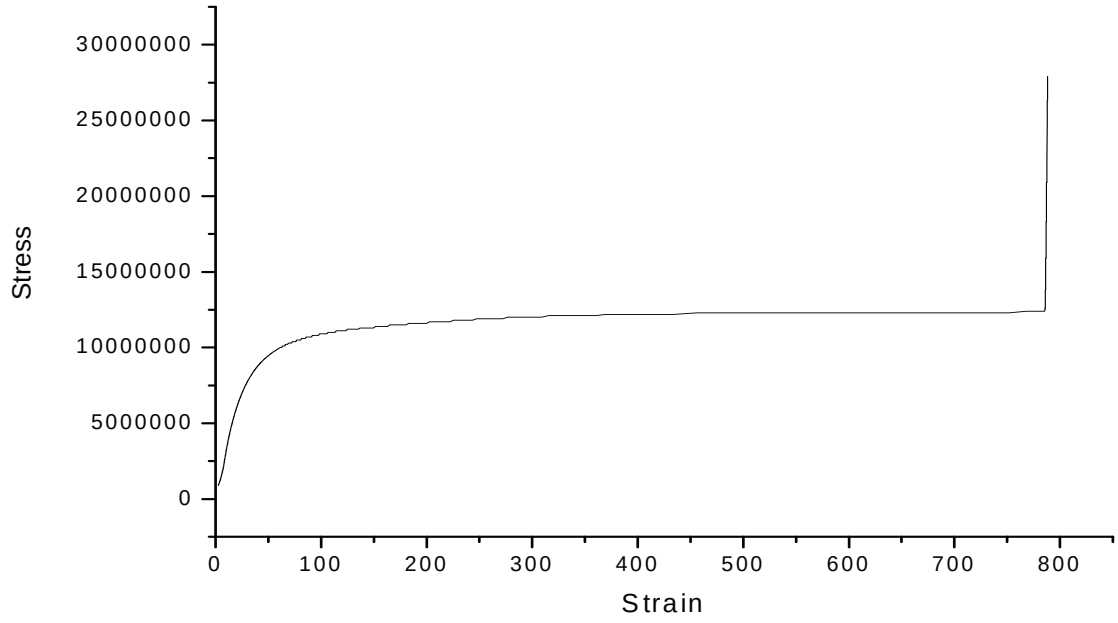

Figure B.1 Bulk material

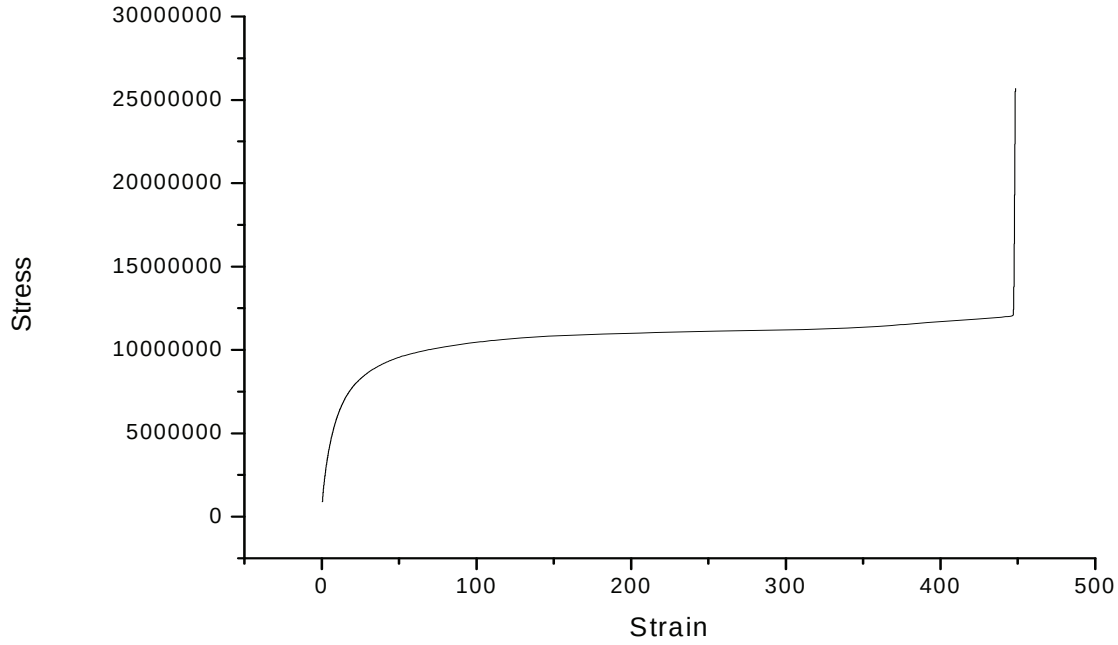

Figure B.2 Sample B1

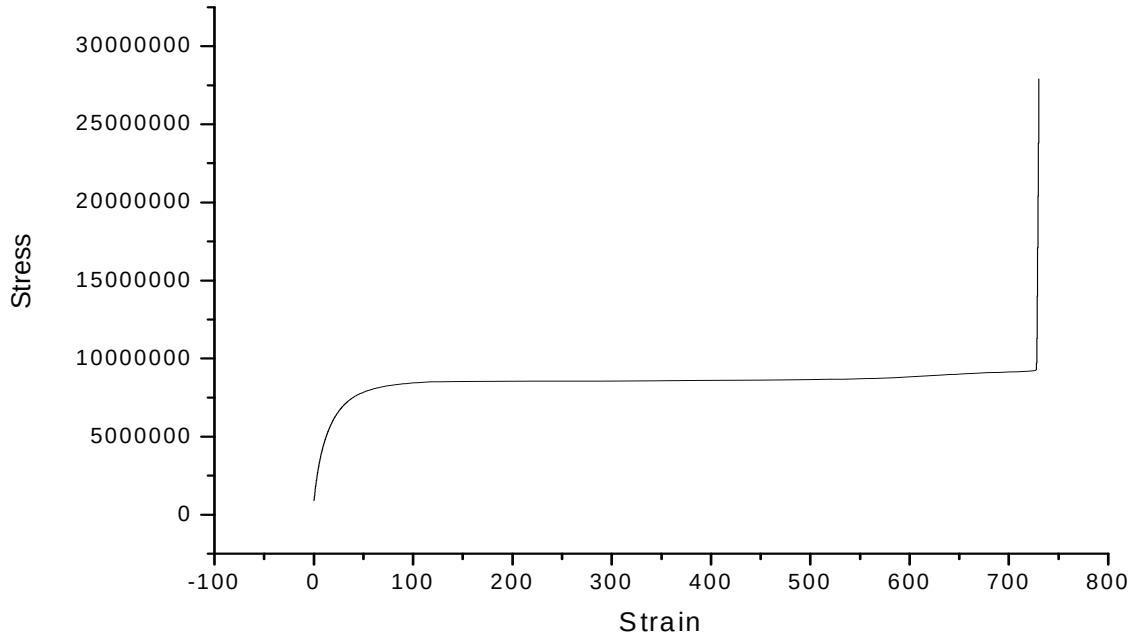

Figure B.3 Sample B2

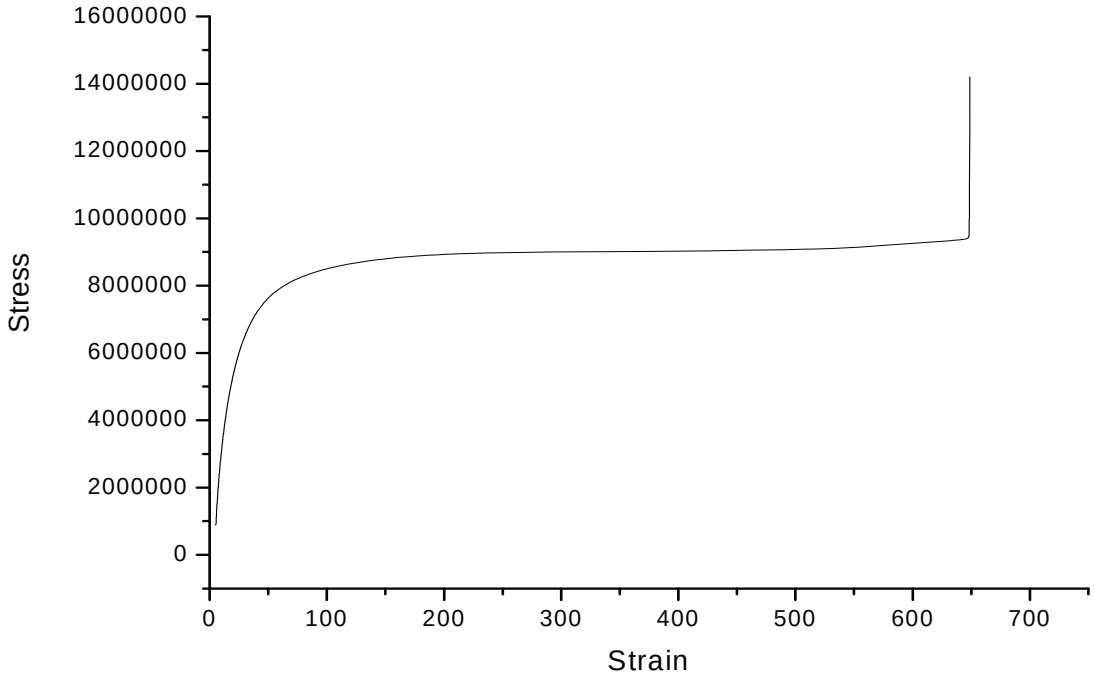

Figure B.4 Sample B3

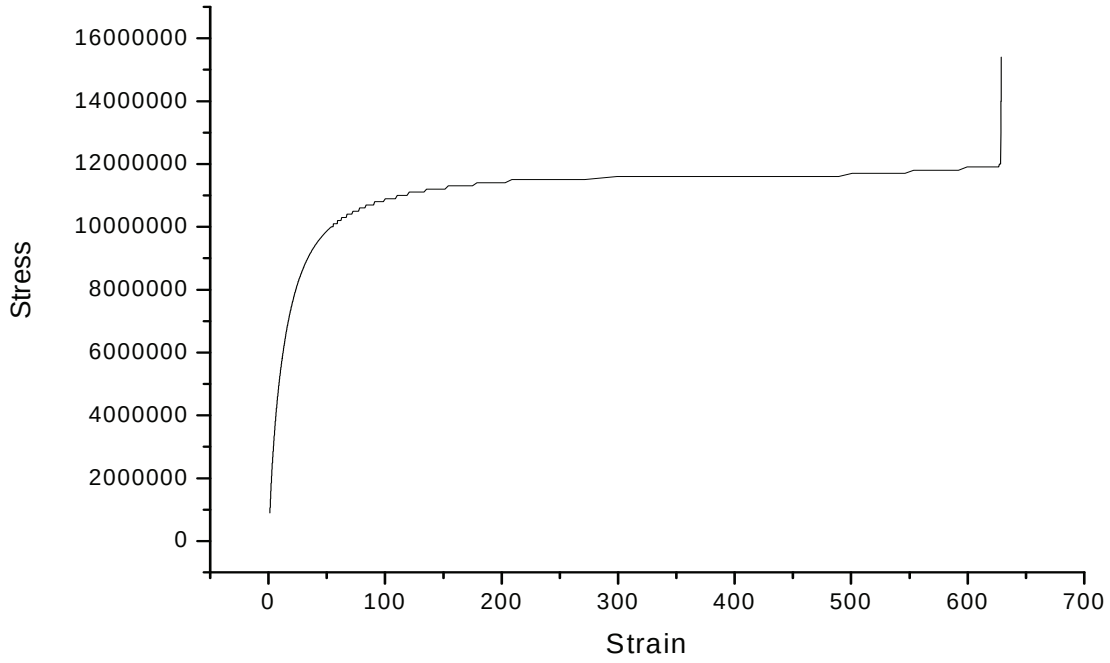

Figure B.5 Sample B4

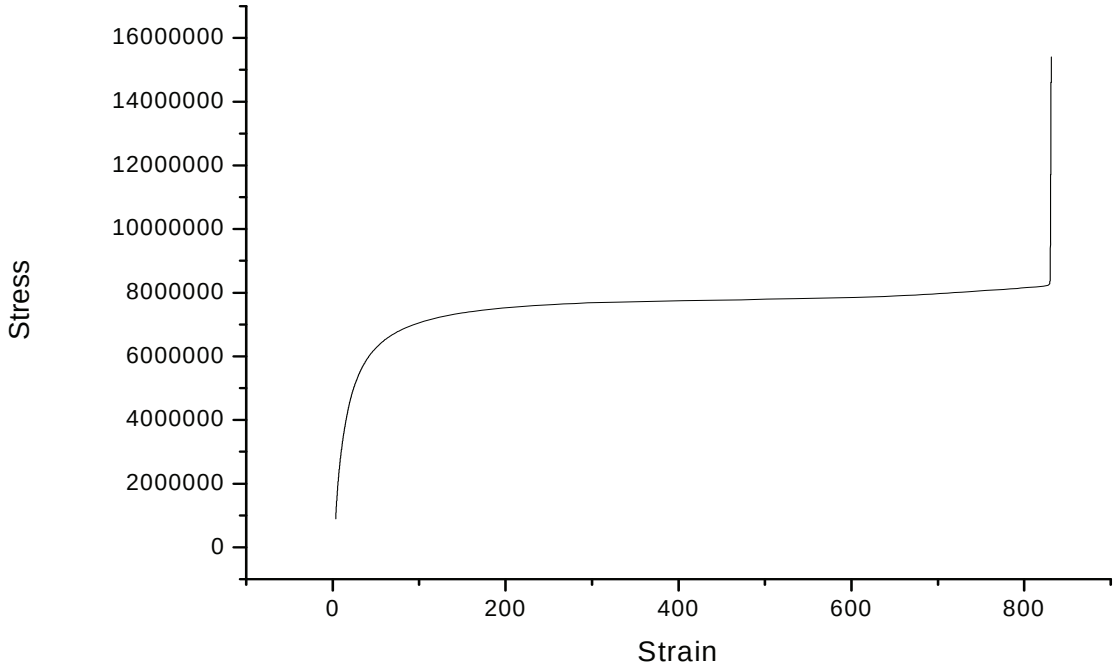

Figure B.6 Sample B5

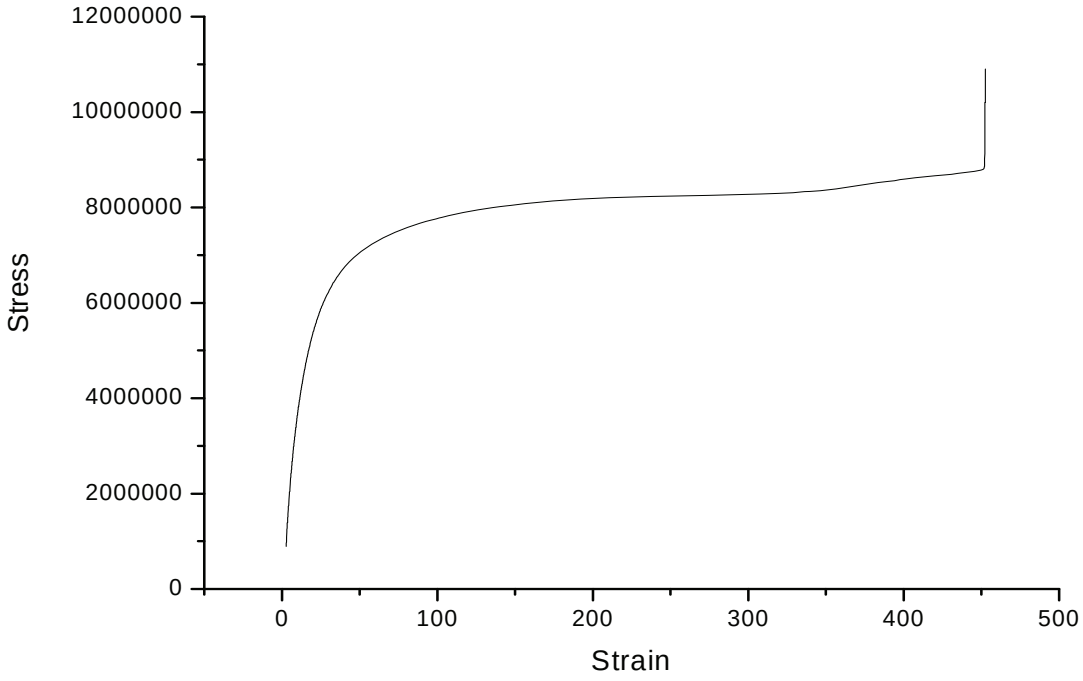

Figure B.7 Sample B6

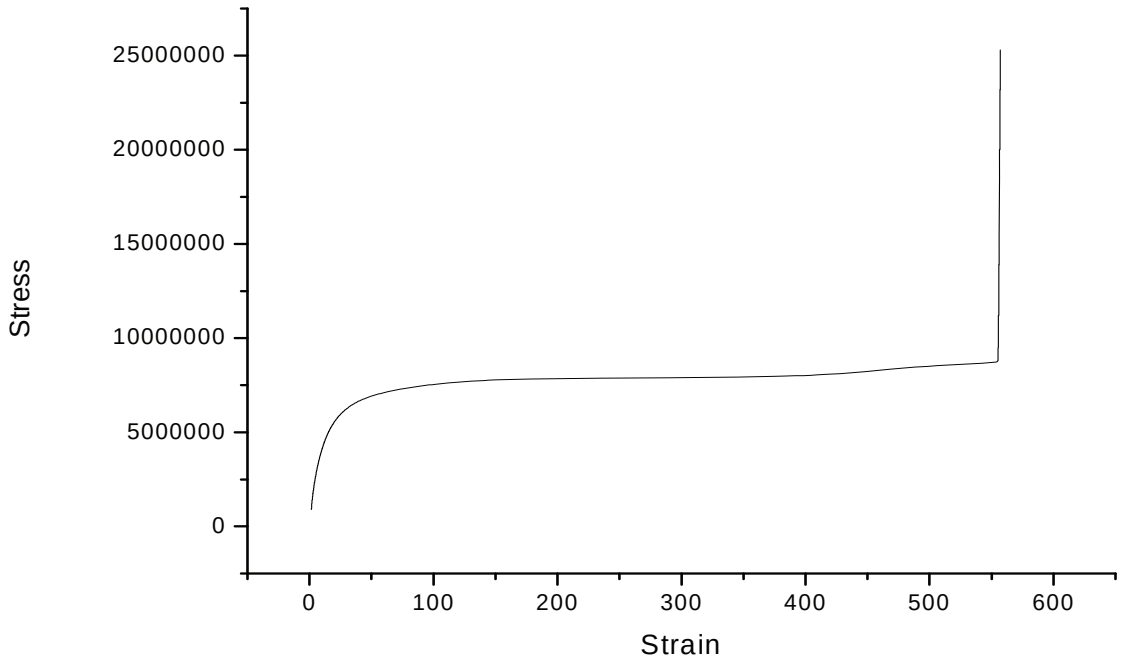

Figure B.8 Sample B7

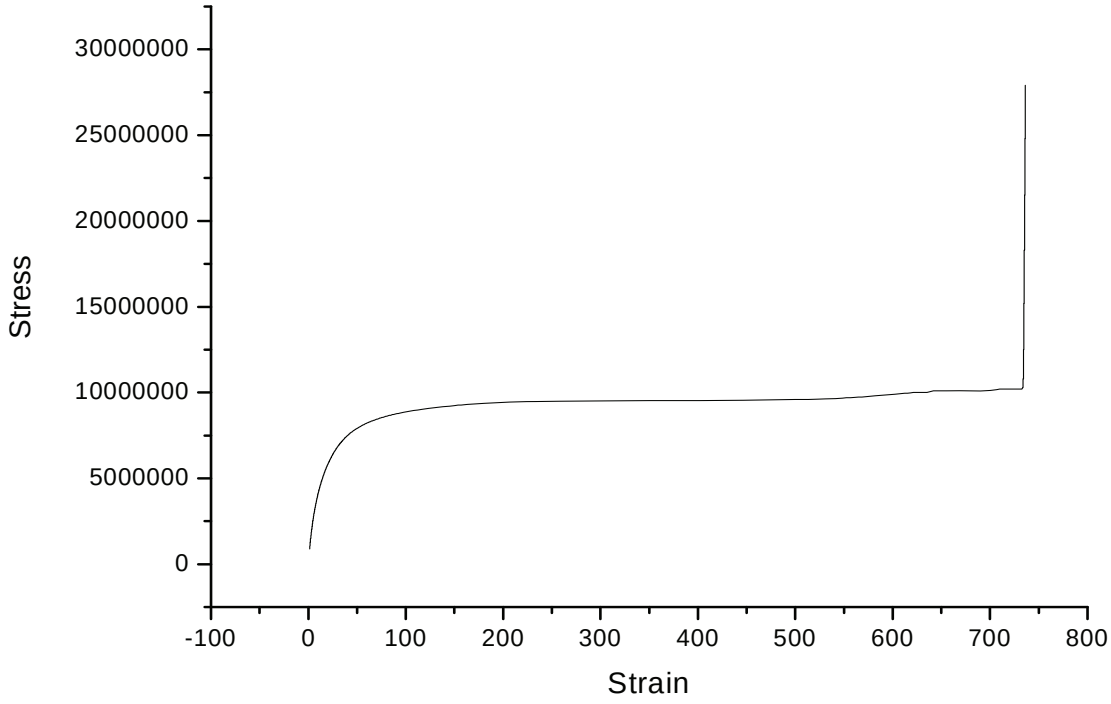

Figure B.9 Sample B8

Appendix C: DSC Data

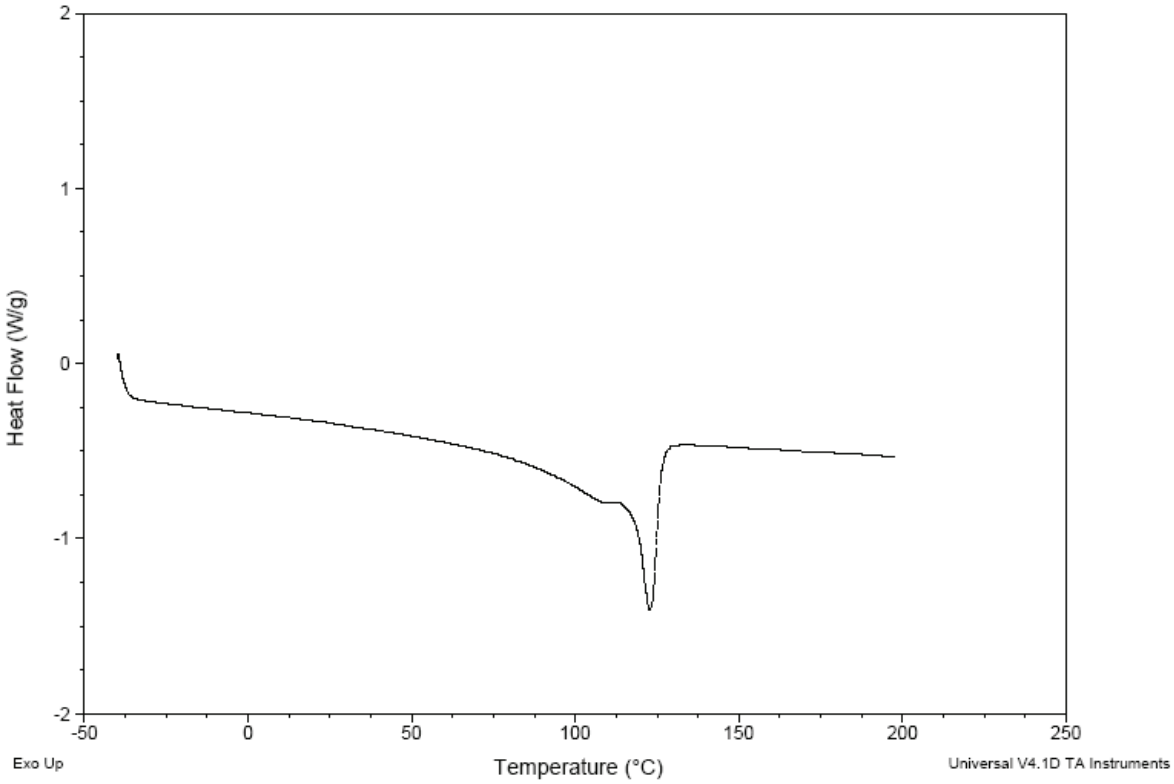

Figure C.1 DSC of bulk material

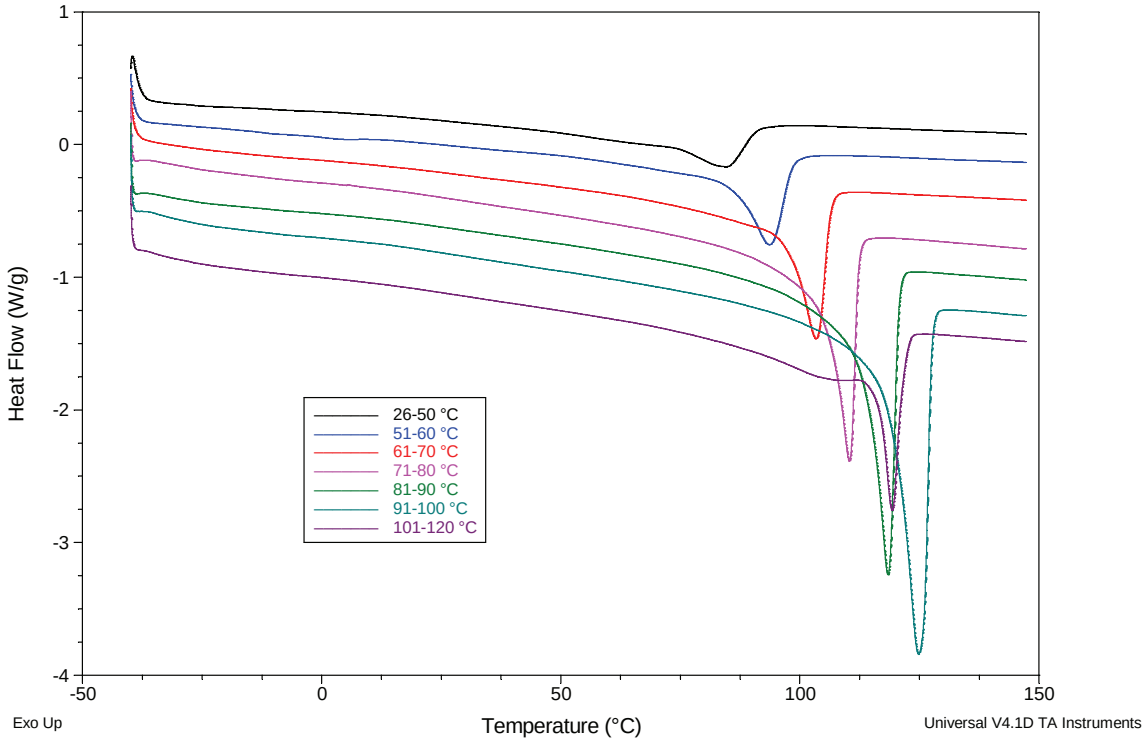

Figure C.2 Waterfall plot of melting endotherms for removed fractions